ADDIS ABABA UNIVERSITY

ADDIS ABABA INSTITUTE OF TECHNOLOGY

AFRICAN RAILWAY CENTER OF EXCELLENCE

TRAIN BRAKE PAD WEAR ANALYSIS USING FINITE ELEMENT METHOD

Case study: Addis Ababa Light Rail Transit (AALRT).

A Thesis in Railway Engineering (Rolling Stock)

By

Nakyanja Philomera

July 04, 2019

Addis Ababa

A Thesis

Submitted in Partial Fulfilment of the Requirements for the Degree of Master of Science in Railway Engineering (Rolling Stock)

The undersigned have examined the thesis entitled '**Train Brake Pad Wear Analysis using Finite Element Method** 'presented by **Nakyanja Philomera**, a candidate for the degree of **Master of Science** and hereby certify that it is worthy of acceptance.

Dr. Ing. Demis Alemu		
Advisor	Signature	Date
Mr. Muluken Masresha		
Internal Examiner	Signature	Date
Dr. Samuel Tesfaye		
External Examiner	Signature	Date
Chairperson	Signature	Date

UNDERTAKING

I certify that the research work titled "**Train Brake Pad Wear Analysis using Finite Element Method**" is my own work. The work has not been presented elsewhere for assessment. Where material has been used from other sources it has been properly acknowledged/referenced.

NakyanjaPhilomera

GSR/3831/10

philomera.nakyanja@aait.edu.et

nphilona@gmail.com

ABSTRACT

Wear is the damaging, gradual removal or deformation of material of contacting solid surfaces in relative motion with each other. During braking, wear occurs at the brake disc-pad contact and is predominant at the brake pad more than the brake disc. If it is not accurately predicted and necessary action taken, the repercussions of the failure of this component can be catastrophic. So, this raises an urge to conduct a study that will help in predicting the wear of the brake pad and plausible maintenance times scheduled.In this thesis, we simulate braking at 22 stations of the AALRT East-West Line from Ayat 2 to Tor Hailoch using FEM to ascertain the train brake pad temperature build up from repeated braking, its effect on contact pressure distribution and wear, ANSYS 2019 R1 is used for this wear simulation. The temperature is obtained from a transient thermal analysis and a thermal structural analysis is adopted to attain the contact pressure whereas the wear depth is evaluated by the Archard's linear wear law absorbed in ANSYS. Generally, the temperature of the brake pad increases after every braking and reduces during the train movement from station to station but does not go back to the initial ambient temperature. The contact pressure increases with increase in temperature, Wear depth is evaluated from contact pressure and temperature distribution, which is obtained from finite element simulation results and is an input into the Archard's wear equation. It is observed that increase in temperature leads to increase in contact pressure which in turn leads to an increase in wear. A maximum Temperature of 385.56℃ was reached and a cumulative wear of 19.085nm was recorded.Therefore, the ability to predict train brake pad wear using Finite Element Analysis will help maintenance personnel to establish the appropriate time for inspection and replacement as well as mitigation of wear.

Keywords: contact pressure, temperature, railway brakes, wear, finite element analysis.

ACKNOWLEDGMENTS

First and foremost, I would like to thank my advisors, Dr. Ing. Demis Alemu and Dr. Celestin Nkundineza for their valuable guidance and advice. They inspired me greatly to work on this thesis and their willingness to motivate me contributed tremendously to my progress. I also would like to show gratitude to Mr. KejelaTemesgen Deressa and Mr. Araya Abera for their support towards directing me on the right track. Additionally, I would like to show my gratitude to all the department's staffs for their comments and suggestions.

I would like to thank all my friends who contributed to my thesis work by giving me supportive materials, data, information and helpful ideas. Finally, I would love to express my utmost gratitude towards my family for their great support and understanding while working on this thesis and through all my graduate study.

TABLE OF CONTENTS

LIST OF TABLES

LIST OF FIGURES

NOMENCLATURE

A= Area

k_x= Thermal conductivity in x-the direction

k_y= Thermal conductivity in y-the direction

k_z= Thermal conductivity in z- the direction

C_p= Specific heat

C= Specific heat capacity

ρ= Specific mass

Q= Internal heat generation rate per unit volume

T= Temperature

h= Convective surface heat transfer coefficient.

T_1= specified surface temperature

q_s = the specified surface heatflux

T_s=Unknown surface temperature

T_∞=Convective exchange temperature

ε= Material's emissivity

σ= Stefan-Boltzmann constant

M= Vehicle mass

k= Correction factor for rotating parts

λ= Proportion of heat entering the brake disc

S_b= Vehicle braking distance

F_T= Tractive force

F_D= Drag force

F_G =Total weight component in the direction of the inclined plane

F_R= Rolling resistance force

a= Train deceleration

g= Acceleration due to gravity

a_T= Train acceleration

T_m= Motor Torque

T_w= Wheel Torque

P= Power

P_b= Braking power

P= Pressure

ω= Angular velocity

η= Mechanical efficiency of transmission

τ= Gear ratio of transmission

r_{wheel}= Radius of the wheel

α= Track gradient

t_b= Braking time required to bring the vehicle to a stop

A_d= Contact swept area

r_o= Outer pad radius

r_i= Inner pad radius

F_{disc}= Brake disc force

$F_{caliper}$= Caliper force

Δh = Wear displacement

t = Sliding time,

k= Dimensionlesswear coefficient,

H = Hardness of softest contacting surfaces

p = Applied contact pressure

v = Sliding velocity

Q =Total volume of wear debris produced

W = Total normal load, k is a constant

L= sliding distance

CHAPTER 1 INTRODUCTION

In East Africa as well as in many other parts of the world, rail networks are distinguished into urban rail network and mainline. In the same regard, Ethiopian networks have Addis Ababa Light Rail Transit and Ethio-Djibouti mainline. The AALRT network supports passenger trains and therefore involves many stoppages at different stations for the loading and alighting of passengers[1]. In order to meet modern railway standards, the braking performance on trains has to be effective which consequently enhances good riding quality of passengers especially during emergency braking[2]. While the basic braking principle is similar to that of road vehicle, the usage and operational features are more complex because of the need to control multiple linked carriages and to be effective on vehicles left without a prime mover[3].

Highly reliable braking systems are a crucial element of railway service safety and there are different types of braking systems among which are, axle-mounted disc brakes and wheel-mounted disc brakes[3]. These brake mechanisms use a brake shoe that applies friction force to the disc.Passenger vehicles usually use disc-type braking systems that are subjected to high contact pressure and temperature, friction, and humidity. The disc brakes are preferred due to the frequent stoppages at stations. In the case for Ethiopian rail networks, disk brakes are used on both the AALRT trains as well as Ethio-Djibouti mainline.

According to[4], trains exploit contact friction to transmit driving power and braking force and since bodies are elasticallydeformable, more or less friction is always involved at contact leading to wear of bodies. During braking, sliding contact of the brake system results in kinetic energy conversion into heat energy at the pad/disc interface[5] also the contact pressure and temperature changes continuously[6]. The contact pressure and temperature changes on the contact surfaces are because of slipping between the brake disc and brake pad especially during emergency braking and these changes are further intensified by significant thermal load due to frictional forces as well as the high velocity of the process [7]. These conditions of operation cause severe wear of the elements of the braking systems resulting in need for frequent replacement of the brake pad. It is not only the cost of replacing a brake pad, but also the damage that excessive temperature/pressure might cause in a braking system. Since both brake pad and rotor surfaces get worn, the useful life of the brake as well as its behavior are affected

[8].Wear of engineering components is a critical factor influencing their service life-span[9]. Typical problems are cracks due to fatigue and material transfer between the friction pad and the disk brake[6].

It is believed that the investigations on the friction and wear behaviors of brake friction materials are valued for controlling friction, reducing wear, developing new fine friction materials, and improving braking reliability [10]. In order for today's railways to stay competitive with other types of transportation, there's need to reduce maintenance costs associated with wear. This would lead to significant savings particularly in form of prevention of accidents associated with brake disc-pad wear.

To reduce associated costs and guarantee safety, wear prediction needs to be in place so that preventive measures are taken at the right time. This issue has been addressed in form of determination of contact pressure distribution or temperature distribution on the pad disc interface but not as a result of both.

Wear of the disc brake is a common occurrence and has been experienced at AALRT; as a result, many expenses are incurred in form of brake pad replacement and other associated maintenance costs which raises the need to address this issue.

With rapid development in computer technology, Finite Element Method (FEM) analysis is a robust tool to investigate the wear characteristics of materials, as it can provide additional analytical tools beside results obtained from experiments, such as parametric studies [11]. It is also helpful in determining preventive maintenance to determine when maintenance and replacement of worn disc-pads should be carried out in order to minimize down time due to repair.

1.1 Problem Statement

A railway brake is an essential feature in order to reduce speed, to maintain its speed when travelling downhill and to completely stop the train. During braking both the brake pad and brake discs are subject to wear causing them to get worn out. At AALRT brake pads were observed to have surface wear. The significant effect of wear is severe damage of the disc brake system and loss of braking efficiency. Brake disc and pad wear can result in extensive costs associated with material loss and associated equipment downtime for repair and replacement of worn components as well as loss of lives from resulting train accidents, if it is not predicted and preventive measures taken timely. Due to this, various research has been done on the brake system for cars but not for AALRT. To limit brake, wear related costs, predicting train brake disc wear through Finite Element Analysis is a means to establish the appropriate time for inspection and replacement.

1.2. Objectives

1.2.1. Main Objective

The main objective of this thesis was to perform a FEM analysis of wearwear on the train brake pad using temperature distribution and contact stress distribution.

1.2.2. Specific Objectives

- To determine the temperature distribution in the brake pad.
- To determine the contact pressure distribution on the brake disc-pad contact.
- To estimate wears depth by using ARCHARD wear model.
- To establish the correlation between temperature, contact pressure distribution and wear.

1.3. Delimitation

The scope of this thesis will be limited to the AALRT East-West Line from Ayat 2 to Tor Hailoch considering train brake pad wear numerical analysis using FEM with the objective of obtaining temperature distribution and contact pressure distribution on the disc brake and the use of the Archard wear model to attain the wear depth. Effect of different brake system material will not be included in this research. However, the effect of material on brake wear has been presented in the literature review section.

CHAPTER 2 LITERATURE REVIEW

This section reviews previous studies on train brake systems in relation to wear. All studies were focused on mechanical brake discs and pads in railway vehicles.

2.1. Disc Brakes

A disc brake is a brake that slows rotation of the wheel by the friction caused by pushing brake pads against a brake disc with a set of calipers. The development and use of disc type brakes began in England in the 1890s [12]**.** In railway locomotives disc brakes are mounted on either wheels or axles to dissipate brake energy. Disc brakes are commonly used because of their simplicity, power, easy maintenance and ease of use of new materials of disc and pad for effective friction and minimal wear. The common material used in disc brakes is grey cast iron, structural steel and in some cases a composition of reinforced carbon-carbon or ceramic matrix composition.

2.1.1. Working principle of disc brake

In a disc brake system, a set of pads is pressed against a rotating disc and due to friction, heat is generated at the disc-pad interface. This heat ultimately transfers to the vehicle and environment and the disc cools down[13]. Figure 2.1 represents the schematic lay out of the disc braking system. When brakes are applied, hydraulically actuated pistons move the friction pads in to contact with the disc, applying equal and opposite pressure on the discs. Due to the friction involved, relative motion between the brake disc and brake pad is constrained thus leading the wheels to reduce speed and eventually stop. On releasing the brakes, the rubber-sealing rings acts as return spring and retracts the pistons and the friction pads away from the disc [14].

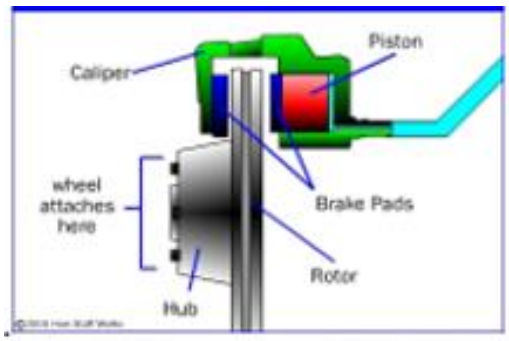

Figure 2.1: How a disc brake works

2.2. Disc Brake Components

A disc brake assembly consists of following major components: brake disc, pad, under layer, back plate, shim and caliper[13], refer to Figure 2.2 below.

Figure 2.2: Disc brake components[15].

2.2.1. Rotor

A brake disc also known as a brake rotor, is fixed to the axle or the wheel, and thus rotates at the same speed as the wheel. Braking power of a disc brake is determined by the rate at which kinetic energy is converted into heat due to frictional forces between the pad and the disc however, ventilation is introduced in the brake discs which increases the cooling rate. Brake discs are divided in two categories; - solid brake discs &ventilated brake discs as in Figure 2.3 below. A solid brake disc is the simplest form and consists of a single solid disc. In a ventilated disc, vanes or pillars or both separate two annular discs and provide a passage for the air to flow[13].

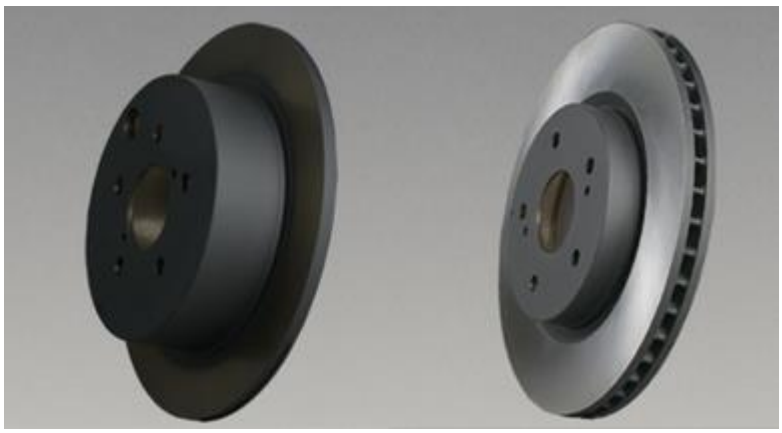

Figure 2.3: Left; Solid disc Right; Ventilated disc[16]

2.2.1.1. Brake pads

A brake pad consists of a friction material which is attached to a stiff back plate. Sometimes the friction material and back plate together are called a brake pad. A brake pad usually incorporates slots on its face and chamfers at the ends. A slot enables the material to bend and avoid cracks. Furthermore, it facilitates to clean the dust collected

between disc and pad surfaces by offering an escape.[13]. Several considerations are weighted in development of brake pads; the coefficient of friction must remain constant over a wide range of temperatures, the brake pads must not wear out rapidly nor should they wear the disc rotors, should withstand the highest temperatures without fading and it should be able to do all this without any noise. Large thermal conductivity is often desirable in order to reduce the thermal loading on the opposing body, i.e. disc/wheel/drum[17, 13, 6].

2.2.1.2. Materials for brake disc and brake pad

Brake disc

The brake disc is usually made of cast iron.High thermal conductivity and specific heat capacity of grey cast iron are two major factors often considered to make cast iron disc brake rotors.

Brake pad

The material used for the brake lining should have the following characteristics;

- It should have high coefficient of friction with minimum fading. In other words, the coefficient of friction should remain constant with change in temperature
- It should have low wear rate
- It should have high heat resistance
- It should have high heat dissipation capacity
- It should have adequate mechanical strength, and
- It should not be affected by moisture and oil.

2.3. Disc Brake Operational Issues

Braking is a process of transferring kinetic energy into heat energy [18]. Efficient brake design enables quick heat dissipation, otherwise the temperature of a disc might rise and affect the performance of a disc brake. The ventilated brake disc types increase cooling rates resulting in lower surface temperature thus reducing the risk of brake fade and also most importantly wear of the disc and pad [19, 13]. However, premature wear and thermal cracking of brake discs is attributed to high thermal stresses during braking, rapid temperature change in components of the sliding systems induces thermal stresses due to thermal expansion [20].

2.4. Disc Brake Wear Phenomenon

Wear takes place when two or more bodies in frictional contact slide against each other. The significant effect of wear particularly in the friction material of the disc brake system is reduction of its life span. According to Jiang [21], damage to materials and mechanical components due to wear has a significant impact on the economics of engineering systems both directly and indirectly in terms of material loss and associated equipment downtime for repair and replacement of worn components and a possibility of worse situations leading to accidents if not detected[21, 22]. A lot of research has been done on the disc brake related to wear analysis.

2.4.1. Wear Damage

Rapid efforts have been made in understanding the mechanisms of wear to improve the wear performance of materials. Sliding wear involves the formation of wear debris particles and their subsequent removal from the rubbing interface[21].Wear debris particles are generated by the relative motion of the rubbing surfaces under load. Some of these are removed from the wear tracks to form loose wear particles, resulting in wear loss. The others are retained within the wear tracks where they are comminute by repeated plastic deformation and fracture while freely moving between the rubbing surfaces [21]. Wear is considered as a critical failure mode that affects the life span of any load-bearing component[11].

2.4.1.1. Forms of wear

Basically, wear is classified in to two; the conditions in which the wear occurs; and the mechanism by which the wear occurs. Conditions used to classify wear include whether or not there is a lubricant present, and whether or not there are hard, abrasive particles present. If there is a lubricant present, it is referred to as lubricated wear, otherwise it is dry wear. If there are abrasive particles causing wear, then it is referred to as abrasive wear, otherwise it is called sliding wear[23]. The current study of brake disc-pad contact wear focuses on dry sliding wear.

Wear resistance is not an essential material property, change to surface and near surface structures during wear contact normally significantly alter local material properties, both mechanically and chemically[24].

Wear mechanisms present in braking systems have been studied by several researchers [22] over the years some of which are discussed briefly;

- Abrasive wear occurs when a hard surface cuts material away from a softer surface making the surface look rough.
- Adhesive wear occurs when the adhesion forces in a sliding contact are high; shear takes place in the weakest material instead of at the surface interface resulting in detachment of fragments from one surface and attachment to the other. Adhesive wear surface often looks quite smooth.
- Oxidative wear occurs under mild contact conditions, when the forces and sliding velocity are low. Under the influence of water and oxygen, oxides form on the surface and will eventually break away in the disc-pad contact.
- Fatigue wear takes place due to repeated loading and unloading. Cracks occur after a while at the surface or underneath. The cracks propagate and after a time, particles from the surface may break out.

However, commonly observed is abrasive wear in brake disc-pad contact[22].

Wear by abrasion is form of wear caused by contact between a particle (grit) and solid material (the loss of material by the passage of hard particles over a surface). The mechanisms of abrasive wear are depicted in Figure 2.3: -

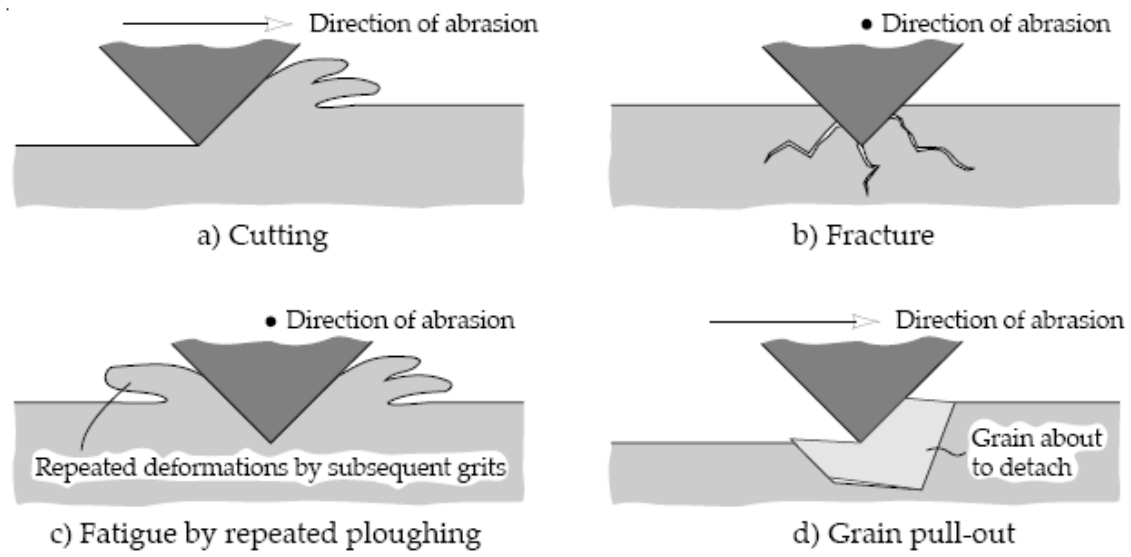

Figure 2.4: Mechanisms of abrasive wear

Depending on the amount of material which is lost from element, the wear may be broadly classified as “mild wear” or “severe wear”.

In mild wear, the wear processes occur at the "outer" surface layers. The surfaces remain relatively smooth and are usually protected by surface oxide layers generated in rubbing. The worn debris consists of small particles down to some nm.

In severe wear, the contact is metallic, the surfaces are deeply torn, and the worn debris consists of metallic particles up to some 100 μm.

Camacho et al[22] did work on the wear mechanisms of disc and shoe brake pads subjected to real service, roughly 8 months in high temperatures between 40-50^{0}C which led to a more rapid wear process. The surface characteristics and the differences in the wear modes of the brake pads showed that high sliding and abrasion wear deformed the disk pad surfaces leading to form third body layers, friction layers and friction films that determined the friction behavior of the automotive brakes. Although sliding wear occurred in shoe pads, the wear mechanism more evident was the formation of fatigue cracks due to impact actions with the drum[22].

2.5. Wear of brake materials

Research by authors [25, 26, 27, 28]found that the friction and wear behaviors of brake friction materials are mainly affected by various factors like **1).** Material characteristics: physical, chemical, and mechanical properties of friction materials. **2).** Braking conditions: braking pressure, initial braking speed, braking times, temperature rise in braking. **3).** surrounding conditions: surrounding temperature, humidity, airflow. **3).** Surface conditions: surface roughness, contact property. **4).** Structural parameters: shape, size, and contact modality of brake pair**.**

Braking condition is one of the most important external factors. Existing researches are mainly focused on these influential factors such as temperature, braking pressure, and initial braking speed as they have most obvious influences on the friction and wear performance of friction materials [28]**.** According to Thuresson[6]**,** conditions such as pressure and temperature are affected by geometry as well as by material properties and boundary conditions in sliding contact. Author[28] observed that the friction coefficient was low while the wear rate increased rapidly under high temperature, braking pressure, or initial braking speed.

Kukutschová. et al. [29] reported that the wear of the brake lining depends on sliding speed, applied pressure and temperature. In their work, they found that the wear debris formed a friction layer on surface of brake lining.

2.5.1. Influence of material properties on wearresistance

Authors [30] investigated the suitable hybrid composite materialwhich is lighter than cast iron and with good Young'smodulus, Yield strength and density properties.Aluminum base metal matrix composite and HighStrength Glass Fiber composites have a promisingfriction and wear behavior as a Disk brake rotor. Thetransient thermo elastic analysis of Disc brakes inrepeated brake applications was performed andthe results were compared. The suitable material forthe braking operation was S2 glass fiber and all thevalues obtained from the analysis were less than theirallowable values.

2.5.2. Effect of surface behaviour on wear

Ghosh [31] investigated the change in the roughness parameters and their effect on wear rate. In their work, they applied a linear elastic material model and the contact parameters were calculated using the Hertzian contact theory. Material removal was simulated by a simple truncation model and Archard's wear law is used at asperity level to evaluate wear depth. It was also predicted that surfaces with high roughness, exhibit higher wear rates.

2.5.3. Influence of temperature on friction and wear resistance

Nearly all the energy dissipated by friction appears as heat and, at all but the slowest speeds of sliding, the temperature within the rubbing bodies raises appreciably[32], the temperature rise affects the frictionand wear. Surface temperature is less than that of asperities, which then leads to the formation of local high-temperature zones. Friction and wear mechanisms alter under different temperatures. At low temperatures, the hard asperities, small debris, and piece shape particles exist on the contact interface. The hard asperities may be embedded in a softer matrix, which results in plastic flowing and plowing called furrow effect [33].With increasing braking pressure and initial braking speed, the friction temperature increases. The wear rate then increases with the increasing temperature and the wear of friction material is more serious at a higher temperature.These temperatures obviously exercise a considerable influence on friction and wear and an estimate of their magnitude is often required [32].

Adamowicz[5]investigated the temperature fields of the solid disc brake during short, emergency braking. In their work, transient thermal analysis of disc brakes in single brake application was performed. A two-dimensional model was used to obtain the numerical simulation parabolic heat conduction equation. The results show that both

evolution of rotating speed of disc and contact pressure with specific material properties intensely effect disc brake temperature fields in the domain of time.

Thuresson[6]did work to investigate the effects of material properties and geometry on pressure and temperature. A continuum thermo mechanical model was used to calculate the interface pressure and temperature that incorporated temperature dependent variables like friction and wear. The model was discretized with finite elements. Design parameters such as the coefficient of friction, and specific heat that were found to have the most significant effect on contact temperature while the pressure was most affected by thermal expansion and the coefficient of wear. The thermal aspects of a friction couple were found to be a restricting factor for the braking capabilities of a system with a thermo elastic instability (TEI) phenomenon as the driving force for excessive pressure and temperature. TEI in friction material appears as slowly moving contact points and the cause being an interaction between wear and thermal expansion[6].

Olshevskiy et al.[34] did work to identify the thermo mechanical factors to be considered in simulation of the braking process, calculation of the distribution of the contact pressure, and temperature and obtain wear patterns for the disc brake system in operation. They reported that the displacements due to thermal deformation affected the distribution of the contact pressures significantly. The contact pressures, in turn, defined the temperature distribution at the surface of the brake block and the brake disc. The wear at the surface was not uniform and depended on the nominal contact pressures and temperature distribution.

Due to relative sliding between a brake pad and disc, wear occurs which affects the behaviour of disc-pad system over time and since the pad material is softer as compared to the brake disc, the wear of the pad is dominant [35]. Higher temperature of the pad surface during braking also affects life of the pad negatively due to increased wear rate[36].Authors [36] dis work on thermomechanicalsimulation of wear and hot bands in a disc brake by adopting an eulerian approach. The results showed that when wear is considered, different distributions of the temperature on disc are obtained for each new brake cycle [36]. This implies that temperature distribution has an implication on wear and therefore an estimate of their magnitude is often required [32].

2.5.4. Influence of braking pressure on friction and wear resistance

Wear has an important effect on the contact conditions. The time evolution of the contact pressure, is an interaction between thermal expansion and wear, where thermal expansion tends to reduce the contact area, and wear increases the contact area[6].The braking pressure affects the friction and wear through the size and deformation of contact area[37]. The number and size of the contact point increases with the increasing braking pressure[27]**.** In addition, more heat generates under a higher braking pressure, which undermines the material structure thus increasing the oxidation wear of the friction material[38].

Authors in[39] did work on mathematical modelling & analysis of brake pad for wear characteristics. In this work, they found that robust braking results in heat generation whose effects may have considerable impact on wear rate and coefficient of friction. However, this was carried out for cars and not for trains yet the conditions are different and needed to be given keen interest and is of paramount value.

Abubakar [40] studied the contact pressure distribution of a solid disc brake as a result of structural modifications. In his work different models were investigated and found that the contact pressure distributions obtained from these four models were different. Sliding frictional contact was analyzed to obtain the interface pressure distributions. His work is helpful to design engineers to obtain a more uniform pressure distribution consequently satisfying customers' needs by making pad life longer.

2.5.5. Wear analysis

Any components in relative motion are subject to surface contact due to loading and additional thermal effect on the contact bodies. The applied loads and relative motion result in high stresses and deformation on the contact surfaces which result in failure due to wear. Wear analysis is mostly performed by experimental procedure in order to analyze the component loss of material with time before and after application of forces. Software simulation of wear analysis is performed by many researchers with FEM simulation method being the commonest for analyzing wear model using ANSYS.

2.6. Analytical Expression for wear model

2.6.1. Linear wear model

Various wear laws are established from experimental results but the most commonly used model for prediction of wear in sliding contacts is the linear wear law proposed by Archard [41]that states that the wear rate is proportional to the normal force. Using Archard's wear model, the abrasive wear of the material can be predicted.A popular generalization of Archard's wear law is based on the assumption that the wear rate at any point on the contact surface is proportional to the applied contact pressure and the relative sliding velocity v according to;

$$\Delta\dot{h} = \frac{\Delta h}{t} = \frac{k}{H} pv, \tag{1.1}$$

where Δh is the wear displacement, t is the sliding time, k is the wear coefficient, H is the hardness of tested material, p is the applied contact pressure and v is the sliding velocity.

For brake systems, Rhee used a modified Archard wear model [42]. In this way, material characteristics are applied to the model.

$$\Delta W = kF^a v^b t^c. \tag{1.2}$$

W is the wear depth and v is the sliding velocity. P, H and k are the normal pressure, the hardness and the wear coefficient, respectively. a, b and c are the wear constants, t is the sliding time. k is the wear rate coefficient obtained from experiments and a, b and c are the set of parameters that are specific to the friction material and the environmental conditions. Rhee stated that a, b and c could be unity in a special case.

Hohmann et al.[43] developed their own wear law based on experimental data. They suggested that the wear displacement of friction material was a function of pressure, temperature, sliding time and apparent contact area A, they computed wear displacement using a 2-dimensional FE model and reported that the predicted results were close to experimental ones. Since there are a number of wear laws available in the literature, it is possible to select one of them and simulate it numerically [43]. Generally, wear process is typically evaluated in terms of its wear rate, weight loss, volume loss, and thickness reduction[44].

2.7. Contact Mechanics

Surfaces are usually rough (have asperities on them) so contact between them can only occur at a limited number of points causing the pressure on those points to be very high. Assumptions can be made about the nature of asperities to establish the area of contact. The point of doing so is to develop the basis for discussions on real area of contact and temperature rise on sliding surfaces. These quantities were prominent in early research and in the development of models for friction and wear[45].

Contact mechanics provides information for safe and energy efficient design of tribology and indentation hardness. The theory of contact mechanics is concerned with the stress and deformations which arise when the surfaces of two solid bodies are brought into contact. There are two types of contact namely; conforming contact when the two surfaces fit exactly or closely together without deformation and non- conforming contact where the surface or one of the two surfaces, deform when there is a contact area in between them. The central aspect of contact mechanics are the pressure and adhesion acting perpendicular to the contacting bodies' surfaces, the normal direction, and the frictional stress acting tangentially between the surfaces. However, this study mainly focuses on normal direction with a friction contact.

Hendric Hertz was the first researcher to introduce the contact stress, he approached the problem by means of theoretical or numerical solutions based on the Hertz's theory Contact mechanics has been applied in railway mainly on wheel and rail contact pantograph and overhead line contact wire which both are in relative motion contact principle[24]. The basic assumptions in Hertzian theory include;

i. The radii of curvature of the contacting bodies are large compared with the radius of the circle of contact
ii. The contacting bodies are in frictionless contact
iii. The dimension of each body is large compared to the radius of the circle of contact
iv. The surfaces in contact are continuous and nonconforming

There are different phenomena between hertz contact theory and FEM based contact. Hertz contact theory has some significant limitations whereas FEM has no assumption and obtains more accurate results. In addition, computing technology has developed more calculation time decline gradually. In this research we use FEM to obtain more accurate results and predict more accurate wear rate on brake disc-pad contact.

2.8. Finite Element Analysis of brakes

The finite element method is an effective tool to obtain the numerical solution of wide range of engineering problems and for verification of analytical contributions.FEM analysis is a robust tool to investigate the wear characteristics of materials, as can provide additional analytical tools beside results obtained from experiments, such as parametric studies [11].The method is generally sufficient to handle any complex shapes or geometries, for any material under different boundary and loading conditions. The generality of the finite element method fits the analysis requirement of present day's complex engineering systems and designs where solutions of governing equilibrium equations are usually not available. It is also an efficient design tool by which designers can perform parametric design studies by considering various design cases, (different shapes & materials) and analyze them to choose the optimum design [46]. The results of numerical simulations for the finite element models can be used in optimizing the disc brake design in order to reduce wear and could be used by the manufacturer for improving efficiency and lifespan of the braking system [34].

In Hohmann et. al.'s work [43], FEM was applied to drum brakes and disc brakes to calculate the distribution of contact forces between the brake pad and counter disc. The temperature distribution was predicted for railway disc brakes by decoupled structural-thermal finite element analyses [47]**.**

Authors in[9] cited that in order to predict wear and eventually the life-span of complex mechanical systems, a finite element (FE) post-processor was the optimum choice, considering the computational expense. They studied the performance of brake for different material on wear and contact pressure.Authorsin[9, 8, 39]all worked on simulation of wear and contact pressure using FEM.Authors in [39] and[8]used ANSYS software package to verify a mathematical model for the disc brake for analysis of wear designed to study the effect of parameters like braking energy, braking power, contact pressure and actuating force on the wear of disc brake whereas the wear simulation approach of authors [9, 8] performed a based on Archard's wear law.

Hegadekatte et. alimplemented their simulation in an FE post-processor that works in association with ABAQUS, to perform a Finite element-based simulation of dry sliding wear. The wear on the interacting surfaces was computed using contact pressure distribution from a two-dimensional or three-dimensional simulation[9]**.** Author [8] they

used general purpose finite element analysis to predict wear of the pad-to-rotor interface using three-dimensional finite element model of the brake pad and the rotor to calculate the pressure distribution in the contact. In their wear routine only wear of the brake pad was simulated and recommended that simulation routine be expanded to consider wear at both contact surfaces hence thefocus of this research.

CHAPTER 3 METHODOLOGY

3.1. Data Collection

3.1.1. Case Study: Addis Ababa Light Rail Transit

Addis Ababa Light Rail Transit (AALRT) Project consists of E-W & N-S lines, with the total length of main line 34.25 km (North-South line 16.9 km and East-West line 17.35 km). 31.025km. The two lines (North-South and East-West lines) use common track of about 2.7 km, The ground line mode is mostly applied in rail laying, while elevated line and underground line are also applied in some sections.

The entire line has 39 stations, consisting of 9 elevated stations (including 5 in the section that uses the same rail, 1 on E-W line, and 3 on S-N line), 2 underground stations, 1 semi-underground, and Ground stations are designed on ground line section, including 27 ground stations along the line (13 ground stations on N-S line, and 14 ground stations on E-W line).

The east-west line phase I project starts from Ayat and ends at Torhailoch. The total length is 17.4km. There are 22 stations, among which 5 are elevated stations, 1 underground station and 16 ground stations. The depot is located at the west ends of the project.

The south-north line phase I project starts from Menelik II Square and ends at Kaliti. The total length is 16.97km. There are 22 stations, among which 9 are elevated stations（5 common stations at the common line, 2 underground station and 11 ground stations. The depot locates at the south end of the project.

For this research, the East West line was considered as the reference. The slope was calculated using Equation 3.0 and the results for the different stations documented in Table 3.1 while Table 3.2. shows the station symbols as well as the distances between consecutive stations.

3.1.2. AALRT E-W route gradient

$$\text{Slope} = \frac{\text{Elevation Distance}}{\text{Horisontal Distance}} \qquad (3.0)$$

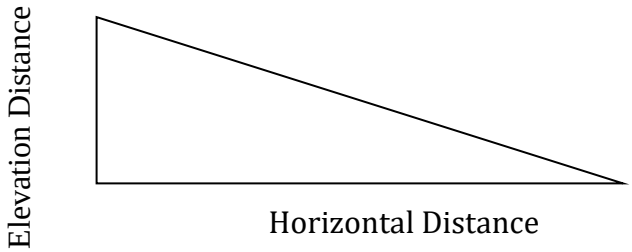

Table 3.1: Addis Ababa light rail transit east- west rail profile gradient.

No	Station name	Gradient/slope	Station types
1	Ayat 2	0.01580 [0.905°]	Ground station [- down]
2	Ayat 1	0.0143[0.818°]	Ground station [level]
3	Meri/CMC 2	0.0160[0.917°]	Ground station [level]
4	CMC 1	0.0483[2.767°]	Ground station [+ up]
6	Civil Service College	0.0178[1.019°]	Ground station [- down]
7	SahliteMhiret Church	0.0138[0.79°]	Ground station [- down]
8	GurdSholla	0.0022[0.127°]	Ground station [- down]
9	Megenagna/Adwa square	0.018[1.031°]	Underground station [+ up]
10	Lem Hotel	0.0063[0.358°]	Ground Station [- down]
11	Mazoria/Traffic Police HQ.	0.0086[0.491°]	Ground Station [Level]
12	Chemical Corporation	0.0253[1.247°]	Elevated station [+ up]
13	Urael Church	0.0243[1.394°]	Ground Station Level]
14	Yordanose Hotel	0.0148[0.849°]	Ground Station [- down]
15	Estifanose/Meskel Square2	0.0027[0.155°]	Ground Station [- down]
16	Stadium/Meskel Square 1	0.0o0016[0.093°]	Elevated station[Level]
17	La Gare	0.008[0.458°]	Elevated station [+ up]
18	Road Authority	0.0018[0.102°]	Ground station [- down]
19	Mexico Square	0.0278[1.591°]	Elevated station [+ up]
20	Lideta	0.0392[1.247°]	Elevated station [- down]
21	Coca Cola	0.0227[1.302°]	Ground station [Level]
22	Tor Hailoch	0.0088[0.504°]	Ground station [- down]

[Source: Addis Ababa (E-W and N-S) route light rail transit project from ERC]

Table 3.2: Seating capacity of the train[48]

Number of passengers (persons)	**Seated (number)**	**Standing (number)**	**Total**
Seats (AW1)	65	**0**	65
Seating capacity (AW2) (standing: 6 persons/m2)	65	189	254
Overload capacity (AW_3)(standing: 8 persons/m^2)	65	252	317

Table 3.3 Weights of the train[48]

Loads	**Car body weight (t)**	**Passenger weight (t)**	**Total weight (t)**
Empty vehicle (t)	44	0	44
Seating capacity (t)	44	15.24	59.24
Overload capacity (t)	44	19.02	63.02
Axle load	≤11（1+3%）t		

Note: Take 60kg as average weight of each passenger.

The data collected from AALRT is captured in Tables 3.3, 3.4 and 3.5 and adopted for use in the analysis. The overload condition is considered for this research thus a maximum load of 63.02t is used for the analysis.

Table 3.4 Vehicle properties

Number of axles per vehicle	4
Number of discs per axle	2
Start speed- V_0 [m/s]	19.44
Mass of the vehicle-M [Kg]	63020
Maximal load per axle [Kg]	11000
Deceleration-a [m/s^2] Service brake =	1.1
Braking time - t_b [s] Service brake =	17.68
Radius of the wheel - r_w [m]	0.33

A speed of !9.44m/s (70km/hr) which is the design speed is adopted for this analysis in order to assess the wear at the maximum speed although a lower speed is adopted for the AALRT. This is due to the fact that the effect of high temperature is significant at the

highest speed and the necessary brake forces required to bring the vehicle to a stop are higher hence the involved contact pressures.

3.1.3. Materials used

The materials used will be grey cast iron for the brake disc whereas the materials for the sintered organic brake padare shown in Table 3.6.

Table 3.5 Material Properties used for brake pad[49] and brake disc

Material Properties	Brake Pad	Brake disc
Thermalconductivity,k[W/m^{0}C]	5	52
Density, ρ [kg/m^3]	1400	7200
Specific heat, C [J/Kg ^{0}C]	1000	447
Poisson's ratio, v	0.25	0.28
Thermal expansion, α [10^{-6}/C]	0.1	0.11
Elastic modulus, E [GPa]	1	110
Mass [kg]	1.2	25

Table 3.6:Geometric properties of the brake disc and pad

Item	Brake disc	Brake pad
Inner radius, [mm]	120	120
Outer radius, [mm]	180	180
Thickness, [mm]	60	10
Effective radius of the disc brake-r_{disc} [m]	0.145	
Surface disc swept area by the pad , A_d[m^2]	0.1608	
Brake pad surface Area [cm^2]	120	
Friction coefficient disc/pad-μ	0.35	

3.1.4. Methodology flow chart

The methodology adopted for this research is summarized in the flow chart in Figure 4.

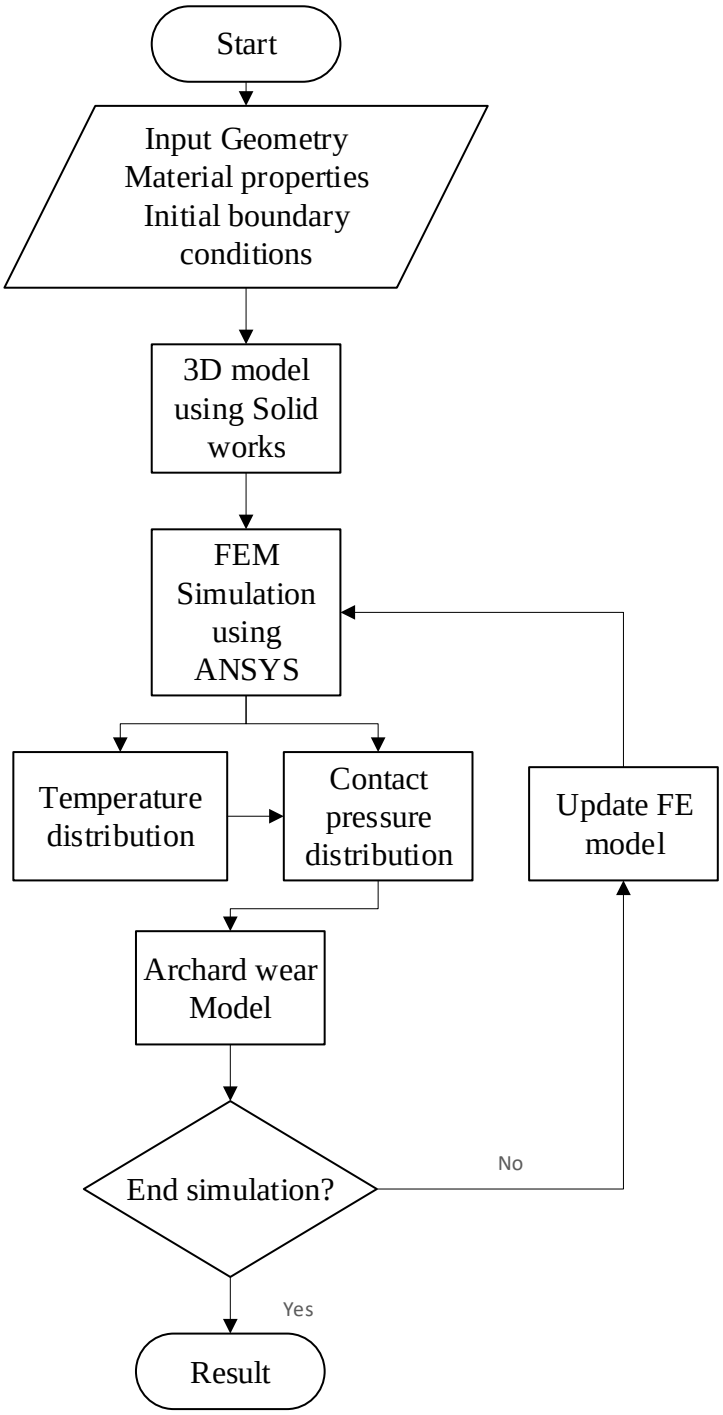

Figure 5 Methodology flow chart

CHAPTER 4 MATHEMATICAL MODEL

4.1. Thermo-mechanical Analysis

4.1.1. Thermal Transient analysis of the brakingsystem

During braking, a thermal analysis that describes the heat transfer and heat generation by friction pad-disc contact, through the disc and pads as well as the heat loss due to cooling effect of the surrounding air by convection is essential to defining the model.

The governing equations for 3-dimensional heat conduction equation under transient conditions for an isotropic material with internal heat generationare as follows: -

$$k_x \frac{d^2T}{dx^2} + k_y \frac{d^2T}{dy^2} + k_z \frac{d^2T}{dz^2} + Q = \rho C_p \frac{dT}{dt}, \quad (3.1)$$

where k_x, k_y and k_z are thermal conductivity in x, y and z-directions, respectively, C_p isthe specific heat, ρ is the specific mass, Q is internal heat generation rate per unit volumeand T is the temperature that varies with position as well as time t.

According to Fourier's law of heat conduction, heat conduction in any direction within the material is given by Equation (3.2): -

$$q = -kA\frac{dT}{dx}. \quad (3.2)$$

Material properties such as thermal conductivity, specific heat and density are required for a transient thermal analysis. A material having the same properties when measured in different directions can be termed as an isotropic material.

The boundary conditions can be quantified by the heat flux entering the model and dissipated by convection or radiation. The heat transfer rate of convection for the braking system dominates the cooling process specified by Newtons law of cooling in Equation (3.3);

$$q_s = -kh(T_s - T_\infty) \text{ where } T_s = T_1(x, y, z), \quad (3.3)$$

where h is the convective surface heat transfer coefficient, T_1 is the specified surface temperature; q_s the specified surface heatflux (positive into a surface); T_s the unknown surface temperature, and T_∞ the convective exchange temperature.

The ANSYS thermal transient simulation will follow using the following equation (3.4) for the FE formulation,

$$[C]\{\frac{dT}{dx}\} + [K]\{T\} = \{\dot{Q}\}. \quad (3.4)$$

Heat transfer by radiation can be neglected as it amounts only to 5 % to 10 % therefore heat transfer due to radiation was neglected for this work.

4.1.2. Braking time and angular velocity

Braking force is the force requiredat the brake disc-pad interface to bring the train to a stop.A train running with initial velocity V_0 is supposed to standstill with constant deceleration (a) and its linear translational velocity as function of time (t) is given by:

$$V(t) = V_0 - at\,. \tag{3.6}$$

The angular velocity (ω) of the wheel is given by;

$$\omega(t) = \frac{v(t)}{r_w}, \tag{3.7}$$

$$\omega_0 = \frac{v_0}{r_w}, \tag{3.8}$$

wherev = velocity of the locomotive, v_0= Initial running velocity of the locomotive, ω_0= Initial angular velocity the wheel, ω = angular velocity of the wheel andr_w= the radius of the wheel.

In brake application, the braking force acts at the effective radius (r_d) of the brake disc. The translational velocity (v_d) of this frictional force expressed in terms of thetranslational velocity v (t) is given as;

$$v_d = \frac{r_d}{r_w} v(t). \tag{3.9}$$

The total braking time and distance can also be obtained from;

$$S_b = v_0 t_b - \frac{1}{2} a t_b^2, \tag{3.10}$$

$$t_b = \frac{v_0}{a} \tag{3.11}$$

where, a is the deceleration. Angular velocity (ω) at time (t) is determined from:

$$\omega = \omega_0 \left(1 - \frac{t}{t_b}\right), \tag{3.12}$$

where,t_b = brake time to stop, S_b = Brake distance

4.1.2.1. Heat flux in brake disc-pad

A time-varying heat flux is applied to the model to simulate the action of the brake pad on the disc. The procedure for determining heat flux is as follows;

Braking energy

$$E_b = \frac{1}{2}MV_0^2 + \frac{1}{2}I\omega^2, \tag{3.13}$$

where; $\frac{1}{2}MV_0^2$ is energy due to kinetic energy of the vehicle and $\frac{1}{2}I\omega^2$ is energy due rotational kinetic energy of rotating parts where I is the rotational inertia while ω is the angular velocity.

From$V_0 = \omega R$, we have

$$E_b = \frac{M}{2} + \frac{1}{R^2M}V_0^2 = \left(\frac{kMV_0^2}{2}\right), \tag{3.14}$$

where, k (correction factor for rotating parts) is estimated to be about 1.1.

$$E_b = \left(\frac{kMV_0^2}{2}\right). \tag{3.15}$$

Heat Energy

During braking, the mechanical energy is transformed into heat energy. This energy is characterized by a total heating of the disc and the pads during braking.

Braking power

Braking power (P_b) is braking energy per unit time therefore;

$$P_b = \frac{E_b}{t_b}, \tag{3.16}$$

$$P_b = \frac{kMV_0^2}{2t_b}. \tag{3.17}$$

Heat flux, $Q(t)$is obtained by dividing the braking power by the swept area of the brake disc.

$$Q(t) = \frac{kMV_0^2}{2A_d t_b}. \tag{3.18}$$

Heat flux is the averaged heat flux generated during braking. The kinetic energy of the vehicle is transformed into heat that is mainly absorbed by the disc and the brake pad[7]. The proportion of heat entering the brake disc or pad is λ. According to [50], at the end of braking, the higher portion of heat generation(approximately 90.88%) at the disc and pad contact surface is absorbed by the disk. Therefore,λ is estimated to be about 0.90 for the brake disc and the remaining 0.1 for the pad[51]. Therefore, the heat flux function from equation 3.18is be modified to be:

$$Q(t) = \lambda\frac{kMV_0^2}{2A_d t_b}. \tag{3.19}$$

4.1.2.2. Braking on a straight Track

Only kinetic energy of the vehicle and rotational kinetic energy of the rotating parts are considered when braking on a flat surface because the gradient of the train is zero hence potential energy is neglected. Due to this kinetic energy, heat is developed between brake disc rotor and pad due to friction.

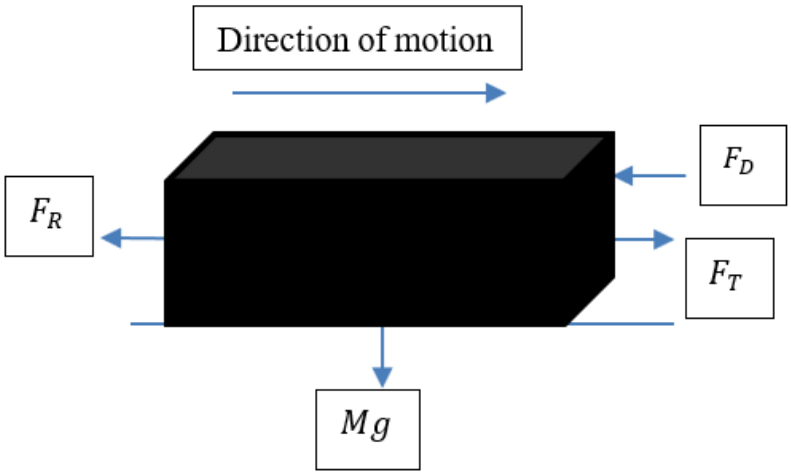

Figure 4.1 : Braking on a straight track

From Newton's second law of motion, for a vehicle is moving along a straight track;

$$Ma_t = F_T - F_D - F_R \quad (3.20)$$

where, M=Total mass of the vehicle including passenger weight, F_T=Tractive force, F_D=Drag force,F_R= Rolling Resistance force. Thus, the heat flux generated isgiven in the aforementioned equation (3.19).

4.1.2.3. Braking on inclined track

The train has both kinetic energy and potential energy due to its motion and its inclination or gradient owing to the alignment of the rail track as a result of different features such as gradient and curves thus increasing the heat energy dissipation from the contact surface to the surrounding.

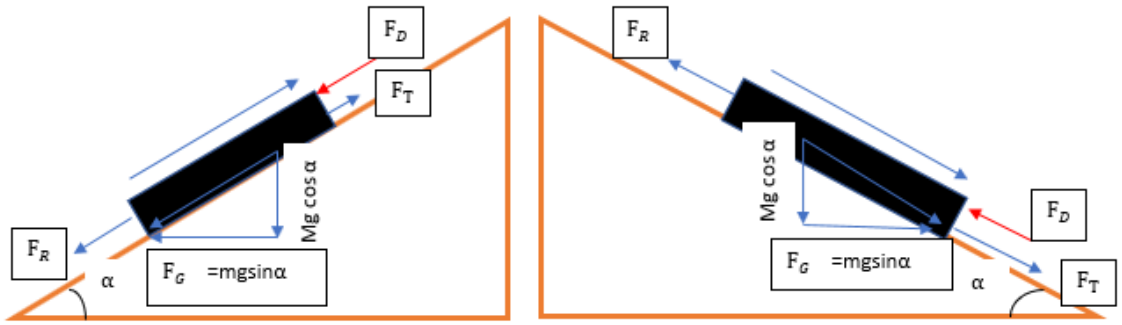

Figure 4.2: Motion on an inclined track

From Newton's second law of motion, for a vehicle moving on an inclined track;

$$Ma_t = F_T - F_D - F_G - F_R(\text{Up hill}), \tag{3.21}$$

$$Ma_t = F_T + F_G - F_D - F_R(\text{down hill}), \tag{3.22}$$

where, F_G= Total weight component in the direction of the inclined plane. For a vehicle moving on an inclined track, the heat flux is expressed as;

$$Q(t) = \lambda\left[\frac{kMV_0^2}{2A_d t_b} \pm \frac{S_b Mg\sin\alpha}{At_b}\right], \tag{3.23}$$

Where, S_b is the braking distance of the vehicle which is $S_b = \frac{V_0^2}{2a}$. Substituting S_b in to Equation (3.23) gives;

$$Q(t) = \lambda\left[\frac{kMV_0^2}{2A_d t_b} \pm \frac{V_0^2 Mg\sin\alpha}{2aAt_b}\right], \tag{3.24}$$

Thus,

$$Q(t) = \lambda\frac{MV_0^2}{2A_d t_b}\left[k - \frac{g\sin\alpha}{a}\right](\text{Up hill}), \tag{3.25}$$

$$Q(t) = \lambda\frac{MV_0^2}{2A_d t_b}\left[k + \frac{g\sin\alpha}{a}\right] \quad (\text{down hill}). \tag{3.26}$$

4.1.2.4. Calculation of braking force [F_B]

$$E_b = \frac{1}{2}kMV_0^2 + MgS_b\sin\alpha, \tag{3.27}$$

$$\text{But } S_b = \frac{V_0^2}{2a}$$

Substituting S_b in to Equation (3.27) gives;

$$E_b = \frac{1}{2}kMV_0^2 + \frac{V_0^2}{2a}Mg\sin\alpha. \tag{3.28}$$

Power dissipated by the brake disc face$P(t)$ is equal to the heat flux $E_b$in the brake disc face;

$$E_b = P(t)dt = 2F_{disc}V_{disc}(t)dt, \tag{3.29}$$

$$\frac{1}{2}kMV_0^2 + \frac{V_0^2}{2a}Mg\sin\alpha = P(t)dt = 2F_{disc}V_{disc}(t)dt, \tag{3.30}$$

where dt is change in time. But from;$V_{vehicle}(t) = V_0 - at_b$ where;

$$a = \frac{V_0}{t_b}, \tag{3.31}$$

$$\frac{V_{vehicle}(t)}{r_w} = \omega(t) = \frac{V_{disc}}{r_{disc}}, \tag{3.32}$$

$$V_{disc} = \frac{r_{disc}}{r_w}\left(V_0 - \frac{V_0}{t_b}\right), \tag{3.33}$$

where,$F_{disc}$is constant with respect to time, and V_{disc} varies only linearly with time so the energy balance equation becomes:

$$\frac{1}{2}kMV_0^2 + \frac{V_0^2}{2a}Mg\sin\alpha = 2F_{disc}V_{disc}(t)dt = 2F_{disc}\frac{r_{disc}}{r_w}\left(V_0t_b - \frac{1}{2}\frac{V_0}{t_b}t_b^2\right), \tag{3.34}$$

$$F_{disc} = \frac{\frac{1}{2}kMV_0^2 + \frac{V_0^2}{2a}Mg\sin\alpha}{2\frac{r_{disc}}{r_w}(V_0t_b - \frac{1}{2}\frac{V_0}{t_b}t_b^2)}. \tag{3.35}$$

4.1.2.5. Calculation of tractive force [F_T]

The force required to overcome the total running resistance at a given driving condition on the wheels is called the traction force of a vehicle. The motor power is transmitted to the wheels through power transmission unit, driveshaft and axle in a vehicle. The traction force on the wheel is proportional to the torque generated by the motor. The motor torque is expressed as;

$$T_m = \frac{P}{\omega}, \tag{3.36}$$

where, T_m= Motor Torque, P= Motor Power, ω= Angular Velocity of the motor

For AALRT, P=130KW and ω= 1800 r.p.m.[48], therefore;

$$T_m = \frac{130x10^3}{1800\ r.p.m} = \frac{130x10^3}{60\pi\ rad/s} = 689.67Nm.$$

The torque on the driven wheels, transmitted from themotor is given by;

$$T_w = T_m x\eta x\tau, \tag{3.37}$$

Where, T_w= Torque on the wheel, η=mechanical efficiency of transmission = 0.98[52] and τ= gear ratio of transmission = 7.43

$$T_w = 689.67x0.98x7.43\ ,$$
$$T_w = 5{,}021.77\text{Nm}.$$

The tractive force of train is therefore;

$$F_T = \frac{T_w}{r_w}, \tag{3.38}$$

Where r_w= Radius of the wheel, Diameter of wheel motor = 660mm

$$F_T = \frac{5021.77\text{Nm}}{330x10^{-3}\text{m}},$$
$$F_T = 15{,}217.48\text{N}.$$

Since there are 4 traction motors, the total traction motor becomes;

$$F_T = 15{,}217.48x4\ ,$$
$$F_T = 60{,}869.94\text{N}.$$

4.1.2.6. Calculation of drag force [F_D]

For a vehicle running on a rail track, relative air movement tends to occur opposite to the direction of motion of the vehicle. Due to this air flow, the vehicle experiences an aerodynamic force such as drag and lift on the body. The Aerodynamic drag force generated on the frontal and rear side of the body acts on the vehicle as a driving resistance. The aerodynamic drag force is expressed as follows:

$$F_D = \frac{1}{2}xC_DxρxAxV_D^2, \tag{3.39}$$

where, C_D= Coefficient of drag = 1.8, ρ= Density of air (1.2 Kg/m^3 for air at NTP), A= Projected frontal area of the vehicle, V_D= Design Velocity of the train = 80Km/hr

$$\text{A= Vehicle width} \times \text{vehicle height}, \tag{3.40}$$

The maximum width of the car body =2650mm and vehicle height=3700mm[48].

$$A = 2650\text{mm}x3700\text{mm} = 9{,}805{,}000\text{mm}^2,$$

$$A = 9.805\text{m}^2,$$

Therefore,

$$F_D = \frac{1}{2}x1.8x1.2x9.805x22.22^2$$
$$F_D = 5228.29\text{N}.$$

4.1.2.7. Calculation of rolling resistance force [F_R]

Rolling resistance refers to the force resisting the motion when a body (such as a wheel) rolls on a surface. It is mainly caused by non-elastic effects.

$$F_R = \mu_R x\, Mg\cos\alpha\,, \tag{3.41}$$

where, μ_R = 0.16, rolling coefficient of friction[48]. M = Total mass of the vehicle including passenger weight, g=acceleration due to gravity, α= gradient of the rail.

$$M = 63.02x\ 10^3 kg.$$

$$F_R = (0.16x\ 63.02x\ 10^3 x\ 9.81x\cos\alpha) = 98{,}916.19\cos\alpha.$$

4.1.2.8. Calculation of Gradient resistance force [F_G]

When a vehicle goes uphill or downhill, its weight produces a component, which is always directed to the downward direction. Thiscomponent either opposes the forward motion or helps the forward motion It experiences gravitational resistance due to its weight and it is called gradient resistance of the vehicle. This force can be expressed as:

$$F_G = Mg\sin\alpha\,, \tag{3.42}$$

$$F_G = 63.02x\ 10^3 x 9.81x\sin\alpha,$$

$$F_G = 618{,}226.2\sin\alpha.$$

4.1.2.9. Calculation of heat flux $Q(t)$

Considering motion of vehicle on an uphillinclined track as in the case for CMC 1. The heat flux generated when the vehicle moving on CMC 1 during braking is:

$$Q(t) = \lambda\frac{MV_0^2}{2A_d t_b}\left[k - \frac{g\sin\alpha}{a}\right],$$

where,a = deceleration of the vehicle, M= Total Mass of the vehicle 63,020kg, V_0= Initial velocity of the vehicle, t_b= braking time required to stop the vehicle, k= Correction factor of the rotating parts= 1.1, λ= Proportion of the heat entering the brake disc= 0.9, g= Acceleration due to gravity, A_d= Contact swept area.

$$A_d = 2\pi(r_o^2 - r_i^2), \tag{3.45}$$

where r_o= outer radius of the brake pad and r_i= inner radius of the brake pad

$r_o = 200$mm and r_i= 120mm

$$A_d = 2\pi(200^2 - 120^2),$$

$$A_d = 160849.54\ mm^2,$$

$$A_d = 0.1608\ m^2.$$

For service brake = $1.1 m/s^2$ and $t_b = 17.68$srefer to Table(3.5).

$$Q(t) = \lambda \frac{MV_0^2}{2A_d t_b}\left[k - \frac{g \sin \alpha}{a}\right],$$

$$t_b = \frac{V_0}{a} = \frac{19.44}{1.1} = 17.68s\ .$$

$$Q(t) = 0.9\frac{63020x19.44^2}{2x0.1608x17.68}\left[1.1 - \frac{9.81 \sin 2.767}{1.1}\right],$$

$$Q(t) = 2{,}523{,}784.63\ W/m^2.$$

The weight distribution of the vehicle considered is equally distributed between the front and rear bogie. The vehicle is equipped with eight mechanical disc brakes. Hence, only an 1/8 of the whole heat flux is applied to one disc from the forward part of the carriage.

$$Q(t)_{\text{eight disks}} = \frac{Q(t)}{8} = 315{,}473.08\ W/m^2.$$

But each disc brake consists of two pads; one pad on each surface of the rotor disc face. Then for the heat flux for one side of the brake pad is calculated as follows:

$$Q(t)_{\text{Sigle disk}} = \frac{Q(t)}{2} = 157{,}736.54\ W/m^2.$$

The same procedure is repeated to attain the percentage absorbed by the brake pad and the results are tabulated in Table 3-7.This heat flux is for one side of the disc brake and is input in to ANSYS workbench for each surface of the brake disc and pad,

Therefore,

The tabulated results in table 3-5 below are obtained from Equations (3.25) and (3.27) for uphill motionand downhill motionconsidering service braking. For stations with level gradient, Equation (3.19) is used to determine the heat flux.

4.1.3. Calculation of braking force

From Equation.3.36 the braking force on the discis;

$$F_{disc} = \frac{\frac{1}{2}(1.1)MV_0^2 + \frac{V_0^2}{2a}Mg \sin \alpha}{2\frac{r_{disc}}{r_w}(V_0 t_b - \frac{1}{2}\frac{V_0}{t_b}t_b^2)},$$

For service brake a = $1.1 m/s^2$, $t_b = 17.68s$

$$F_{disc} = \frac{\frac{1}{2}(1.1)x63020x19.44^2 + \frac{19.44^2}{2x1.1}x63020x9.81x\sin 2.767}{2\frac{0.145}{0.33}(19.44x17.68 - \frac{1}{2}\frac{19.44}{17.68}x17.68^2)},$$

$$F_{disc} = 127{,}886.62\ N.$$

The weight distribution of the vehicle considered is equally distributed between on the front and rear bogie. The vehicle is equipped with eight mechanical disc brakes. Hence,

only 1/8 of the whole brake force is applied to one disc from the forward part of the carriage.

$$F_{disc} = 15{,}985.83 \text{ N.}$$

4.1.4. Calculation of caliper pressure/ hydraulic pressure

The total rotor force applied to both the inboard and out board rotors can be used to calculate the caliper clamping force required to stop the vehicle. The magnitude of the clamping force is found using the columbic friction, μ =0.35[48]:

Service brake

$$F_{caliper} = \frac{F_{disc}}{\mu}, \tag{3.46}$$

$$F_{caliper} = 45{,}673.8 \text{ N.}$$

This force generates a clamping pressure over a contact area of A=0.1608m^2.This force generates a clamping pressure. Brake pads cover a 60^0angle along the brake disc. This results in a contact area of

$$A_d = 0.1608 \text{ m}^2,$$

$$\frac{60}{360} \text{x} 0.1608 = 0.0268.$$

Service brake

$$P = \frac{F_{caliper}}{A}, \tag{3.47}$$

$$P = \frac{45{,}673.8}{0.0268},$$

$$P = 1{,}704{,}246.269 \text{ N/m}^2.$$

4.1.5. Calculation of Centrifugal Load

$$F_c = m_d \omega^2 r_{disc}, \tag{3.48}$$

where,F_c = centrifugal force, m_d -mass of the brake disc = 25kg, ω- Angular velocity, r_{disc}-radius of the brake disc = 0.145

The angular velocity at any time t is:

$$\omega = \omega_0 \left(1 - \frac{t}{t_b}\right),$$

From Equation (3.8), $\omega_0 = \frac{v_0}{r_w} = \frac{19.44}{0.33}\pi = 185 \text{rad/s}.$

At t = 0, $F_c = 25\text{x}185^2\text{x}0.145$ = 124,065.63 N ,

$$F_c = 124{,}065.63 \text{ N}.$$

All the above calculated values are used throughout the finite element analysis as tabulated in Table 4.1. The heat flux and pressure values for the different stations are captured in Table 4.1 based on the corresponding gradients in Table 3.1.

Table 4.1 Heat flux and Pressure values for different stations

Stations	Q(t) Disc	Q(t) Pad	Pressure
Ayat 2	292,342.90	32,482.54	1,303,811.96
Ayat 1	235,610.77	26,178.97	1,289,589.72
Meri/CMC 2	235,610.77	26,178.97	1,305,773.65
CMC 1	157,787.92	17,531.99	1,608,200.75
St.Michael Church	297,950.23	33,105.58	1,328,823.50
Civil Service College	235,610.77	26,178.97	1,322,448.01
SahliteMhiret Church	288,128.08	32,014.23	1,285,012.44
GurdSholla	263,826.98	29,314.11	1,176,629.11
Megenagna/Adwa square	221,382.99	24,598.11	1,324,409.70
Lem Hotel	272,294.12	30,254.90	1,214,391.62
Mazoria/Traffic Police HQ.	235,610.77	26,178.97	1,236,133.68
Chemical Corporation	213,467.16	23,718.57	1,359,720.11
Urael Church	235,610.77	26,178.97	1,383,750.80
Yordanose Hotel	290290.48	32,254.50	1,294,657.41
Estifanose/Meskel Square2	264,853.31	29,428.15	1,181,206.38
Stadium/Meskel Square 1	235,610.77	26,178.97	1,171,070.99
La Gare	242,384.22	26,931.58	1,230,739.04
Road Authority	262,910.62	29,212.29	1,172,542.25
Mexico Square	200,861.85	22,317.98	1,415,955.20
Lideta	304,876.55	33,875.17	1,359,720.11
Coca Cola	235,610.77	26,178.97	1,368,711.18
Tor Hailoch	240,698.17	26,744.24	1,238,258.84

4.2. Wear Simulation

Any components in relative motion are subjected to surface contact due to loading and additional thermal effect on the contact bodies. The applied loads and relative motion result in high stresses and deformation on the contact surfaces which result in wear. Wear analysis is mostly performed experimentally to analyse the component loss of material with time before and after applying the required loads. Recently, FEM simulation of wear analysis isbecoming popular amongst many researchers[8, 9, 24].

4.2.1. Method of Wear Simulation

The following steps are followed to perform the wear simulation;

- Create the model geometry and mesh
- Identify the contact surfaces and material used for each part of model
- Define solution options
- Apply boundary conditions
- Solve the contact problem

4.2.1.1. Model Geometry

The assembly model contains abrake disc that rotates with predetermined velocity, a brake pad that stays stationary on a rotating disc and back plate for holding and applying force on the brake pad.

The followingassumptions are made to simulate wear analysis in ANSYS Workbench.

- A non-linear analysis is conducted.
- The assembly contact between pad and disc is adjust to touch option of ANSYS without any clearance.
- The contact behaviour of modelled elements is taken as asymmetric.
- The coefficient of friction between pad and disc bonded contact is taken as 0.35[48].
- The analysis is performed by assuming the deflections of modelled elements are small and neglected.

4.2.1.2. Designating Contact and target Surfaces

Contact elements are constrained against penetrating the target surface. However, target elements can penetrate through the contact surface. For rigid to flexible contact, the designation is, the target surface is rigid surface and contact surface is deformed surface.

For flexible to flexible contact, the choice of which surface is designated contact or target can cause a different amount of penetration and thus affect the solution accuracy. There are different guidelines when designating the surface, but in this thesis the condition considered is;

- If one surface is stiffer than the other, the softer surface should be the contact surface and the stiffer surface should be the target surface.
- If one surface is markedly larger than the outer surface, such as in the instance where one surface surrounds the other surface, the larger surface should be the target surface.

Therefore, according to above guidelines of contact pair is defined, the disc surface was considered the target and the pad the contact surface.

In defining contact behaviour of disc and pad for contact mechanics analysis the type of surface is added. In this thesis a frictional contact of μ 0.35 Table (3.5) was considered between disc and pad surface. The frictional force is calculated by the software to add into analysis system.

4.2.2. Wear of the brake disc and pad

Improving the endurance of machine elements subjected to friction requires using engineering methods of wear calculation that account for physical and mechanical properties of the contacting bodies, conditions of operation of the friction units (such as load and velocity), environmental conditions, and design features of the frictional junction[34].

4.2.2.1. Wear model

The most frequently used wear model in engineering is the linear Archard wear law. Therefore, it was used as the basis of wear modelling in this study. According to Archard,

$$Q = k\frac{WL}{H} = \frac{k}{H}pv, \tag{3.49}$$

where Q, k, W, L and H are wear volume, dimensionless wear coefficient, total normal load, sliding distance and hardness of the target contacting material, respectively. Diving both sides of equation is divided by “A” (area of contact), then,

$$\frac{V}{A} = k\frac{WL}{HA}, \tag{3.50}$$

$$h = \frac{k}{H}pL. \tag{3.51}$$

where, h and p, are wear depth and contact pressure, respectively.

Wear coefficient is an important parameter in Archard's wear law because it provides a contact betweenexperimental study and simulation. Therefore, the wear resistance of the pad surface corresponded to a wear coefficient with a value of 1×10^{-6} Pa^{-1} and a hardness value of 1MPa adopted from previous literature of experimental results[8]. FE analysis was performed in order to calculate the contact pressure and sliding distance then, the results and measured wear depth are used in equation (3.51) in order to calculate wear depth.

The Archard wear model was chosen based on its simplicity and its critical advantage over other models of wear is that values of 'K' can be determined experimentally, as a result it creates a link between the experimental result and theoretical simulation implying more accurate values.

CHAPTER 5 FINITE ELEMENT ANALYSIS

5.1. Available Software

5.1.1. ANSYS

ANSYS is general purpose finite element analysis (FEA) software package. Finite Element Analysis is a numerical method of deconstructing a complex system into elements. The software implements equations that govern the behaviour of these elements and solves them all and creating a comprehensive explanation of how the system acts as a whole. These results then can be presented in tabular or graphical forms.This type of analysis is typically used for the design and optimization of a system far too complex to analyse by hand.This study used the FEA software ANSYS16.0 and ANSYS 19.2 versions to carry out transient thermal analysis and the coupled thermo-mechanical stresses of a railway brake disc and pad for different stations.

5.1.2. General analysis procedure of ANSYS

Similar to solving problems analytically, definition of the solution domain, the physical model, the boundary conditions and the physical properties of the material used for the model is required.

Then solving the problem and present the results. In numerical methods, the main difference is an extra step called mesh generation is performed. This is the step that divides the complex model into small elements that become solvable in an otherwise too complex situation. Below describes the procedure that need to be followed to carry out thermal and mechanical analysis of brake disc model using ANSYS software.

5.1.2.1.Modeling in ANSYS CFX

In order to determine the convective heat transfer coefficient for the brake pad, the following procedure was followed during modelling in **ANSYS CFX.**

a) **Create/import the Geometry**: Select “Geometry” from the option tabs and select import geometry from the menu since the geometry was developed using Solid works SOFTWARE the file type ‘IGS’ is preferable for this action. Click generate for the geometry to appear. The geometry in Figure (4.1) was created in millimeters and then scaled to meters at the output step.

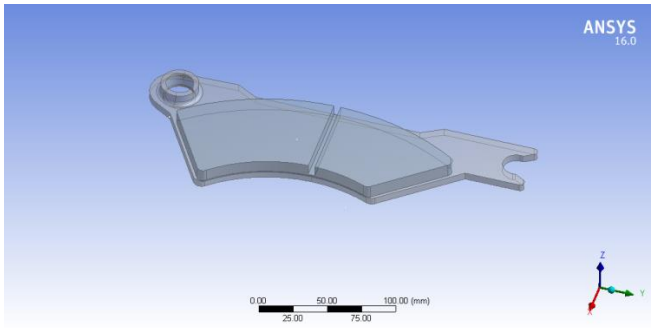

Figure 5.1: Brake pad Geometry

b) Meshing

For the preparation of the mesh of the model, one defines initially various surfaces of the brake pad in integrated computer engineering and manufacturing (ICEM) CFD what was used is a tetrahedral element with nodes and elements as shown in Tables (4.1)and (4.2). A fine mesh was used for accurate results.

c) Physical model

In this step, the physical characteristics of the fluid and the solid are declared. After the meshing is defined, all the parameters of the different models are input to be able to start the analysis.

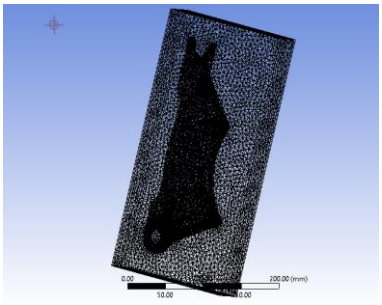

Figure 5.2: ICEM Mesh

Mesh Report

Table 5.1: Mesh Information for CFX

	Nodes	**Elements**
Air	34754	175851
Backplate	8523	38485
Brake Pad	2786	11508
All Domains	46063	225844

Table 5.2: Boundary conditions for CFX

Boundary	Boundary Conditions	Parameters
Inlet	Pressure Inlet	Atmospheric pressure and temperature
Outlet	Pressure Outlet	Atmospheric pressure and temperature
Pad surface	Wall	473K

d) Definition of the domains

Initially one valid the elaborated models and one activate in the option "thermal energy» the calculation of heat transfer «heat transfer" on the outline tree and the domains are loaded as shown in the table.

e) Definition of materials

The materials to be used are selected and for the materials not in the system, they are input manually. In this case steel was selected for the back-plate material and the parameters of the pad organic sintered material are input manually by inserting the thermal properties as captured in Table (3.6).

f) Definition of the boundary conditions &application of the interface domains

The first step is to select the inlet and outlet faces of the heat flux. These options are found in the insertion menu “boundary conditions” in the CFX Pre. The boundary conditions concerning the pads will be also defined. One selects the options “wall”, because there will be the possibility of adjusting a certain number of parameters in the boundary conditions such as flux entering the pad.

The areas of interfaces are commonly used to create the connection or linkage areas. Surfaceslocated between the interaction’s regions (air pad) are reported as solid-fluid interface. They are tabulated as follows;

g) Temporary Condition

Since in this study is to determine the temperature field in a brake pad during the braking phase, we take the following temporal conditions:

- Braking time= 16 [s]
- Increment time = 1 [s]
- Initial time = 0 [s]

Before starting the calculation and the analysis with ANSYS CFX PRE, it can be ensured that the model does not contain any error. The airflow through and around the brake pad was analyzed using the ANSYS CFX software package. The ANSYS-CFX solver automatically calculates heat transfer coefficient at the wall boundary.

Afterwards the heat transfer coefficients considering convection were calculated and organized in such a way, that they could be used as a boundary condition in thermal analysis. Averaged heat transfer coefficient had to be calculated for the brake pad using ANSYS CFX Post, the results and inputs for CFX are as shown in Appendix A, Table (6.1) and (6.2).

5.1.3. Wall heat transfer coefficient

The heat transfer coefficient is a parameter related to the air velocity, the brake disc/pad shape, and many other factors. For different air velocity, the heat transfer coefficient in different parts of the brake disc/pad changes with time. It depends on air flow in the region of brake rotor and on the train speed given that the brake pad is moving with the train speed, but it does not depend on the material. In our simulation, this coefficient is determined as an average value of the coefficient "Wall heat Transfer Coefficient" and variable with time[53].An average value of 94.91 $Wm^{-2}K^{-1}$was adopted for this analysis.

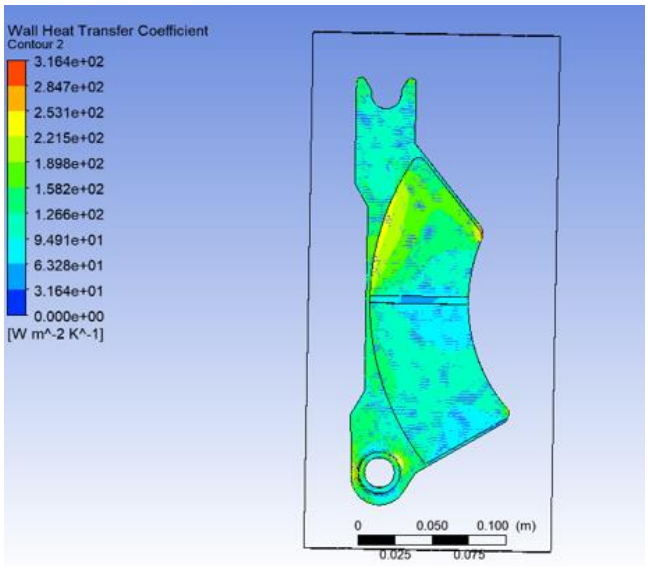

Figure 5.3: Convective heat transfer coefficient of the brake pad

5.1.4. Finite element (FE) model

The selected material of the disc is gray cast iron with high carbon content and the brake pad has an isotropic elastic behaviour whose mechanical characteristics are provided in

tableabove. ANSYS 19.2 (3D) is fully utilized to simulate temperature and contact pressure distribution as well as wear during braking application.

5.1.4.1.Modelling of brake disc and pad.

The 3D model was designed using Solid worksand imported in to ANSYS 2019 R1 Workbench. The model consists of disc and two pads as shown below in Figure 5.4.The model of the disc is incorporated in to the model although the research is about the brake pad so as to study the contact interface with the brake disc with minimal errors involved in neglecting it.

5.1.4.2.Mesh generation

The mesh within the default settings is not adequate enough to give accurate results. The deformable bodies of the subsystem are meshed with a characteristic mesh size of 5mm using general contact elements CONTA173 on the deformable friction material surface and a layer of target elements TARGE170 overlaying the brake disc surface.In this simulation, the meshing was refined in the contact zone (disc-pad) to get a finer mesh and continuous contact pressure (see Figure 5.4).

The greater the numbers of elements near the contact, the better the results will converge within appropriate bounds, Augmented Lagrange Contact formulation method is used in order to avert geometrical penetration over the iterations.

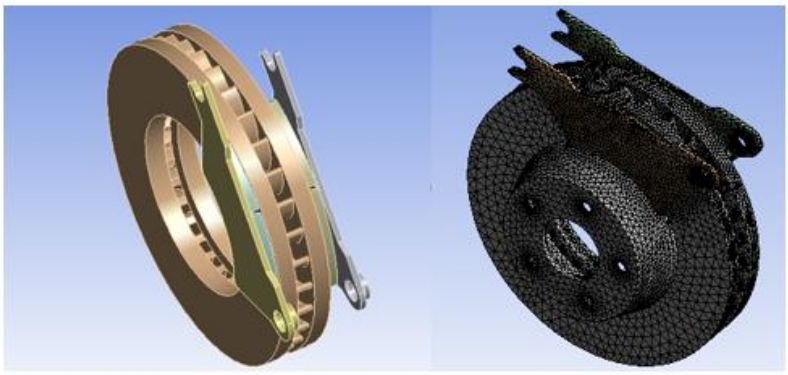

Figure 5.4: Left: Brake disc and Pad assembly Right: Meshed assembly

5.1.4.3.Defining the Contact Region

After importing the geometry from Solid works, the next step is to define the contact between disc and pad. ANSYS 2019 R1 automatically reads the attached geometry for any predefined contacts or other boundary definitions, however these contacts need to berevisited and the right conditions added. The pad-disc interface is modelled as an

asymmetric frictional contact between the top face of the disc and bottom face of the pad see Figure 4.5.

The interface treatment is changed to “Adjust to touch” which option defines the kind of contact between the selected bodies as shown in Figure (4.5) and the detection method is changed to Normal Projected Normal from Contact.

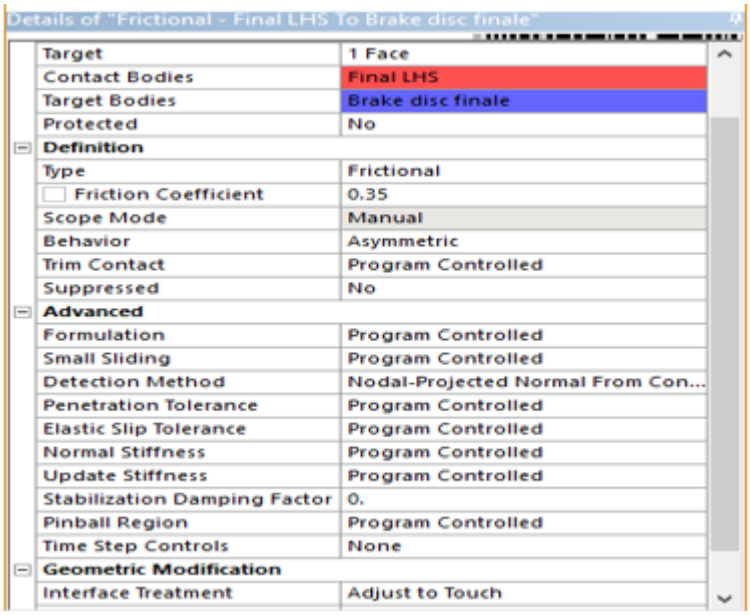

Figure 5.5: Contact Region options

During braking, a point on the brake pad is in constant contact with the brake disc, whereas a point on the brake disc experiences intermittent contact. Although both the brake disc and brake pad are worn, only wear of the brake pad will be considered, by assuming the brake disc has a much higher wear resistance.

5.1.4.4.Wear simulation

The Archard wear law was adopted for this analysis. Therefore, it was used as the basis of wear modelling in this study.

The ANSYS ACT Archard wear model adopted for this analysis makes use of the Archard Equation where$Q = \frac{kWL}{H}$,

where Q is the total volume of wear debris produced, k is a dimensionless constant, W is the total normal load, L is the sliding distance, H is the hardness of the softest contacting surfaces.

The volume of wear in ANSYS is calculated according to the formula:

$$\dot{\omega} = \frac{dh}{dt} = \frac{K}{H}.P^{m}V^{m}. \tag{4.10}$$

Wear thickness

$$(dh) = \left(\frac{K}{H}.P^{m}V^{m}\right)dt, \tag{4.20}$$

Where, K is wearing coefficient, H is material hardness, P is the contact pressure, V is the sliding velocity, m is Pressure exponent, n is Velocity exponent.

Wear on disc is neglected as the amount of wear on disc is negligible compared with wear on the brake pad and the inputs are as shown in Figure 4.6.

Details of "Archard Wear"

Select Component	
Type	Contact
Select Contact	Frictional - pad RHS To Brake disc final...
Definition	
Select LoadStep	All
Archard Wear Inputs	
Wear Coefficient, K	1E-06
Material Hardness, H	1000000 [Pa]
Pressure Exponent, m	1
Velocity Exponent, n	1
Advanced Control	
Use Average Data	Program Controlled
Data Type	Program Controlled
Direction Control	Program Controlled

Figure 5.6 ANSYS ACT Archard wear inputs

Volume loss due to wear results are determined from the ANSYS results and from this the wear thickness value can be determined by the following relation;

$$\text{Wear thickess} = \frac{\text{volume loss due to wear}}{\text{Brake pad surface Area}}. \tag{4.30}$$

CHAPTER 6 RESULTSANDDISCUSSION

6.1. Coupled Thermal –Mechanical Analysis

The purpose of this analysis was to predict the temperatures and the corresponding thermal stresses in the brake pad as well as to analyze the resulting contact pressure distribution. The disc brake system consists of a brake disc that rotates about the axis of a wheel, a caliper-piston assembly where the piston slides inside the caliper which is mounted to the vehicle suspension system and a pair of brake pads. When the hydraulic pressure is applied, the piston is pushed forward to press the inner pad against the disc and simultaneously the outer pad is pressed by the caliper against the disc

6.1.1. Boundary Conditions and Applied Loads

The thermal analysis will be carried out by choosing the transient state and by introducing the thermal expansion, thermal conductivity and the specific heat of the materials. The boundary conditions of friction heat flux and the convection coefficient from Figure 5.3 are applied according to Figure 6-1.

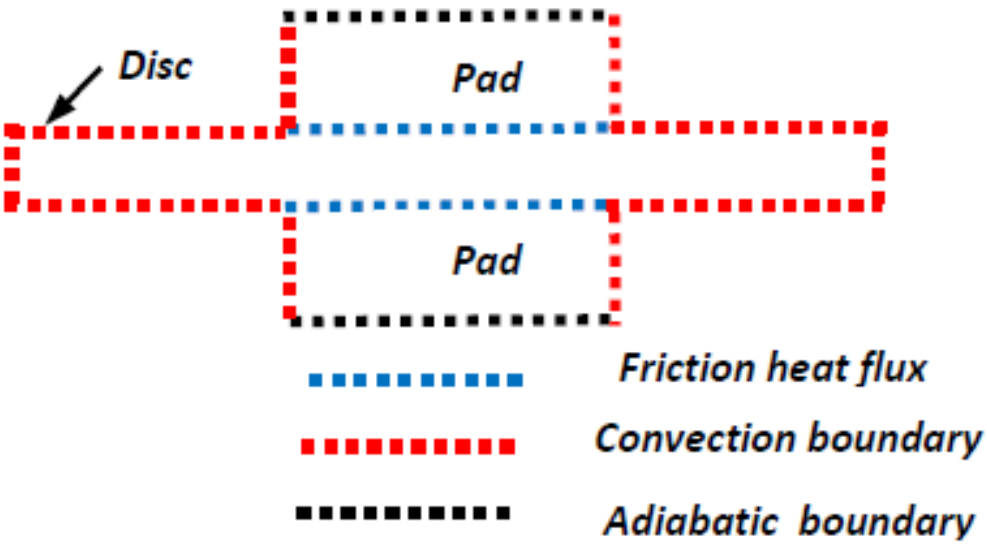

Figure 6.1: Boundary Conditions for transient thermal analysis[49]

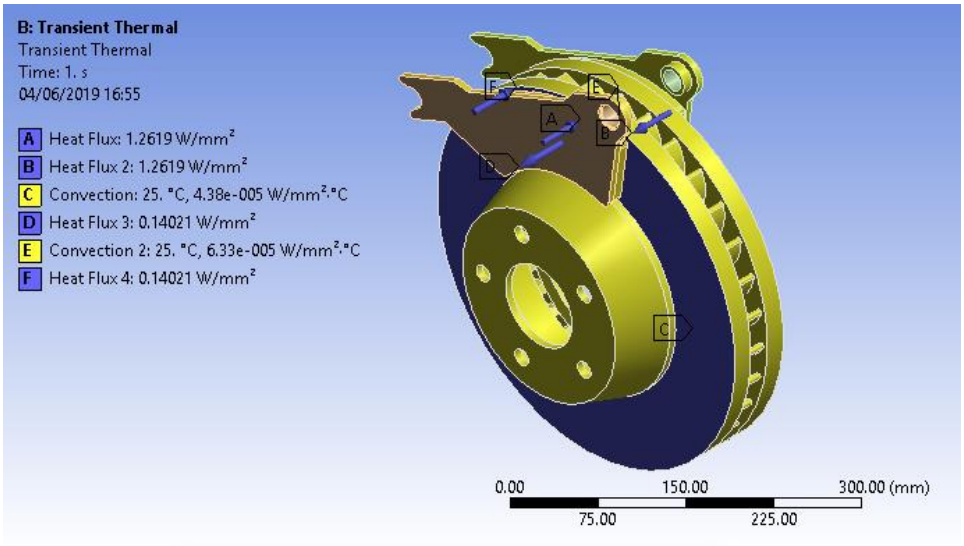

Figure 6.2ANSYS Boundary conditions Thermal Analysis

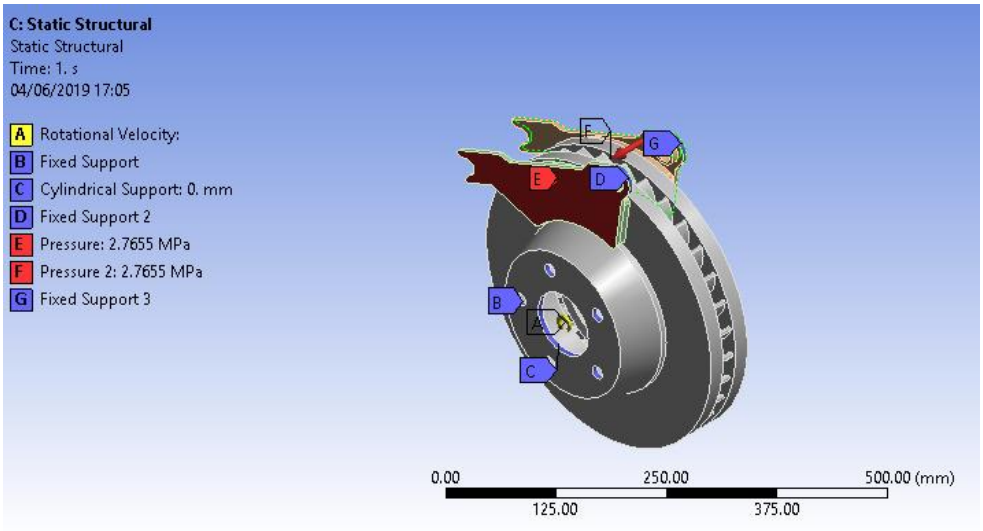

Figure 6.3 Boundary conditions Thermal-Structural Analysis

The structural conditions for the FE model consist of a fixed support, and a cylindrical support with the fixed support placed on the disc bolt holes except in its rotational direction, its angular velocity is constant ω=185 rad/s. The cylindrical support is placed in the model where the bearings would normally sit and constrain the assembly to rotation only.

The boundary conditions applied on the pads are defined according to the movements authorized by the caliper. The caliper retains the pads which have a tendency to follow the movement of the disc when the two structures are in contact. The caliper maintains also the pads in direction Z. Thus, the conditions imposed on the pads are: -

The pad is fixed at the abutment in all degrees of freedom except in the normal direction to allow the pads move up and down and in contact with the disc surface. The friction contact conditions are applied between the surfaces of the disc and pads. In this FE model, boundary conditions are imposed on the models (disc-pad) as shown in Figure 6-3 for applied pressure on both sides of the brake pads.

6.2. Temperature Distribution

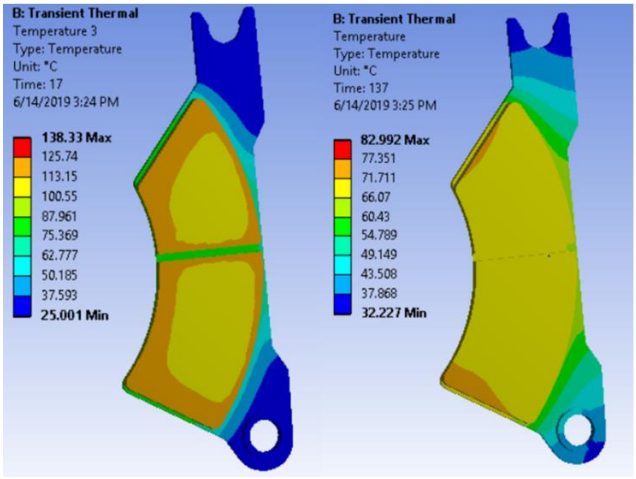

Figure 6.4: Temperature distribution Ayat 2

At the end of the braking session in Figure6-4, the highest temperature of 138.33℃ is observed at the edges and at around the groove of the brake pad. At the end of the cooling period during the train movement from Ayat 2 and Ayat 1, a temperature of 82.992 ℃ is observed to be highest at the leading and the trailing edges of the brake pad in Figure 5-4.

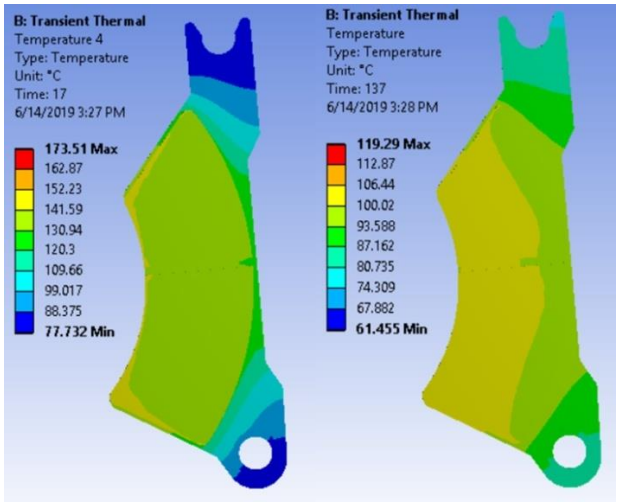

Figure 6.5: Temperature distribution Ayat 1

In Figure6-5, a maximum temperature of 162.87 ℃ is observed at the inner edges of the pad.At the end of the cooling period, a temperature of 112.87 ℃ with a temperature distribution concentrated from inner radius of the brake pad towards the center is depicted in Figure 6-5 before braking again at CMC2.

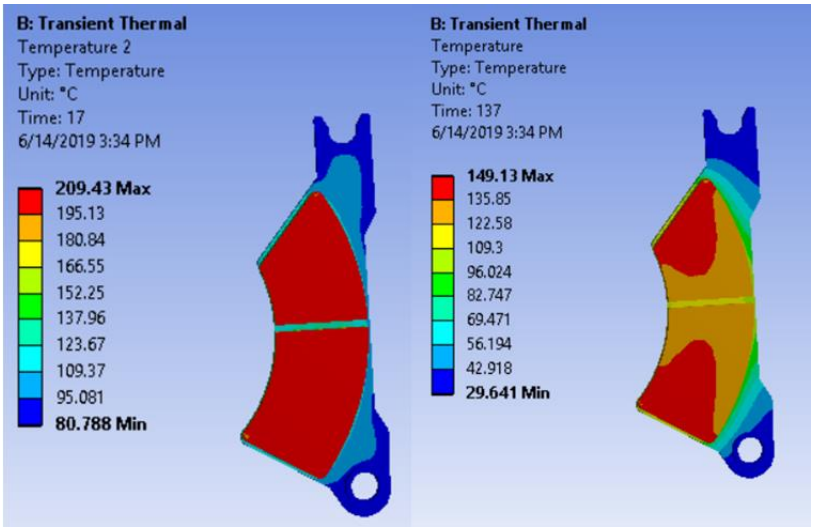

Figure 6.6: Temperature distribution CMC 2

In Figure6-6 left contour,a uniform maximum temperature of 209.43 ℃ is observed at the face of the pad in contact with the brake disc during braking. Upon cooling on the right contour, the temperature then reduces to a maximum of 149.13 ℃ with a concentration at the leading and trailing edges towards the pad groove before braking again at CMC1

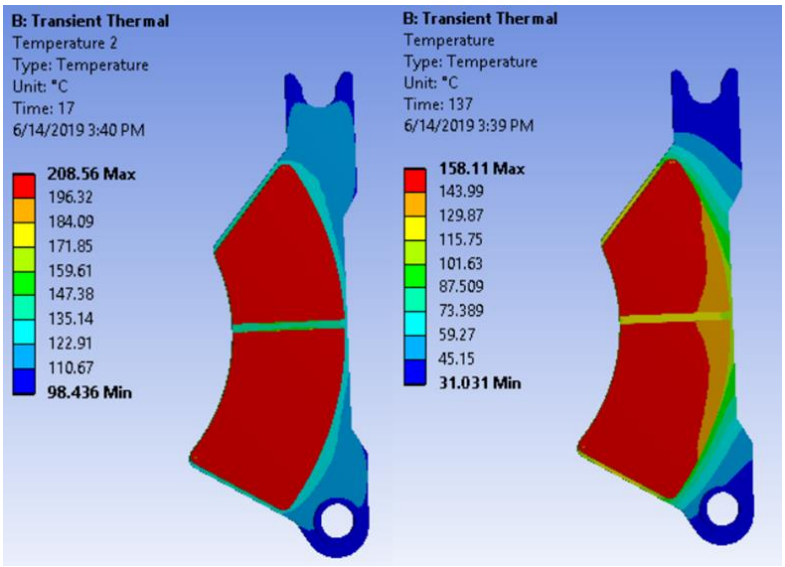

Figure 6.7: Temperature distribution CMC 1

In Figure 6-7left contour,a uniform maximum temperature of 208.56 ℃ is observed at the face of the pad in contact with the brake disc during braking. Upon cooling on the right contour, the temperature then reduces to a maximum of 158.11 ℃ with a concentration inner pad radius towards the centre before braking again at St Micheal Church.

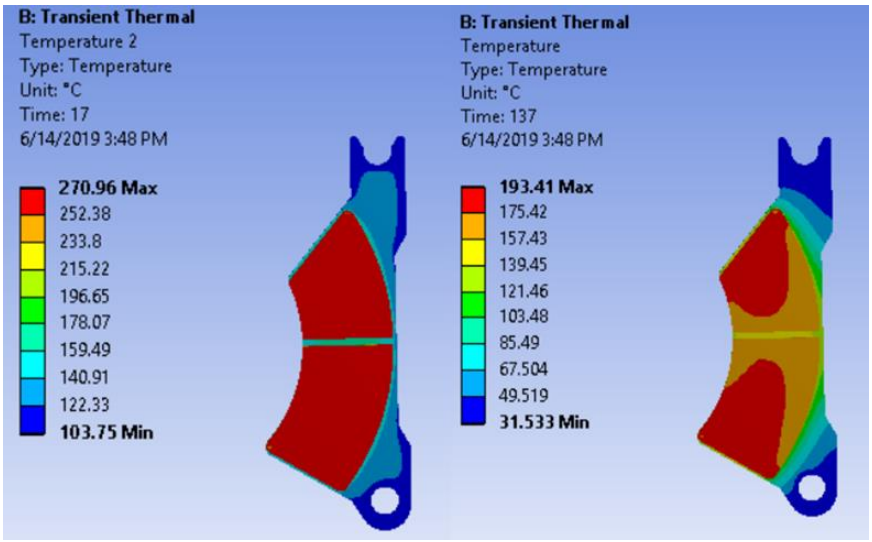

Figure 6.8: Temperature distribution St Micheal Church

Figure6-8, left contour shows a uniform maximum temperature of 270.96 ℃ at the face of the pad in contact with the brake disc. Upon cooling, the temperature then reduces to a maximum of193.41 ℃highest at the leading and trailing edges towards the pad groove before braking again at Civil Service College. The contour observed is similar to the one at CMC 2.

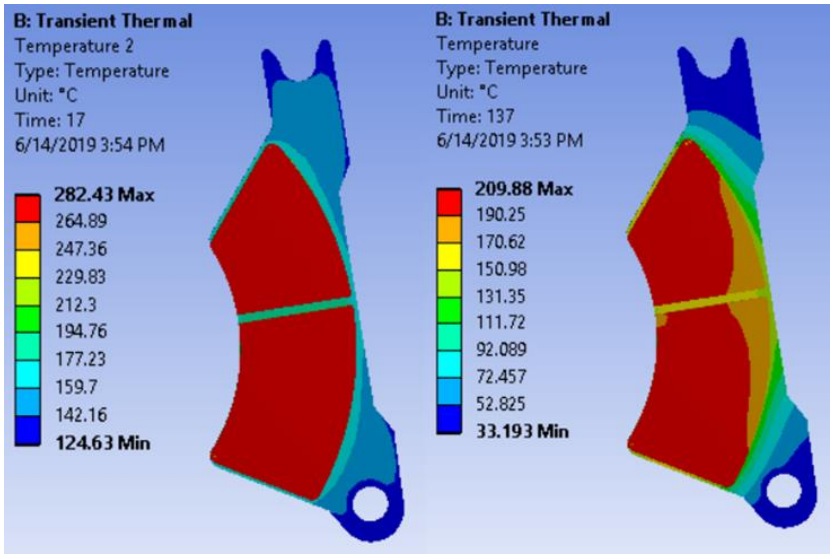

Figure 6.9: Temperature distribution Civil Service College

At Civil Service College shown in Figure6-9, a uniform maximum temperature of 282.43 ℃ is observed at the face of the pad in contact with the brake disc on the left contour. Upon cooling, the temperature then reduces to a maximum of 209.88 ℃ before braking again at SahliteMhiret Church. The temperature distribution changes to that shown in the contour on the right.

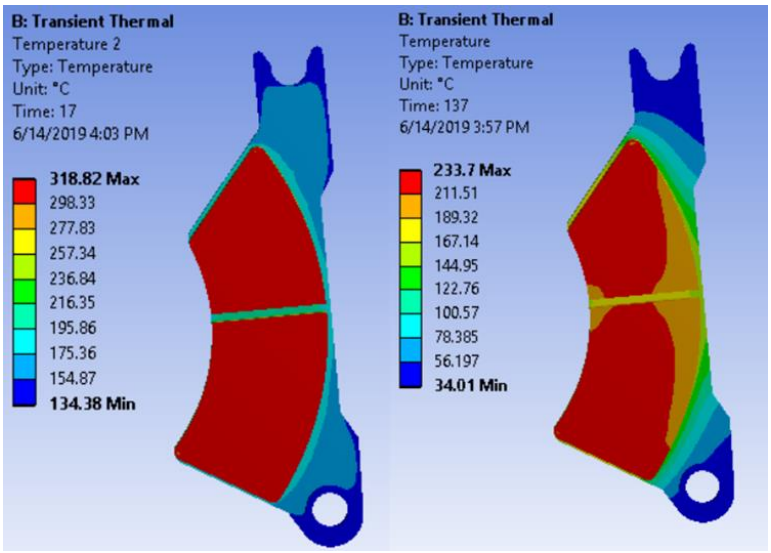

Figure 6.10: Temperature distribution SahliteMhiret Church

At SahliteMhiret Church shown in Figure6-10, a uniform maximum temperature of 318.82 ℃ is observed at the face of the pad in contact with the brake disc on the left contour at the end of braking. Upon cooling, the temperature then reduces to a maximum 233.7 ℃ which is the initial temperature before braking again at GurdSholla. The temperature distribution changes to that shown in the contour on the right.

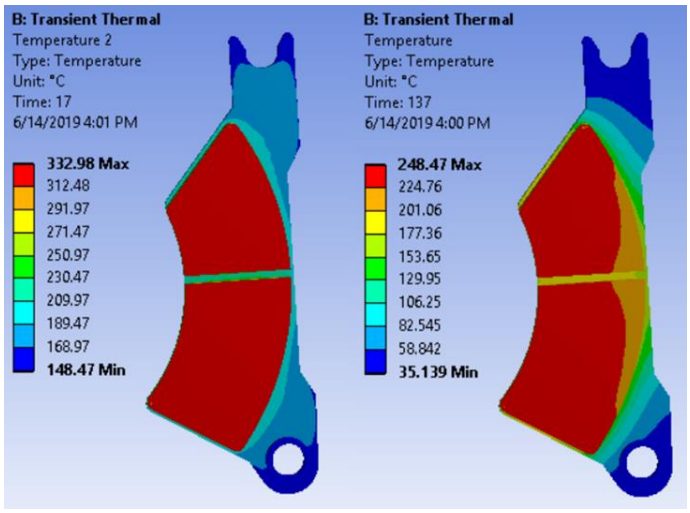

Figure 6.11: Temperature distribution GurdSholla

In Figure6-11, the maximum temperature reached after braking at GurdSholla is 332.98 ℃ while the temperature attained after cooling and initial temperature to Megenagna/Adwa Square is 248.47℃

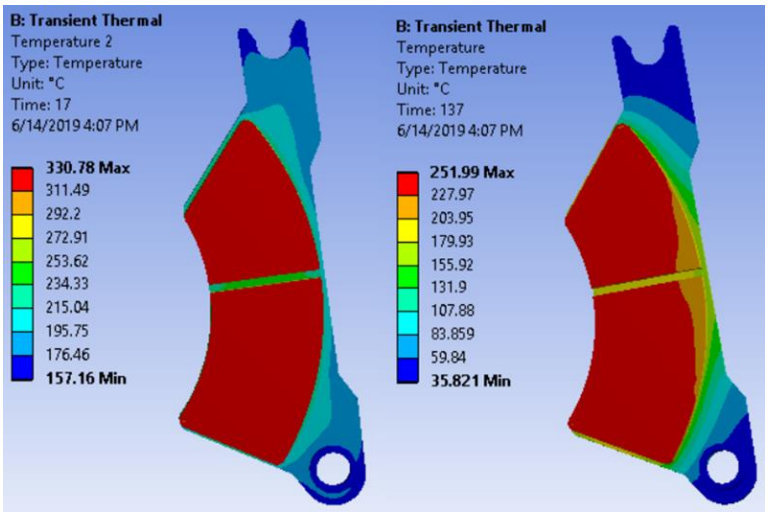

Figure 6.12: Temperature distribution Megenagna/ Adwa Square

In Figure 6-12, the maximum temperature reached after braking at GurdSholla is 330.78 ℃while the temperature attained after cooling and initial temperature to Lem Hotelis251.99 ℃.

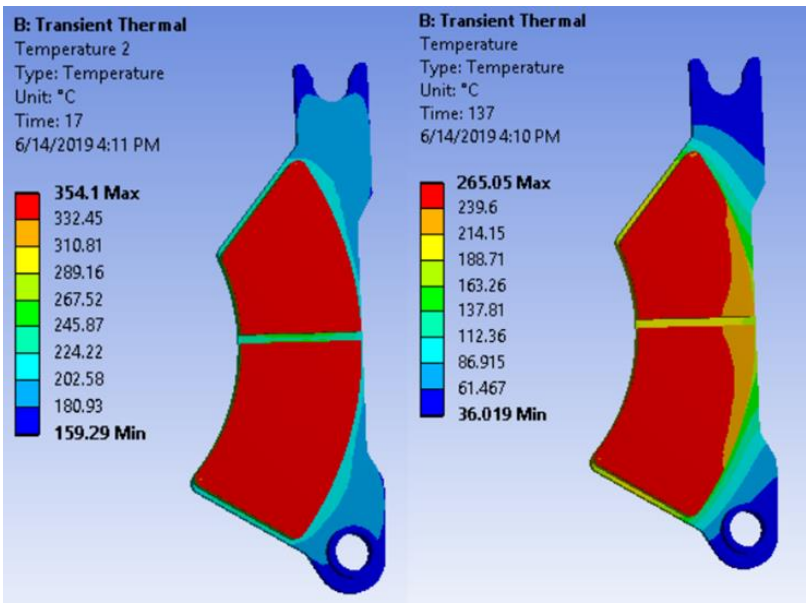

Figure 6.13: Temperature distribution Lem Hotel

In Figure6-13, the maximum temperature reached after braking at Lem Hotel is 354.1 ℃while the temperature attained after cooling and initial temperature to Lem Hotelis265.05 ℃.

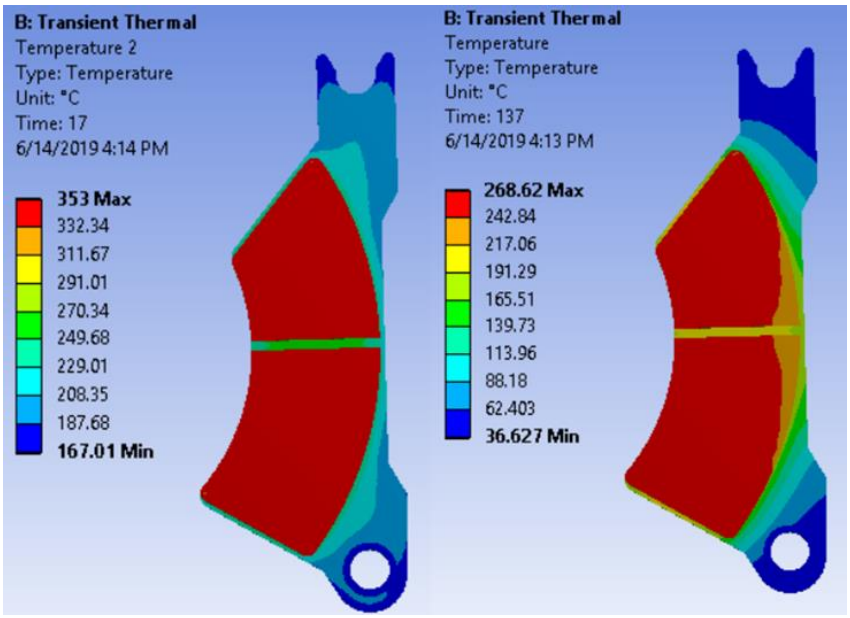

Figure 6.14: Temperature distribution Mazoria / Traffic Police HQ

In Figure6-14, the maximum temperature reached after braking at Mazoria / Traffic Police HQ is 353 ℃while the temperature attained after cooling and initial temperature to the next stationis268.62 ℃ .

The temperature distribution on the brake pad from the first braking operation is shown in the figures above. The braking time is 17seconds whereas it takes 2minutes (120seconds) for the train to move from one station to another. The contours plots show that the temperature increases with time and the highest temperature is reached at the end of the braking time at 17s for every station and due to the temperature build up from previous stations the temperature keeps on increasing while reducing gradually with the help of convection at the end of the train movement from one station to another (at 137s). Upon braking at Ayat 2 which is the first station, the temperature in the pad rises from the ambient temperature of 25 degrees up to a temperature of 138 ℃. This value reduces due to convection and also since brake disc and pad are no longer in contact as the train moves from Ayat 2 to Ayat 1 to a value of 82.992 ℃. This trend is observed in all the following stations but the brake pads don't go back to the ambient temperature since they don't have enough cooling time between the stations. As a result, this temperature is

stored in the brake pad thereby implying that the next braking does not start from ambient temperature.

During braking, some stations experience a higher temperature buildup than others leading to fluctuating temperatures instead of steady rising temperatures. This is due to their gradient orientation among other reasons. The stations on the E-W Line either have positive, negative gradients or are level and as recorded in table 3-1. These gradients affect the heat flux generated at the contact between the brake disc and brake pad in such a way that negative gradients exhibit higher heat fluxes than positive and level gradients.

6.2.1. Summary of Temperature Distribution

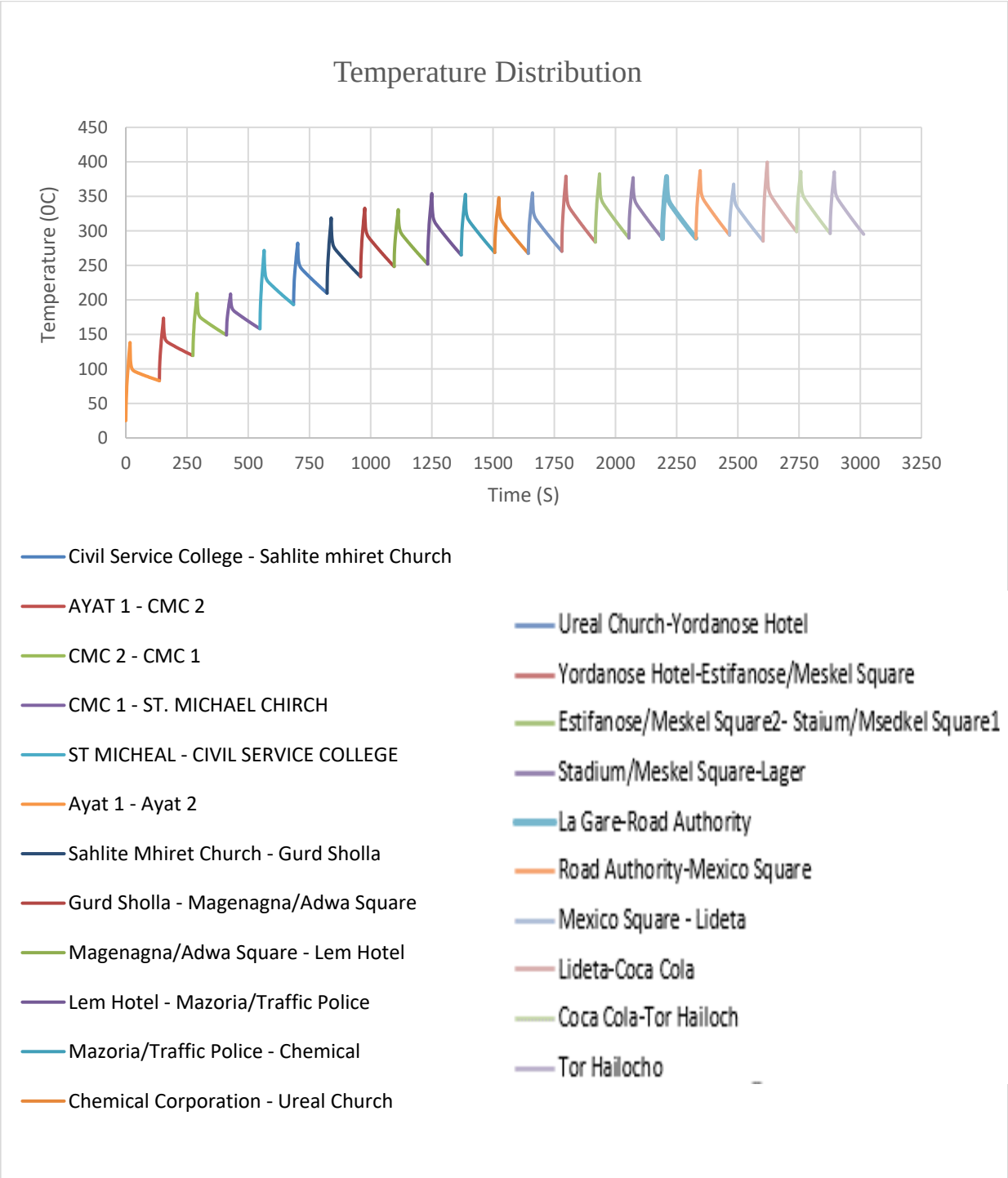

Figure 6.15: Temperature Distribution Ayat 1 –Tor Hailoch AALRT Train Stations

In Figure 6-15, the temperature rise is shown by the rise in temperature during braking while the fall in temperature reflects the time of train movement from station to station

involving convection. Towards the last station, the temperature value is observed to stay almost constant.

When a vehicle is moving on an upward slope, an opposite force of potential energy (mgsinα) acting down the slope counteracts the traction force. This causes a smaller total force that has to be overcome for the vehicle to come to a halt. So, less pressure and force are used. On the other hand, when the vehicle is moving down the slope, both the traction force and mgsinα work in agreement giving a total equivalent force that is high. To overcome such a force for the vehicle to come to a halt, more pressure ought to be used. During braking, all the kinetic energy the vehicle possesses at that instant is converted into heat energy at the brake disc. This heat energy comes about because of friction at the contact surface between the pad and the disc. The more the contact pressure the more the friction force and also the heat flux generated at the contact. The heat flux generated causes the temperature to increase in the bodies in contact. Hence, the higher the energy the vehicle possesses at a point in time, the higher the temperature built up in the body and the resulting thermal stresses due to the high temperatures affect the contact pressure distribution and thus the wear that results.

6.3. Contact Pressure distribution

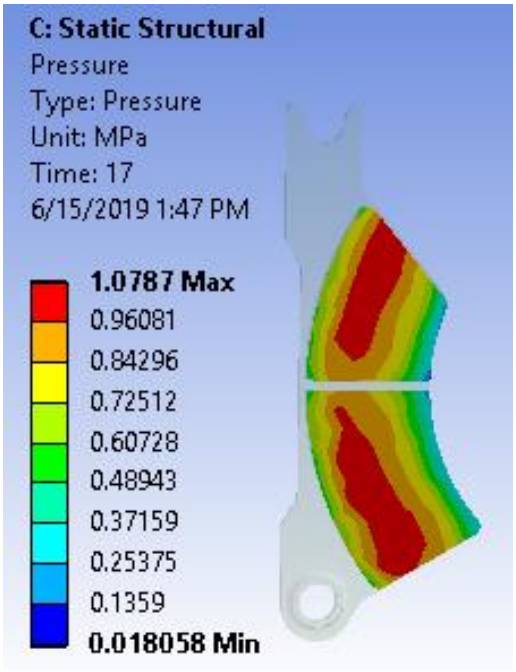

Figure 6.16: Contact pressure distribution Ayat 2

As shown in Figure6-16, the contour plot maximum contact pressure is indicted by red color, which has a value of 1.0787 MPa and a minimum value is 0.018058MPa also

indicated by blue color.The contour depicts that the maximum contact pressure is highest at the leading and trailing edges at the centre of the pad towards the pad groove.

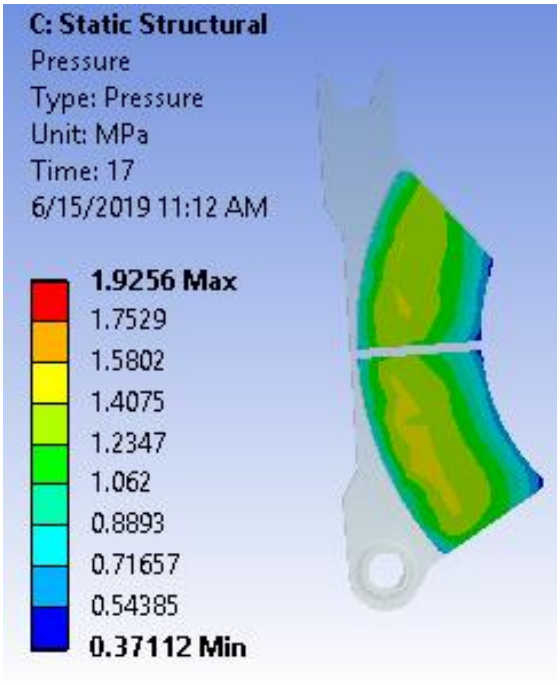

Figure 6.17: Contact pressure distribution Ayat 1

Figure 6-17 shows that the contour plot maximum contact pressure has a value of 1.9256 MPa and a minimum of 0.37112MPa. The figure depicts that the maximum contact pressure is highest at the centre of the pad with a value of 1.5802MPa.

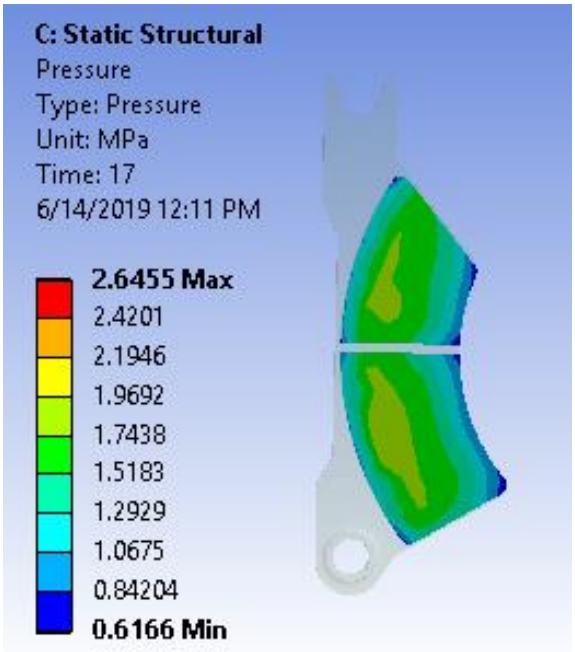

Figure 6.18: Contact pressure distribution CMC 2

Figure 6-18 shows the maximum contact pressure of 1.0787 MPa and a minimum value of 0.6166 MPa. The figure depicts that the maximum contact pressure is highest at the

centre of the brake pad with a value of 2.1946Mpa. The contact pressure distribution is observed to be almost symmetric about the pad groove.

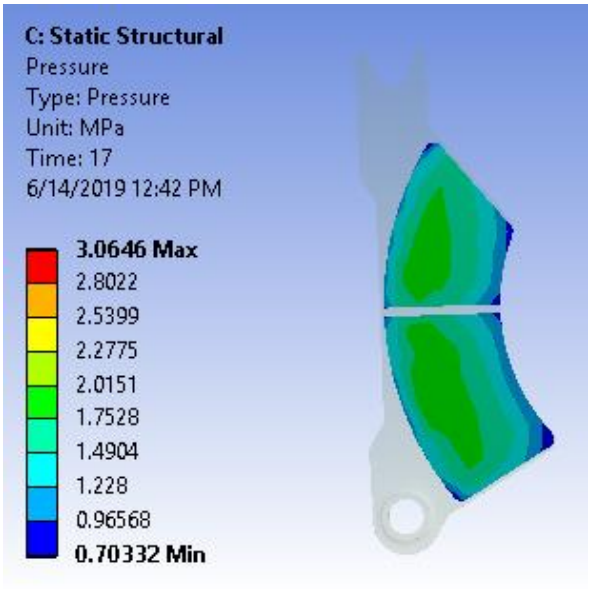

Figure 6.19: Contact pressure distribution CMC 1

As shown in Figure6-19, the contour plot maximum contact pressure with a value of 3.0646MPa and a minimum of 0.70332Mpa is observed. The figure depicts that the maximum contact pressure is highest at the centre of the brake pad with a value of 2.2775Mpa. The contact pressure distribution is observed to be almost symmetric about the pad groove.

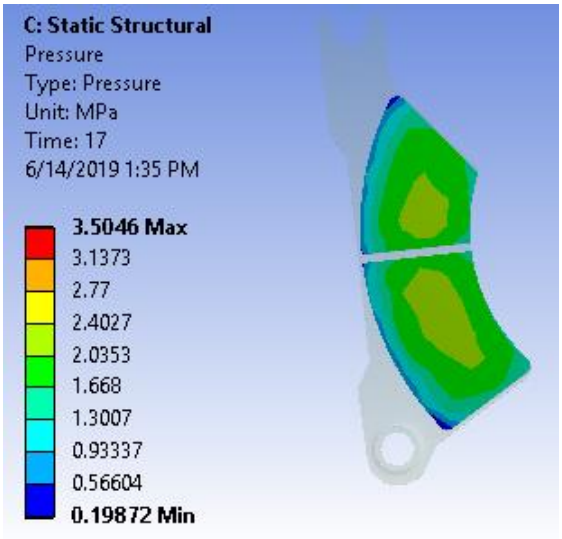

Figure 6.20: Contact pressure distribution St Micheal Church

As shown in Figure6-20,the contour plot maximum contact pressure has a value of 3.5046 MPa and a minimum of 0.19872MPa. Also, the figure depicts that the maximum contact pressure at the centre of the pad with a contact pressure of 2.4027MPa whose distribution is almost symmetric about the pad groove.

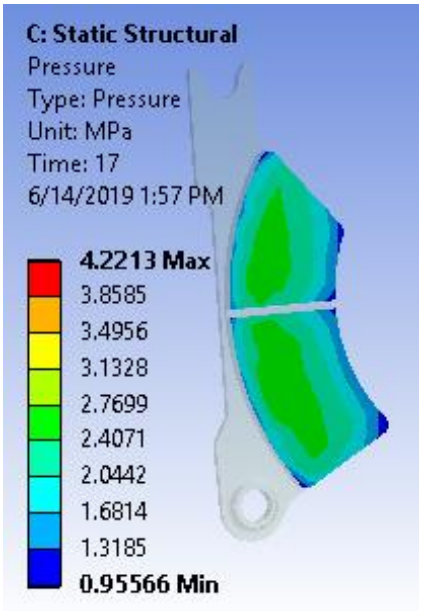

Figure 6.21: Contact pressure distribution Civil Service College

As shown in Figure 6-21 the contour plot maximum contact pressure has a value of 4.2213 MPa and a minimum value of 0.95566MPa. Also, the figure depicts that the maximum contact pressure at the centre of the pad with a contact pressure distribution that is almost symmetric about the pad groove.

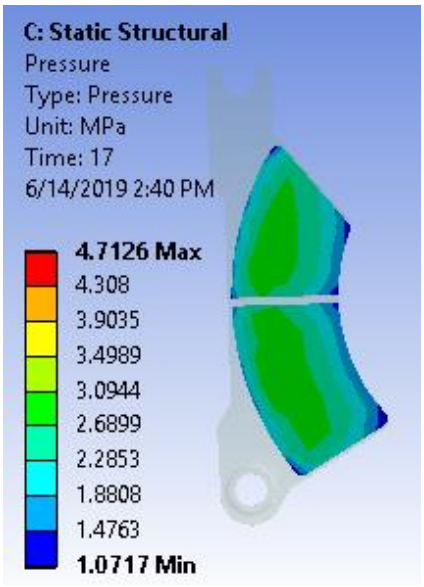

Figure 6.22: Contact pressure distribution SahliteMhiret Church

As shown in Figure6-22, the contour plot maximum contact pressure has a value of 4.7126 MPa and a minimum value of 1.0717MPa. Also, the figure depicts that the maximum contact pressure at the centre of the pad with a contact pressure of 3.4989Mpa whose distribution is almost symmetric about the pad groove.

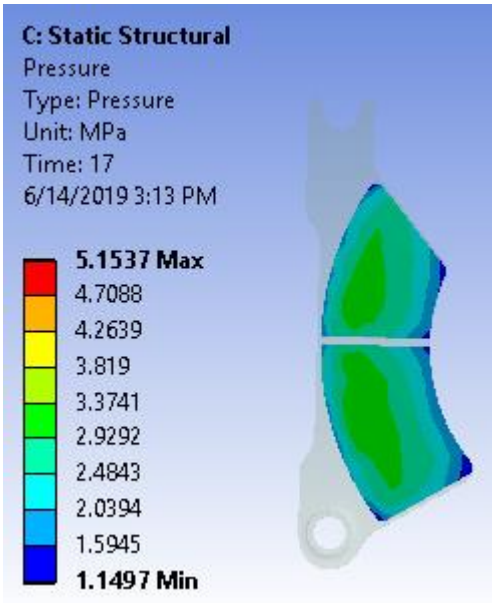

Figure 6.23: Contact pressure distribution GurdSholla

As shown in Figure 6-23, the contour plot maximum contact pressure has a value of 5.1537 MPa and a minimum value of 1.1497MPa. Also, the figure depicts that the maximum contact pressure at the centre of the pad with a contact pressure of 3.819Mpa whose distribution is almost symmetric about the pad groove.

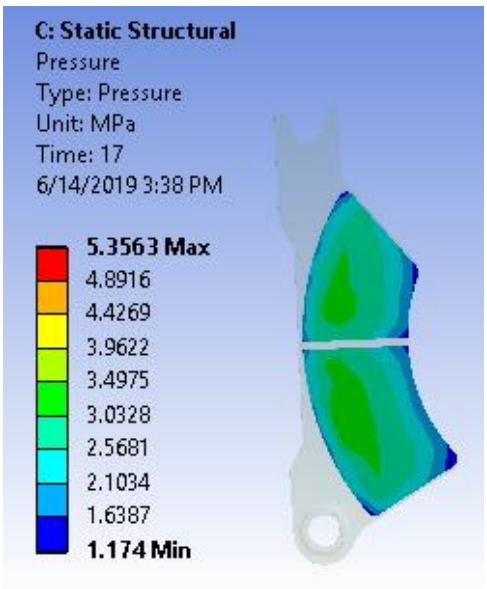

Figure 6.24: Contact pressure distribution Megenagna/Adwa square

As shown in Figure6-24, the contour plot maximum contact pressure has a value of 5.3563 MPa and a minimum value of 1.174MPa. Also, the figure depicts that the maximum contact pressure at the centre of the pad with a contact pressure of 3.9622Mpa whose distribution is almost symmetric about the pad groove.

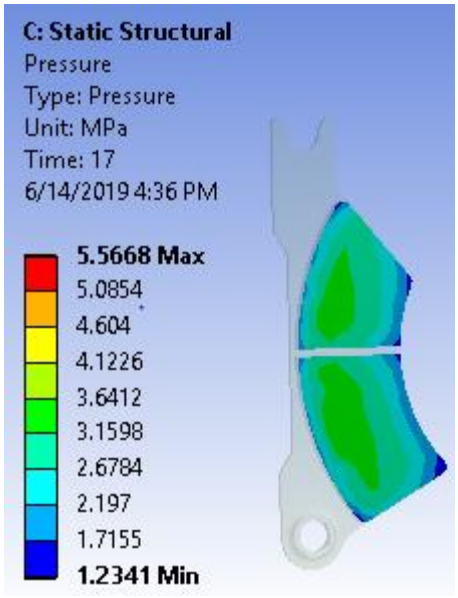

Figure 6.25: Contact pressure distribution Lem Hotel

As shown in Figure6-25, the contour plot maximum contact pressure has a value of 5.5668 MPa and a minimum value of 1.2341MPa. Also, the figure depicts that the maximum contact pressure at the centre of the pad with a contact pressure of 4.1226Mpa whose distribution is almost symmetric about the pad groove.

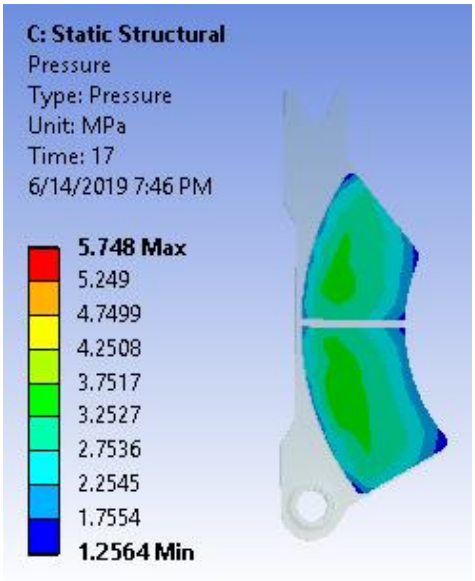

Figure 6.26: Contact pressure distribution Mazoria/Traffic Police HQ.

As shown in Figure6-26, the contour plot maximum contact pressure has a value of 5.748 MPa and a minimum value of 1.2564MPa. Also, the figure depicts that the maximum contact pressure at the centre of the pad with a contact pressure of 4.2508Mpa whose distribution is almost symmetric about the pad groove.

The results of contact pressure at the different times are captured in Table 6-1 and the results for the remaining stations are also captured in the Appendix C.

Contact pressure is as a result of the applied pressure on the brake pads in contact with the brake discs during braking as well as the resulting temperature distribution. The contact pressure increases as the train moves from one station to another because of the effect of temperature. This is due to the effect of convex bending which is caused by thermal deformation of the pad and the back plate, plays a major role in concentration of contact pressure towards the middle of the pad surface.

Convex bending can be explained by the expansion of the pad surface material due to the increase in temperatures. The frictional heat causes the pad surface temperature to rise in a short period of time as compared to the inner region of the pad and the back plate Consequently, the surface expands more than the inner region of the pad and the back plate which results in the convex bending. These phenomena combined with the ramping up of brake pressure in later increments, causes the higher contact pressure in an area which is away from the outer radius of disc.

Table 6.1 Expected Contact pressure values on the railway brake pads

Time (s)	Contact Pressure (MPa) values predicted for AALRT Studied Passenger train Stations										
	Ayat 2	**Ayat 1**	**CMC 2**	**CMC 1**	**St Michea l Church**	**Civil Service Colleg e**	**SahliteMhire t Church**	**GurdSholl a**	**Megenagna/Adw a square**	**Lem Hote l**	**Mazoria/Traffi c Police HQ.**
1	1.066	1.943	2.687	3.110	3.552	4.266	4.758	5.199	5.401	5.612	5.793
2	1.066	1.943	2.686	3.110	3.551	4.266	4.757	5.198	5.401	5.611	5.792
3	1.067	1.942	2.685	3.109	3.551	4.265	4.756	5.197	5.400	5.610	5.791
4	1.067	1.942	2.684	3.108	3.549	4.264	4.755	5.196	5.399	5.609	5.790
5	1.067	1.942	2.683	3.106	3.548	4.263	4.754	5.195	5.397	5.608	5.789
6	1.068	1.941	2.682	3.105	3.546	4.261	4.752	5.193	5.396	5.606	5.787
7	1.068	1.940	2.680	3.102	3.544	4.259	4.750	5.191	5.394	5.604	5.785
8	1.069	1.939	2.678	3.100	3.541	4.257	4.748	5.189	5.391	5.602	5.783
9	1.070	1.938	2.675	3.097	3.539	4.254	4.745	5.186	5.389	5.599	5.780
10	1.071	1.937	2.672	3.094	3.536	4.251	4.742	5.183	5.386	5.596	5.777
11	1.071	1.936	2.669	3.091	3.532	4.248	4.739	5.180	5.383	5.593	5.774
12	1.072	1.934	2.666	3.088	3.528	4.244	4.735	5.176	5.379	5.589	5.771
13	1.074	1.933	2.663	3.084	3.524	4.240	4.731	5.172	5.375	5.585	5.767
14	1.075	1.931	2.659	3.079	3.520	4.236	4.727	5.168	5.371	5.581	5.763
15	1.076	1.930	2.655	3.075	3.515	4.231	4.723	5.164	5.366	5.577	5.758
16	1.077	1.928	2.650	3.070	3.510	4.227	4.718	5.159	5.362	5.572	5.753
17	1.079	1.926	2.646	3.065	3.505	4.221	4.713	5.154	5.356	5.567	5.748

Time (s)	Contact Pressure (MPa) values predicted for AALRT Studied Passenger train Stations										
	Chemical Corporation	**Urael Church**	**Yordanose Hotel**	**Estifanose/ Meskel Square2**	**Stadium/ Meskel Square 1**	**La Gare**	**Road Authority**	**Mexico Square**	**Lideta**	**Coca Cola**	**Tor Hailoch**
1	5.7843	5.8413	6.0508	6.2682	6.317	6.3147	6.3807	6.3137	6.4049	6.5116	6.4697
2	5.7838	5.8408	6.0504	6.2677	6.3166	6.3142	6.3802	6.3133	6.4045	6.5112	6.4693
3	5.783	5.84	6.0496	6.2669	6.3158	6.3134	6.3794	6.3125	6.4037	6.5104	6.4685
4	5.782	5.839	6.0485	6.2659	6.3147	6.3124	6.3784	6.3114	6.4026	6.5093	6.4674
5	5.7806	5.8376	6.0471	6.2645	6.3133	6.311	6.377	6.31	6.4012	6.5079	6.466
6	5.7789	5.8359	6.0454	6.2628	6.3116	6.3093	6.3753	6.3084	6.3995	6.5062	6.4644
7	5.7768	5.8338	6.0434	6.2608	6.3096	6.3073	6.3733	6.3063	6.3975	6.5042	6.4623
8	5.7745	5.8315	6.0411	6.2584	6.3073	6.305	6.3709	6.304	6.3952	6.5019	6.46
9	5.7719	5.8289	6.0384	6.2558	6.3047	6.3023	6.3683	6.3014	6.3926	6.4993	6.4574
10	5.769	5.826	6.0355	6.2529	6.3018	6.2994	6.3654	6.2985	6.3896	6.4964	6.4545
11	5.7657	5.8227	6.0322	6.2496	6.2985	6.2962	6.3621	6.2952	6.3864	6.4931	6.4512
12	5.7621	5.8191	6.0287	6.2461	6.295	6.2926	6.3586	6.2917	6.3828	6.4896	6.4477
13	5.7583	5.8153	6.0248	6.2422	6.2911	6.2887	6.3547	6.2878	6.379	6.4857	6.4438
14	5.7541	5.8111	6.0206	6.238	6.2869	6.2846	6.3505	6.2837	6.3748	6.4816	6.4397
15	5.7496	5.8066	6.0161	6.2335	6.2824	6.2801	6.346	6.2792	6.3703	6.4771	6.4352
16	5.7448	5.8018	6.0113	6.2287	6.2776	6.2753	6.3412	6.2744	6.3655	6.4723	6.4304
17	5.7396	5.7966	6.0062	6.2236	6.2725	6.2702	6.3361	6.2693	6.3604	6.4672	6.4253

6.4. Brake Pad Wear Analysis using ANSYS

The wear value increases within one second to a wear value after which it stays almost constant throughout the braking time. The results of the different volume loss due to wear values at the different times during braking are presented in Figure 6.27.

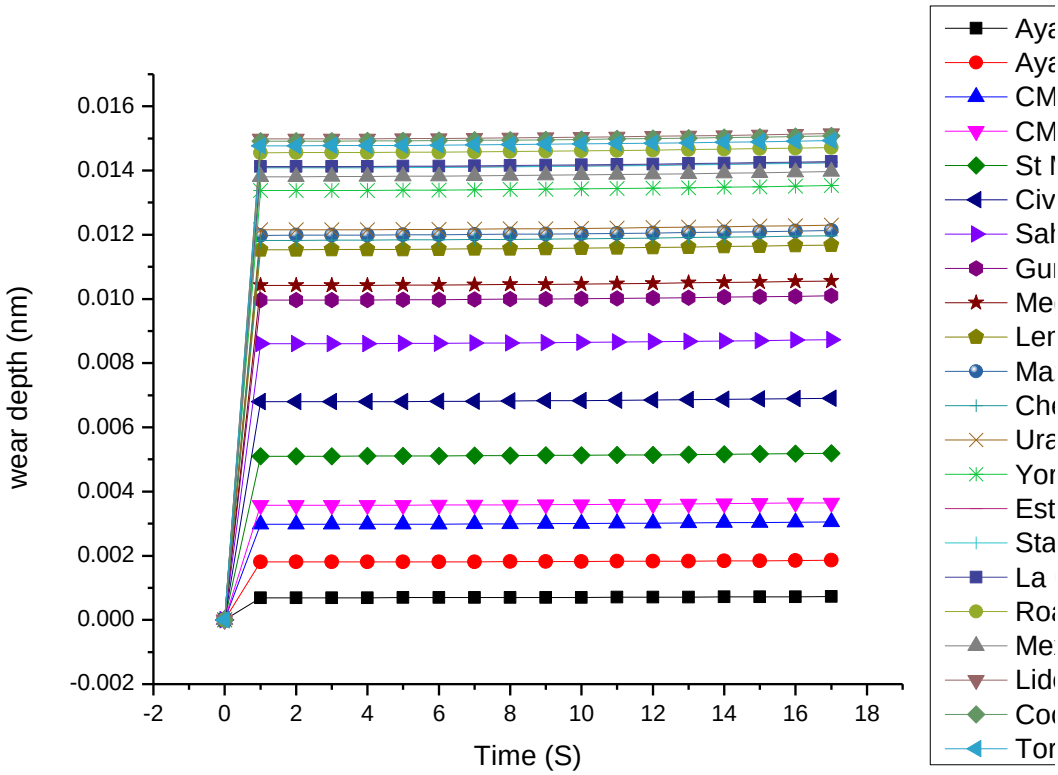

Figure 6.27 A graph of volume loss due to wear against time for different stations

Legend

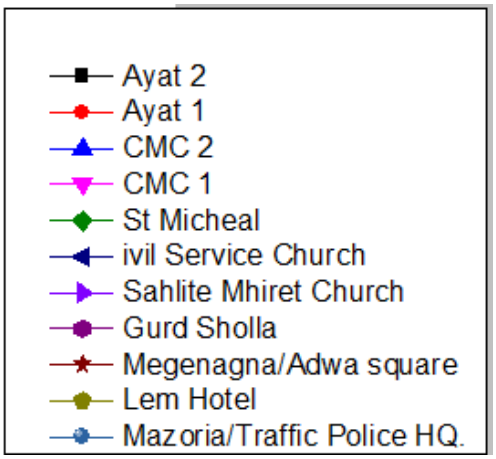

The volume loss due to wear graph Figure 6.27, shows that the wear volume increases from 0 to a value and after which the wear volume stays nearly constant. The wear volume is induced by the high temperatures experienced and the wear volume value is

seen to increase gradually as the train moves from station to station towards the last stations the wear increment is observed to be small. The wear volume values are recorded in Table 6-2 indicating that wear occurs only during the braking time of 17 seconds and no wear is expected during the train movement from station to station due to the fact that there's no contact between the brake disc and pad during that time.In addition, wear is an incremental value which adds on to the wear incurred at the previous station. Therefore, by the last station the wear volume is the summation of the wear accumulated at all the stations.

Wear depth was calculated using Equation 4.30.,by dividing the volume loss due to wear by the surface area of the brake pad of 120cm^2 refer to Table (3.6).

Table 6.2 Expected Volume Loss due to wear values on the railway brake pads

Time (s)	Volume loss due to wear values predicted for AALRT Studied Passenger train Stations										
	Ayat 2	**Ayat 1**	**CMC 2**	**CMC 1**	**St Micheal Church**	**Civil Service College**	**SahliteMhiret Church**	**GurdSholla**	**Megenagna/Adwa square**	**Lem Hotel**	**Mazoria/Traffic Police HQ.**
0	0	0	0	0	0	0	0	0	0	0	0
1	6.89E-04	1.80E-03	2.98E-03	3.57E-03	5.10E-03	6.80E-03	8.60E-03	9.96E-03	1.04E-02	1.15E-02	1.20E-02
2	6.90E-04	1.80E-03	2.98E-03	3.57E-03	5.10E-03	6.80E-03	8.60E-03	9.96E-03	1.04E-02	1.15E-02	1.20E-02
3	6.91E-04	1.81E-03	2.98E-03	3.57E-03	5.10E-03	6.80E-03	8.61E-03	9.97E-03	1.04E-02	1.15E-02	1.20E-02
4	6.92E-04	1.81E-03	2.98E-03	3.57E-03	5.10E-03	6.80E-03	8.61E-03	9.97E-03	1.04E-02	1.15E-02	1.20E-02
5	6.93E-04	1.81E-03	2.98E-03	3.57E-03	5.11E-03	6.80E-03	8.61E-03	9.97E-03	1.04E-02	1.15E-02	1.20E-02
6	6.94E-04	1.81E-03	2.99E-03	3.58E-03	5.11E-03	6.81E-03	8.62E-03	9.98E-03	1.04E-02	1.16E-02	1.20E-02
7	6.96E-04	1.81E-03	2.99E-03	3.58E-03	5.11E-03	6.81E-03	8.62E-03	9.98E-03	1.04E-02	1.16E-02	1.20E-02
8	6.98E-04	1.82E-03	2.99E-03	3.59E-03	5.12E-03	6.82E-03	8.63E-03	9.99E-03	1.04E-02	1.16E-02	1.20E-02
9	7.00E-04	1.82E-03	3.00E-03	3.59E-03	5.12E-03	6.83E-03	8.64E-03	1.00E-02	1.05E-02	1.16E-02	1.20E-02
10	7.03E-04	1.82E-03	3.00E-03	3.60E-03	5.13E-03	6.83E-03	8.65E-03	1.00E-02	1.05E-02	1.16E-02	1.20E-02
11	7.06E-04	1.83E-03	3.01E-03	3.60E-03	5.14E-03	6.84E-03	8.65E-03	1.00E-02	1.05E-02	1.16E-02	1.20E-02
12	7.09E-04	1.83E-03	3.01E-03	3.61E-03	5.14E-03	6.85E-03	8.67E-03	1.00E-02	1.05E-02	1.16E-02	1.21E-02

13	7.12E-04	1.83E-03	3.02E-03	3.62E-03	5.15E-03	6.86E-03	8.68E-03	1.00E-02	1.05E-02	1.16E-02	1.21E-02
14	7.16E-04	1.84E-03	3.03E-03	3.62E-03	5.16E-03	6.87E-03	8.69E-03	1.01E-02	1.05E-02	1.16E-02	1.21E-02
15	7.19E-04	1.84E-03	3.04E-03	3.63E-03	5.17E-03	6.88E-03	8.70E-03	1.01E-02	1.05E-02	1.16E-02	1.21E-02
16	7.24E-04	1.85E-03	3.05E-03	3.64E-03	5.18E-03	6.90E-03	8.71E-03	1.01E-02	1.05E-02	1.17E-02	1.21E-02
17	7.28E-04	1.86E-03	3.05E-03	3.65E-03	5.19E-03	6.91E-03	8.73E-03	1.01E-02	1.06E-02	1.17E-02	1.21E-02

Time (s)	**Volume loss due to wear values predicted for AALRT Studied Passenger train Stations**										
	Chemical Corporation	**Urael Church**	**Yordanose Hotel**	**Estifanose/Meskel Square2**	**Stadium/Meskel Square 1**	**La Gare**	**Road Authority**	**Mexico Square**	**Lideta**	**Coca Cola**	**Tor Hailoch**
0	**0**	**0**	**0**	**0**	**0**	**0**	**0**	**0**	**0**	**0**	**0**
1	1.18E-02	1.21E-02	1.34E-02	1.41E-02	1.41E-02	1.41E-02	1.46E-02	1.38E-02	1.50E-02	1.49E-02	1.48E-02
2	1.18E-02	1.22E-02	1.34E-02	1.41E-02	1.41E-02	1.41E-02	1.46E-02	1.38E-02	1.50E-02	1.49E-02	1.48E-02
3	1.18E-02	1.22E-02	1.34E-02	1.41E-02	1.41E-02	1.41E-02	1.46E-02	1.38E-02	1.50E-02	1.49E-02	1.48E-02
4	1.18E-02	1.22E-02	1.34E-02	1.41E-02	1.41E-02	1.41E-02	1.46E-02	1.38E-02	1.50E-02	1.49E-02	1.48E-02
5	1.18E-02	1.22E-02	1.34E-02	1.41E-02	1.41E-02	1.41E-02	1.46E-02	1.38E-02	1.50E-02	1.49E-02	1.48E-02
6	1.18E-02	1.22E-02	1.34E-02	1.41E-02	1.41E-02	1.41E-02	1.46E-02	1.38E-02	1.50E-02	1.49E-02	1.48E-02
7	1.19E-02	1.22E-02	1.34E-02	1.41E-02	1.41E-02	1.41E-02	1.46E-02	1.38E-02	1.50E-02	1.49E-02	1.48E-02
8	1.19E-02	1.22E-02	1.34E-02	1.41E-02	1.41E-02	1.42E-02	1.46E-02	1.38E-02	1.50E-02	1.49E-02	1.48E-02
9	1.19E-02	1.22E-02	1.34E-02	1.41E-02	1.41E-02	1.42E-02	1.46E-02	1.39E-02	1.50E-02	1.50E-02	1.48E-02
10	1.19E-02	1.22E-02	1.34E-02	1.41E-02	1.41E-02	1.42E-02	1.46E-02	1.39E-02	1.50E-02	1.50E-02	1.48E-02
11	1.19E-02	1.22E-02	1.34E-02	1.42E-02	1.41E-02	1.42E-02	1.46E-02	1.39E-02	1.51E-02	1.50E-02	1.48E-02

12	1.19E-02	1.22E-02	1.35E-02	1.42E-02	1.42E-02	1.42E-02	1.46E-02	1.39E-02	1.51E-02	1.50E-02	1.49E-02
13	1.19E-02	1.22E-02	1.35E-02	1.42E-02	1.42E-02	1.42E-02	1.47E-02	1.39E-02	1.51E-02	1.50E-02	1.49E-02
14	1.19E-02	1.23E-02	1.35E-02	1.42E-02	1.42E-02	1.42E-02	1.47E-02	1.39E-02	1.51E-02	1.50E-02	1.49E-02
15	1.19E-02	1.23E-02	1.35E-02	1.42E-02	1.42E-02	1.42E-02	1.47E-02	1.39E-02	1.51E-02	1.50E-02	1.49E-02
16	1.20E-02	1.23E-02	1.35E-02	1.42E-02	1.42E-02	1.43E-02	1.47E-02	1.39E-02	1.51E-02	1.51E-02	1.49E-02
17	1.20E-02	1.23E-02	1.35E-02	1.43E-02	1.42E-02	1.43E-02	1.47E-02	1.40E-02	1.51E-02	1.51E-02	1.49E-02

6.5. Correlation between temperature distribution contact pressure and wear

Table 6.3Temperature values, contact pressure and wear depth

Stations	Temperature		Contact pressure (MPa)	Volume Loss Due to wear (mm^3)	Cumulative Volume Loss Due to wear (mm3)	Wear thickness/ Wear depth (nm)	Cumulative Wear depth (nm)
	Temp at braking	Initial temp for next braking					
Ayat 2	138.33	82.992	1.0787	7.28E-04	7.28E-04	0.06	0.06
Ayat 1	173.67	119.37	1.9256	1.86E-03	2.59E-03	0.155	0.215
Meri/CMC 2	209.5	149.19	2.6455	3.05E-03	5.64E-03	0.254	0.469
CMC 1	208.62	158.16	3.0646	3.65E-03	1.00E+00	0.304	0.773
St.Michael Church	271.75	193.29	3.5046	5.19E-03	1.01E+00	0.433	1.206
Civil Service College	282.31	209.78	4.2213	6.90E-03	1.01E+00	0.575	1.781
SahliteMhiret Church	318.72	233.62	4.7126	8.73E-03	2.00E+00	0.728	2.509
GurdSholla	332.9	248.4	5.1537	1.01E-02	2.01E+00	0.842	3.351
Megenagna/Adwa square	330.78	251.99	5.3563	1.06E-02	2.02E+00	0.883	4.234
Lem Hotel	354.1	265.05	5.5668	1.17E-02	3.00E+00	0.975	5.209
Mazoria/Traffic Police HQ.	353	268.62	5.748	1.21E-02	3.01E+00	1.008	6.217
Chemical Corporation	335.46	267.33	5.7396	1.20E-02	3.02E+00	0.998	7.215
Urael Church	341.15	270.41	5.7966	1.23E-02	3.04E+00	1.02	8.235
Yordanose Hotel	362.22	283.78	6.0062	1.35E-02	3.05E+00	1.13	9.365
Estifanose/Meskel Square2	366.98	289.7	6.2236	1.43E-02	3.06E+00	1.19	10.555
Stadium/Meskel Square 1	363.16	288.75	6.2725	1.42E-02	3.08E+00	1.19	11.745
La Gare	364.46	289.31	6.2702	1.43E-02	3.09E+00	1.19	12.935
Road Authority	371.78	293.85	6.3361	1.47E-02	3.11E+00	1.23	14.165
Mexico Square	355.78	285.26	6.2693	1.40E-02	3.12E+00	1.16	15.325
Lideta	381.65	298.85	6.3604	1.51E-02	3.14E+00	1.26	16.585
Coca Cola	372.16	296.25	6.4672	1.51E-02	3.15E+00	1.26	17.845
Tor Hailoch	371.28	295.13	6.4253	1.49E-02	3.17E+00	1.24	19.085

Due to thermal deformation, contact area and pressure distribution also change. Thermal and mechanical deformations affect each other strongly and simultaneously. As pressure distributionwasstudied in the context of uneven temperature distribution. It is also noticed that the maximum contact pressure is located on the edges of the pad decreasing from the leading edge towards the trailing edge from friction. This pressure distribution is almost symmetrical about to the groove. The thermal dilation involving temperature

rise and cooling during train movement from station to station leads to a variation of the contact pressure distribution and hence the wear.

6.6. Relationship between temperature, Contact pressure and Wear depth

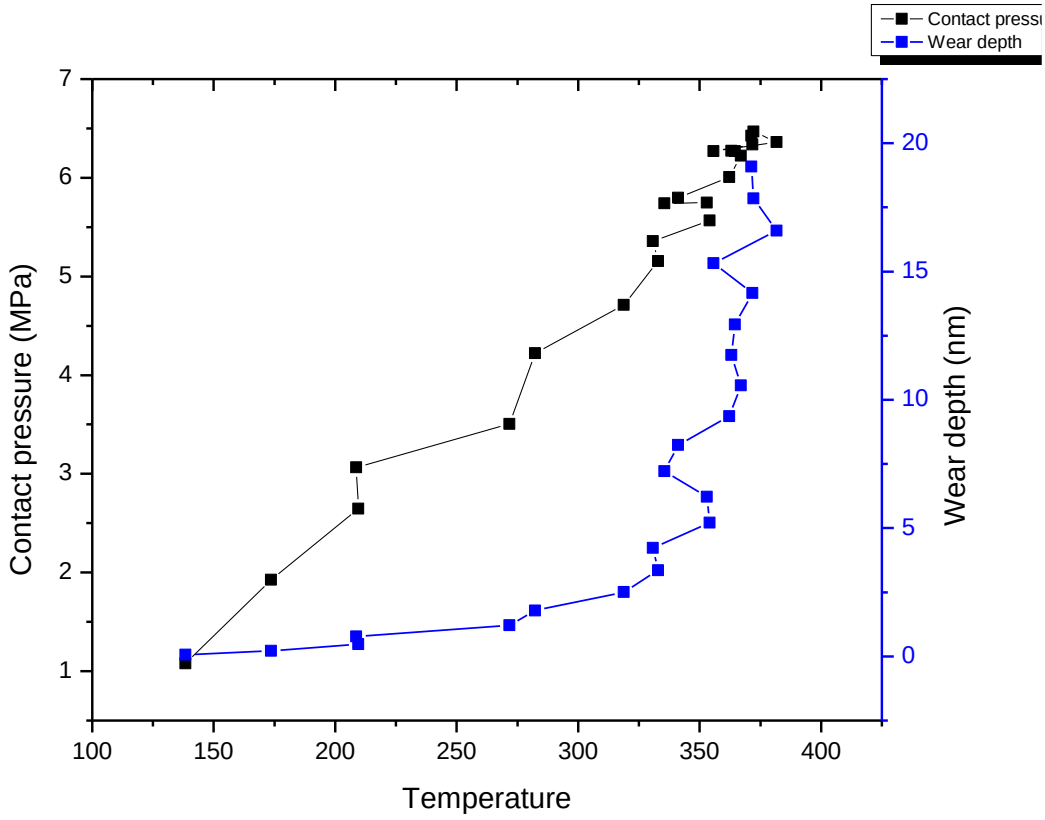

Figure 6.28 Relationship between temperature, contact pressure and wear depth

Figure 6.28 shows that the temperature increases starting from Ayat 2 to Tor Hailoch during the train movement. As a result of this increase in temperature, the contact pressure per station is observed to increase as well. Due to this increase in contact pressure, the wear depth also gradually increases. By the time the train reaches the final station, the temperature is almost constant and the increase in contact pressure is minimal. A temperature of385.56 ℃ is reached resulting in a contact pressure of 6.4253MPa that induces a maximum wear depth of 19.085nm in a period of 3014s.

CHAPTER 7 CONCLUSIONS AND RECCOMENDATIONS

7.1. Conclusion

A wear model was adopted using a finite element model to compute the brake pad to disc contact pressure distribution as a result of temperature distribution. The wear of the brake pad is computed using a generalized form of Archard's wear law based on the resulting contact pressure distribution.

Finite element analysis made it possible to explain and reproduce phenomena observed during braking for 22 stations along the East- West AALRT line from Ayat 2 station to Tor Hailoch. The research considered an overloaded train moving from station to station.

In this thesis, brake pad wear using finite element method is presented considering thermal structural effect. This method can be used to analyse contact pressure and wear in dry sliding contact for mechanical components.

The research discusses how finite element analysis software, ANSYS can be used to analyse the brake disc-pad contact interface in train disc brakes. A FE-based model consisting of two brake pads and the brake disc was modelled. The model was used to study the behaviour of the pad-to-contact interface under different loads and running conditions for different stations namely from Ayat 2 to Tor Hailochon the East-West AALRT Line.

A convection coefficient around the brake pad was determined using ANSYS CFX to be used in the thermal analysis while the brake disc convection coefficient was adopted from previous literature. A simulation replicating the actual train movement for repeated braking phenomenon at different stations was analysed to study the temperature rise and fall at the brake disc-pad contact which in turn affect the contact pressure distribution and wear.

Generally, from this research the conclusions made are;

1. Temperature distribution along disc brake – pad contact was estimated considering braking at different stations as well as cooling during train movement from station to station. The temperature increased gradually during braking and decreased during the time when there was no contact between the brake disc and pad while moving to the next station.
2. The temperature distribution on the brake pad from the temperature contours were concentrated at the outer edges of the brake pad at the first braking action at

Ayat 2 and was observed to be uniform on the contact surface at the end of braking while the temperature distribution contour kept on reducing as the temperature values increased from station to station during the cooling action.

3. Temperature influences the structural and contact behaviour of the brake assembly. The contact pressure is found to increase gradually in the disc-pad model due to the increase in temperature.
4. Wear depth also increases as a result of high contact pressure distribution depending on the high temperatures induced due to high friction and brake pressures leading to a maximum value of 19.085nm by the 22ndstation.

The high temperatures observed on the brake pad surface outer edges, leads to the development of thermal stresses leading to failure of the brake pad due to crack, since these parameters are as function of stress. This was validated by the observation from AALRT brake pads that were characterized by cracks on the outer edges and a lot of surface wear on the middle of the pad also almost symmetric by the brake pad groove as observed in the finite element method results.

The results from this work can be very helpful to railway and maintenance engineers in order to choose materials that minimize wear rate, to determine when maintenance and replacement of brake pads can be done as well as to help designers implement different structural modifications in the brake pads. Also, by taking precaution during braking, wear depth can be minimized by avoiding frequent and unnecessary emergency braking.

7.2. Recommendations

In its present state the model is very simplified and is therefore only suitable for design trend analysis, not for prediction of absolute values.In this work a linear wear model is used to simulate the wear of brake pad. The model was chosen based on its simplicity and its popularity by previous researches. It is also possible to implement other more complex wear models.

Although the use of a global wear coefficient estimated from experimental results is applied to numerical simulations, the numerical approach is not able to completely reproduce experimental results. In order to improve the correlation, an experimental analysis to determine the exact wear coefficient value is recommended. Another factor that may influence the accuracy of the result is the step length during the numerical

integration. Too large a step could lead to poor accuracy, whereas too small a step length could result in unacceptably high computational time.

The following areas are recommended for future research;

1. Experimental study to verify the accuracy of the numerical model developed.
2. Wear analysis making use of temperature dependent brake pad material properties to better quantify the wear value.
3. Thefrictioncoefficientofabrakepadisgenerallydependentontemperature, velocity and contactpressurebutinthiswork, itisassumedtobeconstantatμ= 0.35 torepresentanaveragebehavior.A temperaturedependentbehaviorofthefrictioncoefficientisalso recommended.

REFERENCES

[1] A. A. L. Rail, "WIKIPEDIA," 4 March 2019. [Online]. Available: https://en.m.wikipedia.org/wiki/Addis_Ababa_Rail.

[2] S. C. Wu., S. Q. Zhang and Z. W. .. Xu, "Thermal crack growth-based fatigue life prediction due to braking for a high-speed railway brake disc.," *International Journal of Fatigue,* vol. 87, p. 359–369., 2016.

[3] R. C. D. M. &. P. R. K. Sharma, "Braking systems in railway vehicles.," *International Journal of Engineering Research & Technology,* vol. 4, no. 1, p. 206–211., 2015.

[4] B.-c. Goo and C.-h. L. , "Thermal fatigue of cast iron brake disk materials," *Journal of Mechanical Science and Technology,* vol. 26, no. 6, p. 1719~1724, 2012.

[5] A. &. G. P. Adamowicz, "Analysis of disc brake temperature distribution during single braking under non-axisymmetric load.," *Applied Thermal Engineering,* vol. 31, no. 6–7, p. 1003–1012, 2011.

[6] Daniel Thuresson, "Influence of material properties on sliding contact braking applications," *Wear,* vol. 257, no. 5-6, pp. 451-460, 2004.

[7] A. A. B. A. R. &. B. M. Belhocine, "Thermal and structural analysis of disc brake assembly during single stop braking event.," *Australian Journal of Mechanical Engineering,* vol. 14, no. 1, pp. 26-38, 2016.

[8] S. A. Anders Söderberg, "Simulation of wear and contact pressure distribution at the pad-to-rotor interface in a disc brake using general purpose finite element analysis software," *wear,* vol. 267, p. 2243–2251, 2009.

[9] V. Hegadekatte., N. Huber. and O. Kraft., "Finite element based simulation of dry sliding wear," *Modelling and Simulation in Materials Science and Engineering,* vol. 13, p. 57–75, 2005.

[10] X. Y. Y. B. J. L. L. &. F. X. Xiao, "Review on the friction and wear of brake materials.," *Advances in Mechanical Engineering*, vol. 8, no. 5, p. 1–10, 2016.

[11] M. R. M. G. S. S. Mohammadreza Arjmandi, "Finite element modelling of sliding wear in three-dimensional woven textiles," *Tribology International 115* , p. 452–460, 2017.

[12] P. B. Er. N. B. Shindel, "Literature Review on FEM analysis of Disc brake system," *International Journal Of Engineering And Computer Science*, vol. 4, no. 2, pp. Page No. 10554-19558, february 2015.

[13] A. Rashid, "Overview of Disc Brakes and Related Phenomena- a Review," *International Journal of Vehicle Noise and Vibration*, pp. pp. 257-301., 2014.

[14] A. a. D. M.-C. Floquet, "Non axis Symmetric Effectfor Three Dimensional analysis of a brake," *ASME J. Tribology*, vol. 116, pp. 401-407, 1994.

[15] M. Abdelahamid, ""Brake judder analysis: Case studies"," *SAE, Technical Paper Series,no. 972027.*, 1997.

[16] KIRIU, "https://www.kiriu.co.jp/en/product/brakeparts/," KIRIU, May 2019. [Online]. [Accessed 03 July 2019].

[17] F. Talati and Salman Jalalifar, "Analysis of heat conduction in a disk brake system," 2009.

[18] Z. Z. T. M. e. a. Bao JS, "Dynamic friction heat model for disc brake during emergency braking.," *Adv Sci Lett* , p. 4: 11–12. 31. , 2011.

[19] B. D. c. C. D. A. B. J. T. Grieve D.G, "Design of a light weight automobile brake disc using finite element and Taguchi techniques,," *proc. Instn. Mech. Engrs*, vol. 212, no. 4, pp. 245-254, 1998.

[20] P. G. Adam ADAMOWICZ, "FINITE ELEMENT ANALYSIS OF THERMAL STRESSES IN A PAD-DISC BRAKE SYSTEM (A REVIEW)," *acta mechanica et*

automatica, , vol. 7, no. 4, 2013.

[21] M. S. Jiaren Jiang, "Modelling sliding wear: From dry to wet environments," 2006.

[22] G. J.-M. C. C.-R. V. V.-M. J.R. Laguna-Camacho et al., "A study of the wear mechanisms of disk and shoe brake pads," *Engineering Failure Analysis,* 2015.

[23] N. W. D. B. D. H. B. G. G. S. P. S. W. Kim, "Finite element analysis and experiments of metal/metal wear in oscillatory contacts.," *wear,* vol. 258, pp. 1787-1793, 2005.

[24] F. Gelana, Wear Anakysis of Overhead Line Contact Wire using ANSYS Workbench Software, Addis Ababa: AAIT, 2015.

[25] B. K. Satapathy and J. Bijwe, "Performance of friction materials based on variation in nature of organic fibres Part I. Fade and recovery behaviour," *Wear,* vol. 257, no. 5-6, pp. 573-584, 2004.

[26] B. J. Y. Y. e. a. Zhu ZC, "Frictional catastrophe behaviors and mechanisms of brake shoe for mine hoisters during repetitious emergency braking.," *Ind Lubr Tribol,* p. 65: 245–250., 2012.

[27] J. Bao., JiushengYin., YanLu., Y. Hu., DongyangLu. and Lijian, "A cusp catastrophe model for the friction catastrophe of mine brake material in continuous repeated brakings," *Proceedings of the Institution of Mechanical Engineers, Part J: Journal of Engineering Tribology,* vol. 227, no. 10, pp. 1150-1156, 2013.

[28] X. Xiao., Y. Yin., J. Bao., L. Lu., X. Feng, . and ., "Review on the friction and wear of brake materials,," *Advances in Mechanical Engineering,* 2016.

[29] J. Kukutschová., V. Roubicek., K. Malachova., Z. Pavlickova., R. Holusa., J. K. V. Micka., D. MacCrimmon. and P. Filip., "Wear mechanism in automotive brake materials, wear debris and its potential environmental impact.," *Wear. 267(5–8)* , p. 807–817, 2009.

[30] V.M.M.Thilak., R.Krishnaraj., Dr.M.Sakthivel., K.Kanthavel., D. M. M.G. and R.Palani., "Transient Thermal and Structural Analysis of the Rotor Disc of Disc Brake," *International Journal of Scientific & Engineering Research,* vol. 2, no. 8, August 2011.

[31] F. S. Arnab Ghosh, "A novel approach to model effects of surface roughness parameters on wear," *Wear338-339*, p. 73–94, 2015.

[32] J.F. Archard, "The Temperature of Rubbing Surfaces," 1959.

[33] B. Bhushan, Introduction to Tribology, 2nd Edition March 2013, 2nd ed., Ohio: A John Wiley & Sons, Ltd., 2013.

[34] A. Olshevskiy., O. B. Alexey Olshevskiy and C.-w. Kim., "Finite element analysis of railway disc brake considering structural , thermal , and wear phenomena," pp. 1-16, 2011.

[35] A. AbuBakar and H. Ouyang, " “Wear prediction of friction material and brake squeal using the finite elementmethod”.," *Wear*, vol. 264, no. (11-12), p. 1069–1076, 2008.

[36] A. Rashid and N. Strömberg, "Thermomechanical Simulation of wear and hot bands in a disc brake by adopting Eularian Approach," 2013.

[37] T.Nellemann., N.Bay. and T.Wanheim., "Real area of contact and friction stress - The role of trapped lubricant," *Wear*, vol. 43, no. 1, pp. 45-53, 1977.

[38] L. K. L. H. e. a. Deng H, "Effect of brake pressure and brake speed on the tribological properties of carbon/ carbon composites with different pyrocarbon textures," p. 95–103, 2010.

[39] S. Kakad., R. More. and D. Kamble., "Mathematical Modeling & Analysis of Brake Pad for Wear Characteristics," pp. 1048-1056, 2017.

[40] H. O. a. Q. C. A. R. Abu Bakar, "Interface Pressure Distributions through Structural

Modifications," *SAE Technical Papers,* October 2003.

[41] J. Archard., "Contact and rubbing of flat surfaces," *Journal of Applied Physics,* vol. 24, pp. 981-988, 1953.

[42] S. Rhee., "Wear equation for polymers sliding against metal surfaces.," *wear,* vol. 16, pp. 431-445, 1970.

[43] H. C. S. K. O. K. a. R. H. Hohmann et al., "Contact analysis for drum brakes and disc brakes using ADINA.," *Computers and Structures,* vol. 72, p. 185–198., 1999.

[44] O. O. O. O. A. K. R. S. FONO-TAMO, "Weibull approach to brake pad wear analysis in the Nigerian Market," *Friction,* 2015.

[45] K. Ludema, friction, wear, lubrication a-textbook-in-tribology_3, New York: CRC Press, 1996.

[46] N. A. Pandya, "Computer Aided Design and Analysis of Disc Brake Rotors," *Advances in Automobile Engineering,* vol. 5, no. 2, 2015.

[47] P. Weichert DufreA noy, "Prediction of railway disc temperatures taking the bearing surface variations into account.," *Proc. IMechE, Part F: J. Rail and Rapid Transit,* pp. 209(F1), 67–76., 1995.

[48] C. R. G. CRECG, "South-north Line and East-west Line (Phase I) Light Rail EPC Project of Addis Ababa, Ethiopia," Addis Ababa, July, 2013.

[49] A. Belcohine., O. I. Abdullah., M. Bouchetara. and N. M. Ghazali, "Structural and Contact Analyis of a 3-Dimensional Disc-Pad Model with and without thermal Effects," *Turkish Journal of Engineering, Science and Technology,* vol. 04, pp. 188-202, 2014.

[50] S. J. S. J. a. J. C. H. Mazidi, "Mathematical Modeling of Heat Conduction in a Disk Brake System During Braking," *Asian Journal of Applied Sciences,,* vol. 4, no. 2, pp. 119-136., 2011.

[51] K. K. Leng, "Simulation of Temperature Distribution in Brake Discs," Department of Mechanical Engineering, National University of Singapore, 2008.

[52] X. a. J. Z.Lu, "Design and Control of Disc PMSM Directly Driven Wheel for Tramcar," Institute of Railway and Urban Rail TransitTongji University, , Shanghai, China., 2018.

[53] C.-D. C. M. N. A. R. A. B. A. Belhocine, "Thermal analysis of both ventilated and full disc brake rotorswith frictional heat generation," *Applied and Computational Mechanics*, vol. 8, p. 5–24, 2014.

APPENDIX A: AALRT E-W DISTANCE BETWEEN CONSECUTIVE STATIONS

Table 0.1: Addis Ababa LRT E-W distance between consecutive stations.

No	Addis Ababa LRT E-W route Station name	Addis Ababa LRT E-W route stations symbol	Station distance (km)
1	Ayat 2---------- Ayat	EW1----------EW2	1.30
2	Ayat1----------Meri/CMC 2	EW2----------EW3	1.034
3	Meri/CMC 2-------CMC 1	EW3----------EW4	0.896
4	CMC1---------- St. Michael Church	EW4----------EW5	0.865
5	St. Michael Church--Civil Service College	EW5----------EW6	0.785
6	Civil Service College---SahliteMhiret Church	EW6----------EW7	0.906
7	SahliteMhiret Church-----GurdSholla	EW7----------EW8	0.922
8	Gurd-Sholla----Megenagna/Adwa square	EW8----------EW9	1.004
9	Megenagna/Adwa square--Lem Hotel	EW9----------EW10	1.035
10	Lem Hotel--------Mazoria/Traffic Police	EW10----------EW11	0.838
11	Mazoria/Traffic Police HQ.-Chemical Corporation	EW11----------EW12	0.694
12	Chemical Corporation---Urael church	EW12----------EW13	0.875
13	Urael Church------ Yordanose Hotel	EW13----------EW14	0.570
14	Yordanose Hotel---Estifanose/Meskel Square2	EW14----------EW15	0.569
15	Estifanose/Meskel,Square2--Stadium/Meskel Square 1	EW15----------EW16	0.700
16	Stadium/Meskel Square1---La Gare	EW16----------EW17	0.865
17	LaGare----------Road Authority	EW17----------EW18	0.555
18	Road Authority-----Mexico Square	EW18----------EW19	0.554
19	Mexico Square----------Lideta	EW19----------EW20	0.936
20	Lideta----------Coca Cola	EW20----------EW21	0.848
21	Coca Cola----------Tor Hailoch	EW21----------EW22	1.149

[Source: Addis Ababa (E-W and N-S) route light rail transit project from ERC]

APPENDIX B: **CFX Inputs and Results**

Table 7.1 Domain Physics for CFX

Domain - Air	
Type	Fluid
Location	B413
Materials	
Air at 25 C	
Fluid Definition	Material Library
Morphology	Continuous Fluid
Settings	
Buoyancy Model	Non Buoyant
Domain Motion	Stationary
Reference Pressure	1.0000e+00 [atm]
Heat Transfer Model	Thermal Energy
Turbulence Model	k epsilon
Turbulent Wall Functions	Scalable
Domain - Backplate	
Type	Solid
Location	B93
Settings	
Domain Motion	Stationary
Domain - Brake Pad	
Type	Solid
Location	B229
Settings	
Domain Motion	Stationary
Domain Interface - Default Fluid Solid Interface	
Boundary List1	Default Fluid Solid Interface Side 1
Boundary List2	Default Fluid Solid Interface Side 2, Default Fluid Solid Interface in Backplate Side 2

Interface Type	Fluid Solid
Settings	
Interface Models	General Connection
Heat Transfer	Conservative Interface Flux
Mesh Connection	GGI

Table 7.2: Boundary Physics for CFX

Domain	**Boundaries**		
Air	**Boundary - Inlet**		
	Type	INLET	
	Location	Inlet	
	Settings		
	Flow Regime	Subsonic	
	Heat Transfer	Static Temperature	
	Static Temperature	2.9800e+02 [K]	
	Mass And Momentum	Normal Speed	
	Normal Speed	1.94400e+01 [m s^-1]	
	Turbulence	Medium Intensity and Eddy Viscosity Ratio	
	Boundary - Default Fluid Solid Interface Side 1		
	Type	INTERFACE	
	Location	F420.413, F421.413, F422.413, F423.413, F424.413, F425.413, F426.413, F427.413, F428.413, F429.413, F430.413, F431.413, F432.413, F433.413, F434.413, F435.413, F436.413, F437.413, F438.413, F439.413, F440.413, F441.413, F442.413, F443.413, F444.413, F445.413, F446.413, F447.413, F448.413, F449.413, F450.413, F451.413, F452.413, F453.413, F454.413, F455.413, F456.413, F457.413, F458.413, F459.413, F460.413, F461.413, F462.413, F463.413, F464.413, F465.413, F466.413, F467.413, F468.413	

	Settings		
	Heat Transfer	Conservative Interface Flux	
	Mass and Momentum	No Slip Wall	
	Wall Roughness	Smooth Wall	
	Boundary - Outlet		
	Type	OUTLET	
	Location	Outlet	
	Settings		
	Flow Regime	Subsonic	
	Mass and Momentum	Average Static Pressure	
	Pressure Profile Blend	5.0000e-02	
	Relative Pressure	0.0000e+00 [Pa]	
	Pressure Averaging	Average Over Whole Outlet	
	Boundary - Air Default		
	Type	WALL	
	Location	F414.413, F415.413, F417.413, F419.413	
	Settings		
	Heat Transfer	Adiabatic	
	Mass and Momentum	No Slip Wall	
	Wall Roughness	Smooth Wall	
Backplate	**Boundary - Default Fluid Solid Interface in Backplate Side 2**		
	Type	INTERFACE	
	Location	F100.93, F101.93, F102.93, F103.93, F104.93, F105.93, F106.93, F107.93, F108.93, F109.93, F110.93, F111.93, F112.93, F113.93, F114.93, F115.93, F116.93, F117.93, F118.93, F119.93, F120.93, F121.93, F122.93, F123.93, F124.93, F125.93, F126.93, F94.93, F95.93, F96.93, F97.93, F98.93, F99.93	
	Settings		
	Heat Transfer	Conservative Interface Flux	
Brake Pad	**Boundary - Default Fluid Solid**		

	Interface Side 2		
	Type	INTERFACE	
	Location	F225.229, F226.229, F227.229, F228.229, F231.229, F232.229, F234.229, F235.229, F236.229, F237.229, F238.229, F239.229, F240.229, F241.229	
	Settings		
	Heat Transfer	Conservative Interface Flux	
	Boundary - Surface		
	Type	WALL	
	Location	Surface	
	Settings		
	Heat Transfer	Fixed Temperature	
	Fixed Temperature	2.7300e+02 [K]	

APPENDIX C: **Brake Pad and Brake Disc Drawings**

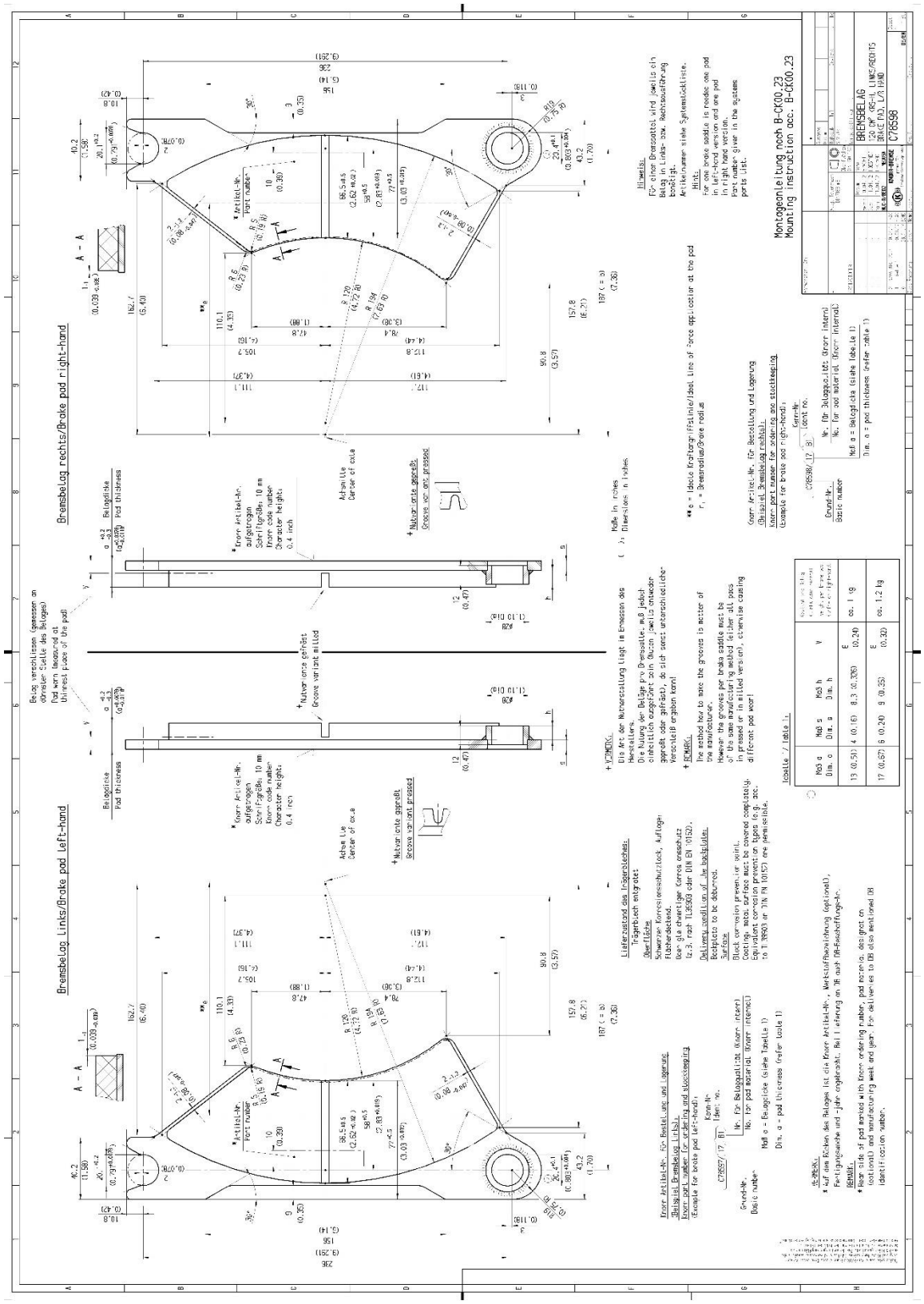

Figure 7.1 Brake Pad drawing dimensions

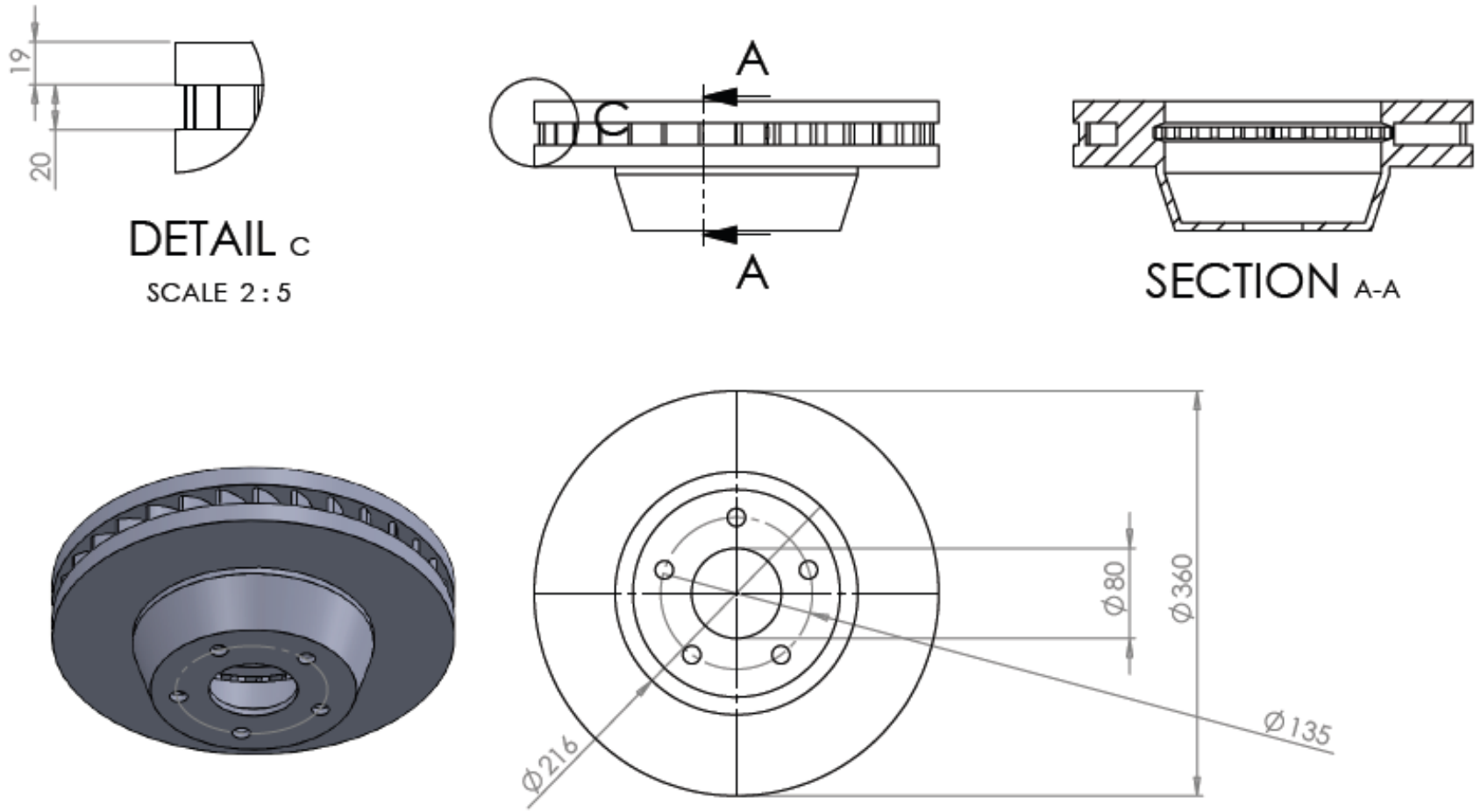

Figure 7.2: Brake disc drawing views

APPENDIX D: **Temperature Distribution and Contact Pressure values for Stations Chemical Corporation to Tor Hailoch**

Table 8.1:Table showing the temperatures during braking and cooling at different stations

Ayat 2 - Ayat 1		Ayat 1-CMC 2		CMC 2 - CMC 1		CMC 1 - ST. MICHEAL CHURCH		St Micheal Church - Civil Service College		Civil Service College-SahliteMhiret Church		SahliteMhiret Church-GurdSholla		GurdSholla-Megenagna/Adwa Square		Magenagna/Adwa Square-Lem Hotel		Lem Hotel-Mazoria/Traffic Police		Mazoria/Traffic Police-Chemical	
Time (S)	Temperature (oC)	Time (S)	Temperature (oC)	Time (S)	Temperature (oC)	Time (S)	Temperature (oC)	Time (S)	Temperature (oC)	Time (S)	Temperature (oC)	Time (S)	Temperature (oC)	Time (S)	Temperature (oC)	Time (S)	Temperature (oC)	Time (S)	Temperature (oC)	Time (S)	Temperature (oC)
0	**25**	**137**	**82.992**	**274**	**119.37**	**411**	**149.19**	**548**	**158.16**	**685**	**193.29**	**822**	**209.78**	**959**	**233.62**	**1096**	**248.4**	**1233**	**251.99**	**1370**	**265.05**
1	48.415	138	101.59	275	137.97	412	161.64	549	181.64	686	211.88	823	232.47	960	254.42	1097	265.81	1234	273.42	1371	283.64
2	59.199	139	110.62	276	146.99	413	167.66	550	193.03	687	220.89	824	243.46	961	264.49	1098	274.23	1235	283.79	1372	292.63
3	67.607	140	117.39	277	153.75	414	172.17	551	201.56	688	227.63	825	251.69	962	272.02	1099	280.51	1236	291.54	1373	299.34
4	74.666	141	123.07	278	159.41	415	175.93	552	208.7	689	233.25	826	258.56	963	278.3	1100	285.75	1237	298.01	1374	304.93
5	80.934	142	128.1	279	164.41	416	179.24	553	215.01	690	238.21	827	264.63	964	283.83	1101	290.35	1238	303.7	1375	309.84
6	86.68	143	132.7	280	168.99	417	182.26	554	220.78	691	242.72	828	270.16	965	288.87	1102	294.53	1239	308.88	1376	314.31
7	92.061	144	137	281	173.25	418	185.06	555	226.15	692	246.93	829	275.31	966	293.56	1103	298.41	1240	313.7	1377	318.45
8	97.179	145	141.08	282	177.3	419	187.72	556	231.25	693	250.91	830	280.18	967	297.99	1104	302.08	1241	318.26	1378	322.36
9	102.11	146	145	283	181.19	420	190.26	557	236.15	694	254.72	831	284.86	968	302.24	1105	305.59	1242	322.62	1379	326.11
10	106.89	147	148.81	284	184.96	421	192.72	558	240.89	695	258.41	832	289.38	969	306.34	1106	308.97	1243	326.84	1380	329.72
11	111.56	148	152.52	285	188.63	422	195.1	559	245.51	696	262	833	293.78	970	310.33	1107	312.26	1244	330.94	1381	333.23
12	116.15	149	156.16	286	192.22	423	197.44	560	250.03	697	265.51	834	298.09	971	314.23	1108	315.46	1245	334.94	1382	336.65
13	120.67	150	159.74	287	195.76	424	199.73	561	254.48	698	268.95	835	302.31	972	318.06	1109	318.61	1246	338.87	1383	340.01
14	125.14	151	163.27	288	199.24	425	201.99	562	258.86	699	272.35	836	306.48	973	321.83	1110	321.71	1247	342.74	1384	343.32
15	129.57	152	166.76	289	202.69	426	204.22	563	263.2	700	275.7	837	310.6	974	325.56	1111	324.76	1248	346.57	1385	346.58
16	133.96	153	170.23	290	206.11	427	206.43	564	267.49	701	279.02	838	314.68	975	329.24	1112	327.79	1249	350.35	1386	349.81
17	138.33	154	173.67	291	209.5	428	208.62	565	271.75	702	282.31	839	318.72	976	332.9	1113	330.78	1250	354.1	1387	353
18	121.35	155	159.92	292	195.71	429	199.31	566	254.33	703	268.44	840	301.82	977	317.35	1114	317.71	1251	338.07	1388	339.04
19	113.58	156	153.52	293	189.24	430	194.9	567	246.14	704	261.87	841	293.83	978	309.98	1115	311.47	1252	330.45	1389	332.37

20	109.11	157	149.8	294	185.45	431	192.27	568	241.33	705	257.96	842	289.09	979	305.58	1116	307.72	1253	325.9	1390	328.37
21	106.14	158	147.31	295	182.91	432	190.47	569	238.1	706	255.3	843	285.87	980	302.57	1117	305.14	1254	322.79	1391	325.61
22	104.05	159	145.52	296	181.07	433	189.15	570	235.76	707	253.36	844	283.54	981	300.37	1118	303.21	1255	320.5	1392	323.55
23	102.52	160	144.17	297	179.68	434	188.14	571	233.99	708	251.87	845	281.75	982	298.67	1119	301.72	1256	318.73	1393	321.96
24	101.35	161	143.13	298	178.59	435	187.32	572	232.59	709	250.67	846	280.31	983	297.3	1120	300.51	1257	317.31	1394	320.66
25	100.44	162	142.3	299	177.7	436	186.64	573	231.45	710	249.68	847	279.14	984	296.17	1121	299.49	1258	316.12	1395	319.57
26	99.718	163	141.62	300	176.97	437	186.07	574	230.51	711	248.85	848	278.15	985	295.21	1122	298.62	1259	315.11	1396	318.63
27	99.13	164	141.06	301	176.36	438	185.57	575	229.71	712	248.12	849	277.3	986	294.37	1123	297.85	1260	314.23	1397	317.81
28	98.647	165	140.59	302	175.83	439	185.12	576	229.02	713	247.49	850	276.55	987	293.63	1124	297.16	1261	313.45	1398	317.07
29	98.241	166	140.17	303	175.36	440	184.72	577	228.41	714	246.91	851	275.88	988	292.95	1125	296.52	1262	312.74	1399	316.39
30	97.892	167	139.81	304	174.94	441	184.35	578	227.86	715	246.39	852	275.26	989	292.34	1126	295.94	1263	312.08	1400	315.76
31	97.589	168	139.48	305	174.56	442	184.01	579	227.36	716	245.9	853	274.7	990	291.76	1127	295.38	1264	311.47	1401	315.17
32	97.319	169	139.18	306	174.21	443	183.69	580	226.89	717	245.44	854	274.17	991	291.22	1128	294.86	1265	310.9	1402	314.61
33	97.077	170	138.9	307	173.88	444	183.38	581	226.45	718	245	855	273.66	992	290.7	1129	294.36	1266	310.35	1403	314.07
34	96.856	171	138.64	308	173.57	445	183.08	582	226.04	719	244.58	856	273.18	993	290.2	1130	293.87	1267	309.81	1404	313.55
35	96.653	172	138.39	309	173.27	446	182.79	583	225.64	720	244.17	857	272.71	994	289.72	1131	293.39	1268	309.3	1405	313.04
36	96.462	173	138.16	310	172.98	447	182.51	584	225.25	721	243.78	858	272.26	995	289.24	1132	292.93	1269	308.8	1406	312.54
37	96.281	174	137.93	311	172.7	448	182.23	585	224.88	722	243.39	859	271.81	996	288.78	1133	292.47	1270	308.3	1407	312.05
38	96.108	175	137.71	312	172.42	449	181.96	586	224.51	723	243.01	860	271.38	997	288.33	1134	292.02	1271	307.82	1408	311.56
39	95.941	176	137.49	313	172.15	450	181.69	587	224.15	724	242.64	861	270.95	998	287.88	1135	291.57	1272	307.34	1409	311.09
40	95.779	177	137.28	314	171.89	451	181.43	588	223.8	725	242.27	862	270.53	999	287.44	1136	291.13	1273	306.86	1410	310.61
41	95.621	178	137.07	315	171.63	452	181.17	589	223.45	726	241.9	863	270.11	1000	287	1137	290.7	1274	306.39	1411	310.14
42	95.466	179	136.86	316	171.37	453	180.91	590	223.1	727	241.53	864	269.7	1001	286.56	1138	290.26	1275	305.93	1412	309.68
43	95.314	180	136.66	317	171.11	454	180.65	591	222.75	728	241.17	865	269.28	1002	286.13	1139	289.83	1276	305.46	1413	309.21

Ayat 2 - Ayat 1	Ayat 1-CMC 2	CMC 2 - CMC 1	CMC 1 - ST. MICHEAL CHURCH	St Micheal Church - Civil Service College	Civil Service College-SahliteMhiret Church	SahliteMhiret Church-GurdSholla	GurdSholla-Megenagna/Adwa	Magenagna/Adwa Square-Lem Hotel	Lem Hotel-Mazoria/Traffic	Mazoria/Traffic Police-Chemical

														Square				Police			
Time (S)	Temperature (oC)	Time (S)	Temperature (oC)	Time (S)	Temperature (oC)	Time (S)	Temperature (oC)	Time (S)	Temperature (oC)	Time (S)	Temperature (oC)	Time (S)	Temperature (oC)	Time (S)	Temperature (oC)	Time (S)	Temperature (oC)	Time (S)	Temperature (oC)	Time (S)	Temperature (oC)
44	95.164	181	136.45	318	170.85	455	180.39	592	222.41	729	240.81	866	268.87	1003	285.69	1140	289.4	1277	305	1414	308.75
45	95.015	182	136.25	319	170.6	456	180.13	593	222.07	730	240.45	867	268.46	1004	285.26	1141	288.97	1278	304.54	1415	308.29
46	94.868	183	136.05	320	170.35	457	179.88	594	221.73	731	240.1	868	268.06	1005	284.84	1142	288.54	1279	304.08	1416	307.83
47	94.722	184	135.85	321	170.1	458	179.62	595	221.4	732	239.74	869	267.65	1006	284.41	1143	288.11	1280	303.62	1417	307.37
48	94.576	185	135.65	322	169.85	459	179.37	596	221.06	733	239.39	870	267.25	1007	283.98	1144	287.69	1281	303.17	1418	306.92
49	94.431	186	135.45	323	169.6	460	179.12	597	220.73	734	239.03	871	266.84	1008	283.56	1145	287.26	1282	302.71	1419	306.46
50	94.287	187	135.26	324	169.35	461	178.86	598	220.39	735	238.68	872	266.44	1009	283.13	1146	286.84	1283	302.25	1420	306
51	94.143	188	135.06	325	169.1	462	178.61	599	220.06	736	238.32	873	266.04	1010	282.71	1147	286.41	1284	301.8	1421	305.55
52	94	189	134.86	326	168.85	463	178.36	600	219.72	737	237.97	874	265.64	1011	282.28	1148	285.99	1285	301.35	1422	305.09
53	93.857	190	134.66	327	168.6	464	178.11	601	219.39	738	237.62	875	265.24	1012	281.86	1149	285.57	1286	300.89	1423	304.64
54	93.714	191	134.47	328	168.35	465	177.85	602	219.06	739	237.27	876	264.84	1013	281.44	1150	285.14	1287	300.44	1424	304.19
55	93.572	192	134.27	329	168.11	466	177.6	603	218.73	740	236.92	877	264.44	1014	281.02	1151	284.72	1288	299.99	1425	303.73
56	93.429	193	134.08	330	167.86	467	177.35	604	218.4	741	236.57	878	264.04	1015	280.6	1152	284.3	1289	299.54	1426	303.28
57	93.287	194	133.88	331	167.61	468	177.1	605	218.07	742	236.21	879	263.64	1016	280.17	1153	283.88	1290	299.09	1427	302.83
58	93.146	195	133.69	332	167.37	469	176.85	606	217.74	743	235.87	880	263.24	1017	279.75	1154	283.46	1291	298.64	1428	302.38
59	93.004	196	133.49	333	167.12	470	176.6	607	217.41	744	235.52	881	262.85	1018	279.34	1155	283.04	1292	298.19	1429	301.93
60	92.863	197	133.3	334	166.88	471	176.35	608	217.08	745	235.17	882	262.45	1019	278.92	1156	282.62	1293	297.75	1430	301.48
61	92.722	198	133.1	335	166.63	472	176.1	609	216.75	746	234.82	883	262.05	1020	278.5	1157	282.2	1294	297.3	1431	301.03
62	92.581	199	132.91	336	166.39	473	175.85	610	216.42	747	234.47	884	261.66	1021	278.08	1158	281.78	1295	296.85	1432	300.58
63	92.441	200	132.72	337	166.14	474	175.6	611	216.09	748	234.12	885	261.26	1022	277.66	1159	281.37	1296	296.4	1433	300.13
64	92.3	201	132.52	338	165.9	475	175.35	612	215.76	749	233.78	886	260.87	1023	277.25	1160	280.95	1297	295.96	1434	299.69
65	92.16	202	132.33	339	165.66	476	175.11	613	215.44	750	233.43	887	260.47	1024	276.83	1161	280.53	1298	295.51	1435	299.24

Ayat 2 - Ayat 1		Ayat 1-CMC 2		CMC 2 - CMC 1		CMC 1 - ST. MICHEAL CHURCH		St Micheal Church - Civil Service College		Civil Service College-SahliteMhiret Church		SahliteMhiret Church-GurdSholla		GurdSholla-Megenagna/Adwa Square		Magenagna/Adwa Square-Lem Hotel		Lem Hotel-Mazoria/Traffic Police		Mazoria/Traffic Police-Chemical	
Time (S)	Temperature (oC)	Time (S)	Temperature (oC)	Time (S)	Temperature (oC)	Time (S)	Temperature (oC)	Time (S)	Temperature (oC)	Time (S)	Temperature (oC)	Time (S)	Temperature (oC)	Time (S)	Temperature (oC)	Time (S)	Temperature (oC)	Time (S)	Temperature (oC)	Time (S)	Temperature (oC)
66	92.021	203	132.14	340	165.41	477	174.86	614	215.11	751	233.08	888	260.08	1025	276.42	1162	280.12	1299	295.07	1436	298.79
67	91.882	204	131.95	341	165.17	478	174.61	615	214.79	752	232.74	889	259.69	1026	276	1163	279.7	1300	294.62	1437	298.35
68	91.743	205	131.75	342	164.93	479	174.36	616	214.46	753	232.39	890	259.29	1027	275.59	1164	279.29	1301	294.18	1438	297.9
69	91.604	206	131.56	343	164.69	480	174.12	617	214.14	754	232.05	891	258.9	1028	275.17	1165	278.87	1302	293.74	1439	297.46
70	91.466	207	131.37	344	164.45	481	173.87	618	213.81	755	231.7	892	258.51	1029	274.76	1166	278.46	1303	293.29	1440	297.01
71	91.328	208	131.18	345	164.2	482	173.63	619	213.49	756	231.36	893	258.12	1030	274.35	1167	278.04	1304	292.85	1441	296.57
72	91.19	209	130.99	346	163.96	483	173.38	620	213.17	757	231.02	894	257.73	1031	273.94	1168	277.63	1305	292.41	1442	296.13
73	91.052	210	130.8	347	163.72	484	173.13	621	212.84	758	230.67	895	257.34	1032	273.52	1169	277.22	1306	291.97	1443	295.69
74	90.915	211	130.61	348	163.48	485	172.89	622	212.52	759	230.33	896	256.95	1033	273.11	1170	276.81	1307	291.53	1444	295.24
75	90.778	212	130.42	349	163.24	486	172.64	623	212.2	760	229.99	897	256.56	1034	272.7	1171	276.4	1308	291.09	1445	294.8
76	90.642	213	130.23	350	163	487	172.4	624	211.88	761	229.65	898	256.17	1035	272.29	1172	275.99	1309	290.65	1446	294.36
77	90.505	214	130.04	351	162.77	488	172.16	625	211.56	762	229.31	899	255.79	1036	271.88	1173	275.58	1310	290.21	1447	293.92
78	90.369	215	129.85	352	162.53	489	171.91	626	211.24	763	228.97	900	255.4	1037	271.47	1174	275.17	1311	289.78	1448	293.48
79	90.234	216	129.66	353	162.29	490	171.67	627	210.92	764	228.63	901	255.01	1038	271.07	1175	274.76	1312	289.34	1449	293.05
80	90.098	217	129.48	354	162.05	491	171.43	628	210.6	765	228.29	902	254.63	1039	270.66	1176	274.35	1313	288.9	1450	292.61
81	89.963	218	129.29	355	161.82	492	171.18	629	210.28	766	227.95	903	254.24	1040	270.25	1177	273.94	1314	288.47	1451	292.17
82	89.829	219	129.1	356	161.58	493	170.94	630	209.96	767	227.61	904	253.86	1041	269.85	1178	273.54	1315	288.03	1452	291.73
83	89.694	220	128.91	357	161.34	494	170.7	631	209.65	768	227.28	905	253.47	1042	269.44	1179	273.13	1316	287.6	1453	291.3
84	89.56	221	128.73	358	161.11	495	170.46	632	209.33	769	226.94	906	253.09	1043	269.04	1180	272.72	1317	287.16	1454	290.86
85	89.427	222	128.54	359	160.87	496	170.22	633	209.01	770	226.6	907	252.71	1044	268.63	1181	272.32	1318	286.73	1455	290.43
86	89.294	223	128.36	360	160.64	497	169.98	634	208.7	771	226.27	908	252.33	1045	268.23	1182	271.91	1319	286.3	1456	289.99

Ayat 2 - Ayat 1		Ayat 1-CMC 2		CMC 2 - CMC 1		CMC 1 - ST. MICHEAL CHURCH		St Micheal Church - Civil Service College		Civil Service College-SahliteMhiret Church		SahliteMhiret Church-GurdSholla		GurdSholla-Megenagna/Adwa Square		Magenagna/Adwa Square-Lem Hotel		Lem Hotel-Mazoria/Traffic Police		Mazoria/Traffic Police-Chemical	
Time (S)	Temperature (oC)	Time (S)	Temperature (oC)	Time (S)	Temperature (oC)	Time (S)	Temperature (oC)	Time (S)	Temperature (oC)	Time (S)	Temperature (oC)	Time (S)	Temperature (oC)	Time (S)	Temperature (oC)	Time (S)	Temperature (oC)	Time (S)	Temperature (oC)	Time (S)	Temperature (oC)
87	89.161	224	128.17	361	160.4	498	169.74	635	208.38	772	225.93	909	251.95	1046	267.82	1183	271.51	1320	285.86	1457	289.56
88	89.028	225	127.99	362	160.17	499	169.5	636	208.07	773	225.59	910	251.57	1047	267.42	1184	271.1	1321	285.43	1458	289.13
89	88.896	226	127.8	363	159.94	500	169.26	637	207.75	774	225.26	911	251.19	1048	267.02	1185	270.7	1322	285	1459	288.69
90	88.765	227	127.62	364	159.7	501	169.02	638	207.44	775	224.93	912	250.81	1049	266.62	1186	270.3	1323	284.57	1460	288.26
91	88.633	228	127.44	365	159.47	502	168.78	639	207.13	776	224.59	913	250.43	1050	266.22	1187	269.9	1324	284.14	1461	287.83
92	88.502	229	127.25	366	159.24	503	168.54	640	206.81	777	224.26	914	250.05	1051	265.81	1188	269.49	1325	283.71	1462	287.4
93	88.372	230	127.07	367	159	504	168.3	641	206.5	778	223.93	915	249.67	1052	265.42	1189	269.09	1326	283.28	1463	286.97
94	88.242	231	126.89	368	158.77	505	168.06	642	206.19	779	223.59	916	249.29	1053	265.02	1190	268.69	1327	282.86	1464	286.54
95	88.112	232	126.7	369	158.54	506	167.82	643	205.88	780	223.26	917	248.92	1054	264.62	1191	268.29	1328	282.43	1465	286.11
96	87.982	233	126.52	370	158.31	507	167.59	644	205.57	781	222.93	918	248.54	1055	264.22	1192	267.89	1329	282	1466	285.68
97	87.853	234	126.34	371	158.08	508	167.35	645	205.26	782	222.6	919	248.17	1056	263.82	1193	267.5	1330	281.58	1467	285.25
98	87.725	235	126.16	372	157.85	509	167.11	646	204.95	783	222.27	920	247.79	1057	263.42	1194	267.1	1331	281.15	1468	284.83
99	87.596	236	125.98	373	157.62	510	166.88	647	204.64	784	221.94	921	247.42	1058	263.03	1195	266.7	1332	280.73	1469	284.4
100	87.469	237	125.8	374	157.39	511	166.64	648	204.33	785	221.61	922	247.04	1059	262.63	1196	266.3	1333	280.3	1470	283.97
101	87.341	238	125.62	375	157.16	512	166.41	649	204.02	786	221.28	923	246.67	1060	262.24	1197	265.91	1334	279.88	1471	283.55
102	87.214	239	125.44	376	156.93	513	166.17	650	203.72	787	220.96	924	246.3	1061	261.84	1198	265.51	1335	279.46	1472	283.12
103	87.087	240	125.26	377	156.71	514	165.94	651	203.41	788	220.63	925	245.92	1062	261.45	1199	265.11	1336	279.03	1473	282.7
104	86.961	241	125.08	378	156.48	515	165.7	652	203.1	789	220.3	926	245.55	1063	261.06	1200	264.72	1337	278.61	1474	282.27
105	86.835	242	124.9	379	156.25	516	165.47	653	202.8	790	219.97	927	245.18	1064	260.66	1201	264.32	1338	278.19	1475	281.85
106	86.709	243	124.72	380	156.02	517	165.23	654	202.49	791	219.65	928	244.81	1065	260.27	1202	263.93	1339	277.77	1476	281.43
107	86.583	244	124.54	381	155.8	518	165	655	202.19	792	219.32	929	244.44	1066	259.88	1203	263.54	1340	277.35	1477	281.01
108	86.458	245	124.37	382	155.57	519	164.77	656	201.88	793	219	930	244.07	1067	259.49	1204	263.14	1341	276.93	1478	280.58

Ayat 2 - Ayat 1		Ayat 1-CMC 2		CMC 2 - CMC 1		CMC 1 - ST. MICHEAL CHURCH		St Micheal Church - Civil Service College		Civil Service College-SahliteMhiret Church		SahliteMhiret Church-GurdSholla		GurdSholla-Megenagna/Adwa Square		Magenagna/Adwa Square-Lem Hotel		Lem Hotel-Mazoria/Traffic Police		Mazoria/Traffic Police-Chemical	
Time (S)	Temperature (oC)	Time (S)	Temperature (oC)	Time (S)	Temperature (oC)	Time (S)	Temperature (oC)	Time (S)	Temperature (oC)	Time (S)	Temperature (oC)	Time (S)	Temperature (oC)	Time (S)	Temperature (oC)	Time (S)	Temperature (oC)	Time (S)	Temperature (oC)	Time (S)	Temperature (oC)
109	86.334	246	124.19	383	155.35	520	164.53	657	201.58	794	218.67	931	243.7	1068	259.1	1205	262.75	1342	276.51	1479	280.16
110	86.209	247	124.01	384	155.12	521	164.3	658	201.28	795	218.35	932	243.34	1069	258.71	1206	262.36	1343	276.1	1480	279.74
111	86.085	248	123.84	385	154.9	522	164.07	659	200.97	796	218.02	933	242.97	1070	258.32	1207	261.97	1344	275.68	1481	279.32
112	85.962	249	123.66	386	154.67	523	163.84	660	200.67	797	217.7	934	242.6	1071	257.93	1208	261.58	1345	275.26	1482	278.9
113	85.839	250	123.48	387	154.45	524	163.61	661	200.37	798	217.38	935	242.24	1072	257.54	1209	261.19	1346	274.85	1483	278.48
114	85.716	251	123.31	388	154.22	525	163.37	662	200.07	799	217.06	936	241.87	1073	257.15	1210	260.8	1347	274.43	1484	278.07
115	85.594	252	123.13	389	154	526	163.14	663	199.77	800	216.74	937	241.51	1074	256.77	1211	260.41	1348	274.02	1485	277.65
116	85.472	253	122.96	390	153.78	527	162.91	664	199.47	801	216.41	938	241.14	1075	256.38	1212	260.02	1349	273.6	1486	277.23
117	85.351	254	122.79	391	153.55	528	162.68	665	199.17	802	216.09	939	240.78	1076	255.99	1213	259.63	1350	273.19	1487	276.82
118	85.23	255	122.61	392	153.33	529	162.45	666	198.87	803	215.77	940	240.41	1077	255.61	1214	259.25	1351	272.78	1488	276.4
119	85.109	256	122.44	393	153.11	530	162.22	667	198.57	804	215.45	941	240.05	1078	255.22	1215	258.86	1352	272.36	1489	275.99
120	84.988	257	122.27	394	152.89	531	162	668	198.27	805	215.13	942	239.69	1079	254.84	1216	258.47	1353	271.95	1490	275.57
121	84.868	258	122.09	395	152.67	532	161.77	669	197.97	806	214.82	943	239.33	1080	254.46	1217	258.09	1354	271.54	1491	275.16
122	84.748	259	121.92	396	152.45	533	161.54	670	197.68	807	214.5	944	238.97	1081	254.07	1218	257.7	1355	271.13	1492	274.75
123	84.629	260	121.75	397	152.23	534	161.31	671	197.38	808	214.18	945	238.61	1082	253.69	1219	257.32	1356	270.72	1493	274.33
124	84.51	261	121.58	398	152.01	535	161.08	672	197.09	809	213.86	946	238.25	1083	253.31	1220	256.93	1357	270.31	1494	273.92
125	84.391	262	121.4	399	151.79	536	160.86	673	196.79	810	213.55	947	237.89	1084	252.93	1221	256.55	1358	269.9	1495	273.51
126	84.273	263	121.23	400	151.57	537	160.63	674	196.5	811	213.23	948	237.53	1085	252.55	1222	256.17	1359	269.5	1496	273.1
127	84.155	264	121.06	401	151.35	538	160.4	675	196.2	812	212.91	949	237.17	1086	252.17	1223	255.79	1360	269.09	1497	272.69
128	84.037	265	120.89	402	151.13	539	160.18	676	195.91	813	212.6	950	236.81	1087	251.79	1224	255.4	1361	268.68	1498	272.28
129	83.919	266	120.72	403	150.91	540	159.95	677	195.61	814	212.28	951	236.45	1088	251.41	1225	255.02	1362	268.28	1499	271.87
130	83.802	267	120.55	404	150.7	541	159.72	678	195.32	815	211.97	952	236.1	1089	251.03	1226	254.64	1363	267.87	1500	271.46

Ayat 2 - Ayat 1		Ayat 1-CMC 2		CMC 2 - CMC 1		CMC 1 - ST. MICHEAL CHURCH		St Micheal Church - Civil Service College		Civil Service College-SahliteMhiret Church		SahliteMhiret Church-GurdSholla		GurdSholla-Megenagna/Adwa Square		Magenagna/Adwa Square-Lem Hotel		Lem Hotel-Mazoria/Traffic Police		Mazoria/Traffic Police-Chemical	
Time (S)	Temperature (oC)	Time (S)	Temperature (oC)	Time (S)	Temperature (oC)	Time (S)	Temperature (oC)	Time (S)	Temperature (oC)	Time (S)	Temperature (oC)	Time (S)	Temperature (oC)	Time (S)	Temperature (oC)	Time (S)	Temperature (oC)	Time (S)	Temperature (oC)	Time (S)	Temperature (oC)
131	83.685	268	120.38	405	150.48	542	159.5	679	195.03	816	211.66	953	235.74	1090	250.65	1227	254.26	1364	267.47	1501	271.05
132	83.569	269	120.21	406	150.26	543	159.27	680	194.74	817	211.34	954	235.39	1091	250.28	1228	253.88	1365	267.06	1502	270.65
133	83.453	270	120.04	407	150.05	544	159.05	681	194.45	818	211.03	955	235.03	1092	249.9	1229	253.5	1366	266.66	1503	270.24
134	83.337	271	119.88	408	149.83	545	158.83	682	194.16	819	210.72	956	234.68	1093	249.52	1230	253.12	1367	266.25	1504	269.83
135	83.222	272	119.71	409	149.62	546	158.6	683	193.87	820	210.4	957	234.32	1094	249.15	1231	252.75	1368	265.85	1505	269.43
136	83.107	273	119.54	410	149.4	547	158.38	684	193.58	821	210.09	958	233.97	1095	248.77	1232	252.37	1369	265.45	1506	269.02
137	82.992	274	119.37	411	149.19	548	158.16	685	193.29	822	209.78	959	233.62	1096	248.4	1233	251.99	1370	265.05	1507	268.62

Chemical corporation - Urael Church		Urael Church-Yordanose Hotel		Yordanose Hotel-Estifanose/Meskel Square2		Estifanose/Meskel Square2-Stadium/Meskel Square 1		Stadium/Meskel Square 1-La Gare		La Gare-Road Authority		Road Authority-Mexico Square		Mexico Square-Lideta		Lideta-Coca Cola		Coca Cola-Tor Hailoch		Tor Hailoch	
Time (S)	Temperature (oC)	Time (S)	Temperature (oC)	Time (S)	Temperature (oC)	Time (S)	Temperature (oC)	Time (S)	Temperature (oC)	Time (S)	Temperature (oC)	Time (S)	Temperature (oC)	Time (S)	Temperature (oC)	Time (S)	Temperature (oC)	Time (S)	Temperature (oC)	Time (S)	Temperature (oC)
1507	268.62	1644	267.33	1781	270.41	1918	283.78	2055	289.7	2192	288.8	2329	289.31	2466	293.85	2603	285.26	2740	298.85	2877	296.25
1508	285.43	1645	285.89	1782	293.28	1919	304.64	2056	308.26	2193	307.8	2330	310.02	2467	309.67	2604	309.28	2741	317.41	2878	315.21
1509	293.56	1646	294.86	1783	304.35	1920	314.73	2057	317.23	2194	317.1	2331	320.04	2468	317.31	2605	320.9	2742	326.38	2879	324.37
1510	299.62	1647	301.56	1784	312.62	1921	322.27	2058	323.92	2195	324	2332	327.51	2469	323	2606	329.59	2743	333.07	2880	331.21
1511	304.66	1648	307.14	1785	319.52	1922	328.55	2059	329.49	2196	329.7	2333	333.74	2470	327.72	2607	336.83	2744	338.63	2881	336.89
1512	309.09	1649	312.04	1786	325.59	1923	334.07	2060	334.38	2197	334.7	2334	339.22	2471	331.86	2608	343.21	2745	343.51	2882	341.89
1513	314.84	1650	316.5	1787	331.12	1924	339.09	2061	338.82	2198	339.3	2335	344.19	2472	335.62	2609	349.02	2746	347.94	2883	346.43
1514	317.72	1651	320.64	1788	336.26	1925	343.75	2062	342.93	2199	343.5	2336	348.81	2473	339.09	2610	354.41	2747	352.05	2884	350.63
1515	321	1652	324.54	1789	341.12	1926	348.15	2063	346.81	2200	347.5	2337	353.17	2474	342.36	2611	359.51	2748	355.93	2885	354.59
1516	324.25	1653	328.28	1790	345.78	1927	352.36	2064	350.53	2201	351.4	2338	357.35	2475	345.48	2612	364.4	2749	359.63	2886	358.39
1517	327.43	1654	331.88	1791	350.27	1928	356.42	2065	354.11	2202	355.1	2339	361.37	2476	348.49	2613	369.12	2750	363.2	2887	362.04
1518	330.53	1655	335.38	1792	354.64	1929	360.37	2066	357.58	2203	358.6	2340	365.29	2477	351.4	2614	373.71	2751	366.66	2888	365.59
1519	333.57	1656	338.79	1793	358.91	1930	364.23	2067	360.97	2204	362.1	2341	369.1	2478	354.24	2615	378.19	2752	370.04	2889	369.05
1520	336.56	1657	342.14	1794	363.1	1931	368.01	2068	364.29	2205	365.6	2342	372.85	2479	357.02	2616	382.59	2753	373.35	2890	372.45
1521	339.5	1658	345.44	1795	367.23	1932	371.73	2069	367.56	2206	368.9	2343	376.54	2480	359.75	2617	386.92	2754	376.61	2891	375.79
1522	342.4	1659	348.69	1796	371.31	1933	375.41	2070	370.79	2207	372.3	2344	380.17	2481	362.45	2618	391.2	2755	379.83	2892	379.08
1523	345.28	1660	351.91	1797	375.34	1934	379.04	2071	373.98	2208	375.6	2345	383.77	2482	365.11	2619	395.43	2756	383	2893	382.34
1524	348.13	1661	355.1	1798	379.34	1935	382.64	2072	377.13	2209	378.8	2346	387.34	2483	367.75	2620	399.62	2757	386.15	2894	385.56
1525	335.46	1662	341.15	1799	362.22	1936	366.98	2073	363.16	2210	364.5	2347	371.78	2484	355.78	2621	381.65	2758	372.16	2895	371.28
1526	329.39	1663	334.49	1800	354.09	1937	359.52	2074	356.47	2211	357.6	2348	364.36	2485	350.02	2622	373.1	2759	365.46	2896	364.45
1527	325.73	1664	330.49	1801	349.23	1938	355.04	2075	352.44	2212	353.5	2349	359.91	2486	346.52	2623	368	2760	361.42	2897	360.33
1528	323.19	1665	327.73	1802	345.91	1939	351.95	2076	349.65	2213	350.6	2350	356.83	2487	344.08	2624	364.5	2761	358.62	2898	357.48
1529	321.29	1666	325.68	1803	343.46	1940	349.66	2077	347.56	2214	348.5	2351	354.55	2488	342.24	2625	361.93	2762	356.51	2899	355.34
1530	319.81	1667	324.08	1804	341.57	1941	347.89	2078	345.93	2215	346.8	2352	352.78	2489	340.8	2626	359.93	2763	354.87	2900	353.68

Chemical corporation - Urael Church		Urael Church-Yordanose Hotel		Yordanose Hotel-Estifanose/Meskel Square2		Estifanose/Meskel Square2-Stadium/Meskel Square 1		Stadium/Meskel Square 1-La Gare		La Gare-Road Authority		Road Authority-Mexico Square		Mexico Square-Lideta		Lideta-Coca Cola		Coca Cola-Tor Hailoch		Tor Hailoch	
Time (S)	Temperature (oC)	Time (S)	Temperature (oC)	Time (S)	Temperature (oC)	Time (S)	Temperature (oC)	Time (S)	Temperature (oC)	Time (S)	Temperature (oC)	Time (S)	Temperature (oC)	Time (S)	Temperature (oC)	Time (S)	Temperature (oC)	Time (S)	Temperature (oC)	Time (S)	Temperature (oC)
1531	318.6	1668	322.78	1805	340.04	1942	346.45	2079	344.6	2216	345.4	2353	351.34	2490	339.6	2627	358.33	2764	353.53	2901	352.32
1532	317.57	1669	321.69	1806	338.77	1943	345.24	2080	343.48	2217	344.3	2354	350.13	2491	338.58	2628	356.99	2765	352.39	2902	351.17
1533	316.68	1670	320.75	1807	337.69	1944	344.21	2081	342.51	2218	343.3	2355	349.09	2492	337.7	2629	355.85	2766	351.41	2903	350.18
1534	315.9	1671	319.92	1808	336.75	1945	343.3	2082	341.65	2219	342.4	2356	348.17	2493	336.9	2630	354.86	2767	350.54	2904	349.3
1535	315.19	1672	319.18	1809	335.91	1946	342.48	2083	340.88	2220	341.7	2357	347.35	2494	336.18	2631	353.97	2768	349.75	2905	348.51
1536	314.54	1673	318.5	1810	335.14	1947	341.73	2084	340.16	2221	340.9	2358	346.6	2495	335.51	2632	353.17	2769	349.02	2906	347.78
1537	313.94	1674	317.87	1811	334.44	1948	341.04	2085	339.5	2222	340.3	2359	345.91	2496	334.88	2633	352.43	2770	348.35	2907	347.1
1538	313.36	1675	317.28	1812	333.78	1949	340.39	2086	338.87	2223	339.6	2360	345.25	2497	334.29	2634	351.73	2771	347.71	2908	346.46
1539	312.81	1676	316.71	1813	333.16	1950	339.78	2087	338.28	2224	339	2361	344.63	2498	333.71	2635	351.08	2772	347.1	2909	345.85
1540	312.29	1677	316.17	1814	332.57	1951	339.19	2088	337.7	2225	338.5	2362	344.03	2499	333.16	2636	350.45	2773	346.51	2910	345.26
1541	311.77	1678	315.64	1815	332	1952	338.61	2089	337.14	2226	337.9	2363	343.45	2500	332.62	2637	349.85	2774	345.94	2911	344.69
1542	311.27	1679	315.13	1816	331.44	1953	338.06	2090	336.6	2227	337.3	2364	342.89	2501	332.1	2638	349.26	2775	345.38	2912	344.13
1543	310.78	1680	314.62	1817	330.9	1954	337.51	2091	336.06	2228	336.8	2365	342.34	2502	331.58	2639	348.69	2776	344.83	2913	343.58
1544	310.3	1681	314.13	1818	330.37	1955	336.98	2092	335.54	2229	336.3	2366	341.8	2503	331.07	2640	348.13	2777	344.3	2914	343.04
1545	309.83	1682	313.65	1819	329.85	1956	336.45	2093	335.02	2230	335.8	2367	341.26	2504	330.57	2641	347.57	2778	343.76	2915	342.51
1546	309.36	1683	313.17	1820	329.33	1957	335.93	2094	334.51	2231	335.2	2368	340.74	2505	330.07	2642	347.03	2779	343.24	2916	341.99
1547	308.89	1684	312.69	1821	328.82	1958	335.41	2095	334	2232	334.7	2369	340.21	2506	329.57	2643	346.49	2780	342.72	2917	341.47
1548	308.43	1685	312.22	1822	328.31	1959	334.9	2096	333.49	2233	334.2	2370	339.7	2507	329.08	2644	345.95	2781	342.2	2918	340.95
1549	307.96	1686	311.75	1823	327.81	1960	334.39	2097	332.99	2234	333.7	2371	339.18	2508	328.59	2645	345.42	2782	341.68	2919	340.44
1550	307.51	1687	311.28	1824	327.31	1961	333.89	2098	332.49	2235	333.2	2372	338.67	2509	328.11	2646	344.89	2783	341.17	2920	339.93
1551	307.05	1688	310.81	1825	326.81	1962	333.39	2099	332	2236	332.7	2373	338.16	2510	327.62	2647	344.36	2784	340.66	2921	339.42
1552	306.59	1689	310.35	1826	326.32	1963	332.88	2100	331.5	2237	332.2	2374	337.65	2511	327.14	2648	343.84	2785	340.15	2922	338.91
1553	306.14	1690	309.89	1827	325.82	1964	332.38	2101	331.01	2238	331.7	2375	337.14	2512	326.66	2649	343.32	2786	339.64	2923	338.4
1554	305.69	1691	309.43	1828	325.33	1965	331.88	2102	330.51	2239	331.2	2376	336.64	2513	326.17	2650	342.8	2787	339.14	2924	337.9

Chemical corporation - Urael Church		Urael Church-Yordanose Hotel		Yordanose Hotel-Estifanose/Meskel Square2		Estifanose/Meskel Square2-Stadium/Meskel Square 1		Stadium/Meskel Square 1-La Gare		La Gare-Road Authority		Road Authority-Mexico Square		Mexico Square-Lideta		Lideta-Coca Cola		Coca Cola-Tor Hailoch		Tor Hailoch	
Time (S)	Temperature (oC)	Time (S)	Temperature (oC)	Time (S)	Temperature (oC)	Time (S)	Temperature (oC)	Time (S)	Temperature (oC)	Time (S)	Temperature (oC)	Time (S)	Temperature (oC)	Time (S)	Temperature (oC)	Time (S)	Temperature (oC)	Time (S)	Temperature (oC)	Time (S)	Temperature (oC)
1555	305.24	1692	308.97	1829	324.84	1966	331.39	2103	330.02	2240	330.7	2377	336.13	2514	325.69	2651	342.28	2788	338.63	2925	337.39
1556	304.79	1693	308.51	1830	324.35	1967	330.89	2104	329.53	2241	330.2	2378	335.63	2515	325.21	2652	341.76	2789	338.13	2926	336.89
1557	304.34	1694	308.05	1831	323.86	1968	330.39	2105	329.04	2242	329.8	2379	335.12	2516	324.73	2653	341.24	2790	337.63	2927	336.39
1558	303.89	1695	307.59	1832	323.37	1969	329.9	2106	328.55	2243	329.3	2380	334.62	2517	324.26	2654	340.72	2791	337.12	2928	335.89
1559	303.44	1696	307.13	1833	322.88	1970	329.4	2107	328.06	2244	328.8	2381	334.12	2518	323.78	2655	340.21	2792	336.62	2929	335.39
1560	302.99	1697	306.68	1834	322.39	1971	328.91	2108	327.57	2245	328.3	2382	333.62	2519	323.3	2656	339.69	2793	336.12	2930	334.89
1561	302.54	1698	306.22	1835	321.91	1972	328.42	2109	327.09	2246	327.8	2383	333.12	2520	322.82	2657	339.18	2794	335.62	2931	334.39
1562	302.09	1699	305.77	1836	321.42	1973	327.92	2110	326.6	2247	327.3	2384	332.62	2521	322.35	2658	338.66	2795	335.12	2932	333.89
1563	301.65	1700	305.31	1837	320.94	1974	327.43	2111	326.11	2248	326.8	2385	332.12	2522	321.87	2659	338.15	2796	334.62	2933	333.39
1564	301.2	1701	304.86	1838	320.45	1975	326.94	2112	325.63	2249	326.3	2386	331.62	2523	321.4	2660	337.64	2797	334.12	2934	332.89
1565	300.75	1702	304.4	1839	319.97	1976	326.45	2113	325.14	2250	325.8	2387	331.12	2524	320.92	2661	337.13	2798	333.63	2935	332.4
1566	300.31	1703	303.95	1840	319.48	1977	325.96	2114	324.66	2251	325.4	2388	330.63	2525	320.45	2662	336.61	2799	333.13	2936	331.9
1567	299.87	1704	303.5	1841	319	1978	325.47	2115	324.17	2252	324.9	2389	330.13	2526	319.98	2663	336.1	2800	332.63	2937	331.4
1568	299.42	1705	303.05	1842	318.52	1979	324.98	2116	323.69	2253	324.4	2390	329.63	2527	319.5	2664	335.59	2801	332.13	2938	330.91
1569	298.98	1706	302.59	1843	318.04	1980	324.49	2117	323.21	2254	323.9	2391	329.14	2528	319.03	2665	335.08	2802	331.64	2939	330.41
1570	298.54	1707	302.14	1844	317.56	1981	324	2118	322.72	2255	323.4	2392	328.64	2529	318.56	2666	334.57	2803	331.14	2940	329.92
1571	298.09	1708	301.69	1845	317.08	1982	323.52	2119	322.24	2256	322.9	2393	328.15	2530	318.09	2667	334.07	2804	330.65	2941	329.43
1572	297.65	1709	301.24	1846	316.6	1983	323.03	2120	321.76	2257	322.4	2394	327.66	2531	317.62	2668	333.56	2805	330.16	2942	328.94
1573	297.21	1710	300.79	1847	316.12	1984	322.54	2121	321.28	2258	322	2395	327.16	2532	317.15	2669	333.05	2806	329.66	2943	328.44
1574	296.77	1711	300.34	1848	315.64	1985	322.06	2122	320.8	2259	321.5	2396	326.67	2533	316.68	2670	332.55	2807	329.17	2944	327.95
1575	296.33	1712	299.9	1849	315.16	1986	321.57	2123	320.32	2260	321	2397	326.18	2534	316.21	2671	332.04	2808	328.68	2945	327.46
1576	295.89	1713	299.45	1850	314.68	1987	321.09	2124	319.84	2261	320.5	2398	325.69	2535	315.74	2672	331.54	2809	328.19	2946	326.97
1577	295.45	1714	299	1851	314.21	1988	320.61	2125	319.37	2262	320	2399	325.2	2536	315.27	2673	331.03	2810	327.7	2947	326.48
1578	295.01	1715	298.55	1852	313.73	1989	320.12	2126	318.89	2263	319.6	2400	324.71	2537	314.81	2674	330.53	2811	327.21	2948	325.99

Chemical corporation - Urael Church		Urael Church-Yordanose Hotel		Yordanose Hotel-Estifanose/Meskel Square2		Estifanose/Meskel Square2-Stadium/Meskel Square 1		Stadium/Meskel Square 1-La Gare		La Gare-Road Authority		Road Authority-Mexico Square		Mexico Square-Lideta		Lideta-Coca Cola		Coca Cola-Tor Hailoch		Tor Hailoch	
Time (S)	Temperature (oC)	Time (S)	Temperature (oC)	Time (S)	Temperature (oC)	Time (S)	Temperature (oC)	Time (S)	Temperature (oC)	Time (S)	Temperature (oC)	Time (S)	Temperature (oC)	Time (S)	Temperature (oC)	Time (S)	Temperature (oC)	Time (S)	Temperature (oC)	Time (S)	Temperature (oC)
1579	294.58	1716	298.11	1853	313.26	1990	319.64	2127	318.41	2264	319.1	2401	324.22	2538	314.34	2675	330.03	2812	326.72	2949	325.51
1580	294.14	1717	297.66	1854	312.78	1991	319.16	2128	317.94	2265	318.6	2402	323.73	2539	313.87	2676	329.52	2813	326.23	2950	325.02
1581	293.7	1718	297.22	1855	312.31	1992	318.68	2129	317.46	2266	318.1	2403	323.24	2540	313.41	2677	329.02	2814	325.74	2951	324.53
1582	293.27	1719	296.77	1856	311.83	1993	318.2	2130	316.98	2267	317.6	2404	322.76	2541	312.94	2678	328.52	2815	325.25	2952	324.04
1583	292.83	1720	296.33	1857	311.36	1994	317.72	2131	316.51	2268	317.2	2405	322.27	2542	312.48	2679	328.02	2816	324.76	2953	323.56
1584	292.39	1721	295.89	1858	310.89	1995	317.24	2132	316.04	2269	316.7	2406	321.78	2543	312.01	2680	327.52	2817	324.28	2954	323.07
1585	291.96	1722	295.45	1859	310.42	1996	316.76	2133	315.56	2270	316.2	2407	321.3	2544	311.55	2681	327.02	2818	323.79	2955	322.59
1586	291.53	1723	295	1860	309.95	1997	316.28	2134	315.09	2271	315.7	2408	320.81	2545	311.09	2682	326.53	2819	323.31	2956	322.1
1587	291.09	1724	294.56	1861	309.48	1998	315.81	2135	314.62	2272	315.3	2409	320.33	2546	310.63	2683	326.03	2820	322.82	2957	321.62
1588	290.66	1725	294.12	1862	309.01	1999	315.33	2136	314.15	2273	314.8	2410	319.85	2547	310.16	2684	325.53	2821	322.34	2958	321.14
1589	290.23	1726	293.68	1863	308.54	2000	314.85	2137	313.68	2274	314.3	2411	319.36	2548	309.7	2685	325.04	2822	321.85	2959	320.66
1590	289.8	1727	293.24	1864	308.07	2001	314.38	2138	313.21	2275	313.9	2412	318.88	2549	309.24	2686	324.54	2823	321.37	2960	320.17
1591	289.36	1728	292.8	1865	307.6	2002	313.9	2139	312.74	2276	313.4	2413	318.4	2550	308.78	2687	324.05	2824	320.89	2961	319.69
1592	288.93	1729	292.37	1866	307.14	2003	313.43	2140	312.27	2277	312.9	2414	317.92	2551	308.32	2688	323.55	2825	320.41	2962	319.21
1593	288.5	1730	291.93	1867	306.67	2004	312.96	2141	311.8	2278	312.4	2415	317.44	2552	307.86	2689	323.06	2826	319.93	2963	318.73
1594	288.07	1731	291.49	1868	306.2	2005	312.48	2142	311.33	2279	312	2416	316.96	2553	307.41	2690	322.57	2827	319.45	2964	318.25
1595	287.64	1732	291.06	1869	305.74	2006	312.01	2143	310.86	2280	311.5	2417	316.48	2554	306.95	2691	322.08	2828	318.97	2965	317.78
1596	287.22	1733	290.62	1870	305.27	2007	311.54	2144	310.4	2281	311	2418	316.01	2555	306.49	2692	321.58	2829	318.49	2966	317.3
1597	286.79	1734	290.19	1871	304.81	2008	311.07	2145	309.93	2282	310.6	2419	315.53	2556	306.04	2693	321.09	2830	318.01	2967	316.82
1598	286.36	1735	289.75	1872	304.35	2009	310.6	2146	309.47	2283	310.1	2420	315.05	2557	305.58	2694	320.6	2831	317.53	2968	316.35
1599	285.93	1736	289.32	1873	303.89	2010	310.13	2147	309	2284	309.6	2421	314.58	2558	305.13	2695	320.12	2832	317.06	2969	315.87
1600	285.51	1737	288.88	1874	303.42	2011	309.66	2148	308.54	2285	309.2	2422	314.1	2559	304.67	2696	319.63	2833	316.58	2970	315.4
1601	285.08	1738	288.45	1875	302.96	2012	309.19	2149	308.08	2286	308.7	2423	313.63	2560	304.22	2697	319.14	2834	316.1	2971	314.92
1602	284.66	1739	288.02	1876	302.5	2013	308.73	2150	307.61	2287	308.2	2424	313.15	2561	303.76	2698	318.65	2835	315.63	2972	314.45

Chemical corporation - Urael Church		Urael Church-Yordanose Hotel		Yordanose Hotel-Estifanose/Meskel Square2		Estifanose/Meskel Square2-Stadium/Meskel Square 1		Stadium/Meskel Square 1-La Gare		La Gare-Road Authority		Road Authority-Mexico Square		Mexico Square-Lideta		Lideta-Coca Cola		Coca Cola-Tor Hailoch		Tor Hailoch	
Time (S)	Temperature (oC)	Time (S)	Temperature (oC)	Time (S)	Temperature (oC)	Time (S)	Temperature (oC)	Time (S)	Temperature (oC)	Time (S)	Temperature (oC)	Time (S)	Temperature (oC)	Time (S)	Temperature (oC)	Time (S)	Temperature (oC)	Time (S)	Temperature (oC)	Time (S)	Temperature (oC)
1603	284.23	1740	287.59	1877	302.04	2014	308.26	2151	307.15	2288	307.8	2425	312.68	2562	303.31	2699	318.17	2836	315.15	2973	313.97
1604	283.81	1741	287.16	1878	301.59	2015	307.8	2152	306.69	2289	307.3	2426	312.21	2563	302.86	2700	317.68	2837	314.68	2974	313.5
1605	283.39	1742	286.73	1879	301.13	2016	307.33	2153	306.23	2290	306.9	2427	311.74	2564	302.41	2701	317.2	2838	314.21	2975	313.03
1606	282.97	1743	286.3	1880	300.67	2017	306.87	2154	305.77	2291	306.4	2428	311.26	2565	301.96	2702	316.71	2839	313.74	2976	312.56
1607	282.54	1744	285.87	1881	300.21	2018	306.4	2155	305.31	2292	305.9	2429	310.79	2566	301.51	2703	316.23	2840	313.26	2977	312.09
1608	282.12	1745	285.44	1882	299.76	2019	305.94	2156	304.85	2293	305.5	2430	310.32	2567	301.06	2704	315.75	2841	312.79	2978	311.62
1609	281.7	1746	285.01	1883	299.3	2020	305.48	2157	304.39	2294	305	2431	309.86	2568	300.61	2705	315.27	2842	312.32	2979	311.15
1610	281.28	1747	284.58	1884	298.85	2021	305.01	2158	303.94	2295	304.6	2432	309.39	2569	300.16	2706	314.79	2843	311.85	2980	310.68
1611	280.86	1748	284.16	1885	298.39	2022	304.55	2159	303.48	2296	304.1	2433	308.92	2570	299.71	2707	314.3	2844	311.38	2981	310.21
1612	280.44	1749	283.73	1886	297.94	2023	304.09	2160	303.02	2297	303.6	2434	308.45	2571	299.27	2708	313.82	2845	310.91	2982	309.75
1613	280.02	1750	283.31	1887	297.49	2024	303.63	2161	302.57	2298	303.2	2435	307.99	2572	298.82	2709	313.35	2846	310.45	2983	309.28
1614	279.61	1751	282.88	1888	297.03	2025	303.17	2162	302.11	2299	302.7	2436	307.52	2573	298.37	2710	312.87	2847	309.98	2984	308.81
1615	279.19	1752	282.46	1889	296.58	2026	302.72	2163	301.66	2300	302.3	2437	307.05	2574	297.93	2711	312.39	2848	309.51	2985	308.35
1616	278.77	1753	282.03	1890	296.13	2027	302.26	2164	301.2	2301	301.8	2438	306.59	2575	297.48	2712	311.91	2849	309.05	2986	307.88
1617	278.36	1754	281.61	1891	295.68	2028	301.8	2165	300.75	2302	301.4	2439	306.13	2576	297.04	2713	311.44	2850	308.58	2987	307.42
1618	277.94	1755	281.19	1892	295.23	2029	301.34	2166	300.3	2303	300.9	2440	305.66	2577	296.59	2714	310.96	2851	308.12	2988	306.96
1619	277.53	1756	280.77	1893	294.78	2030	300.89	2167	299.85	2304	300.5	2441	305.2	2578	296.15	2715	310.49	2852	307.65	2989	306.49
1620	277.11	1757	280.35	1894	294.33	2031	300.43	2168	299.4	2305	300	2442	304.74	2579	295.71	2716	310.01	2853	307.19	2990	306.03
1621	276.7	1758	279.92	1895	293.89	2032	299.98	2169	298.95	2306	299.5	2443	304.28	2580	295.27	2717	309.54	2854	306.73	2991	305.57
1622	276.28	1759	279.5	1896	293.44	2033	299.52	2170	298.5	2307	299.1	2444	303.82	2581	294.83	2718	309.07	2855	306.26	2992	305.11
1623	275.87	1760	279.08	1897	292.99	2034	299.07	2171	298.05	2308	298.6	2445	303.36	2582	294.38	2719	308.6	2856	305.8	2993	304.65
1624	275.46	1761	278.67	1898	292.55	2035	298.62	2172	297.6	2309	298.2	2446	302.9	2583	293.94	2720	308.12	2857	305.34	2994	304.19
1625	275.05	1762	278.25	1899	292.1	2036	298.16	2173	297.15	2310	297.7	2447	302.44	2584	293.5	2721	307.65	2858	304.88	2995	303.73
1626	274.64	1763	277.83	1900	291.66	2037	297.71	2174	296.7	2311	297.3	2448	301.98	2585	293.07	2722	307.18	2859	304.42	2996	303.27

Chemical corporation - Urael Church		Urael Church-Yordanose Hotel		Yordanose Hotel-Estifanose/Meskel Square2		Estifanose/Meskel Square2-Stadium/Meskel Square 1		Stadium/Meskel Square 1-La Gare		La Gare-Road Authority		Road Authority-Mexico Square		Mexico Square-Lideta		Lideta-Coca Cola		Coca Cola-Tor Hailoch		Tor Hailoch	
Time (S)	Temperature (oC)	Time (S)	Temperature (oC)	Time (S)	Temperature (oC)	Time (S)	Temperature (oC)	Time (S)	Temperature (oC)	Time (S)	Temperature (oC)	Time (S)	Temperature (oC)	Time (S)	Temperature (oC)	Time (S)	Temperature (oC)	Time (S)	Temperature (oC)	Time (S)	Temperature (oC)
1627	274.23	1764	277.41	1901	291.22	2038	297.26	2175	296.25	2312	296.8	2449	301.52	2586	292.63	2723	306.72	2860	303.96	2997	302.81
1628	273.82	1765	277	1902	290.77	2039	296.81	2176	295.81	2313	296.4	2450	301.07	2587	292.19	2724	306.25	2861	303.5	2998	302.36
1629	273.41	1766	276.58	1903	290.33	2040	296.36	2177	295.36	2314	296	2451	300.61	2588	291.75	2725	305.78	2862	303.04	2999	301.9
1630	273	1767	276.16	1904	289.89	2041	295.91	2178	294.92	2315	295.5	2452	300.15	2589	291.32	2726	305.31	2863	302.59	3000	301.45
1631	272.59	1768	275.75	1905	289.45	2042	295.47	2179	294.47	2316	295.1	2453	299.7	2590	290.88	2727	304.85	2864	302.13	3001	300.99
1632	272.18	1769	275.34	1906	289.01	2043	295.02	2180	294.03	2317	294.6	2454	299.25	2591	290.44	2728	304.38	2865	301.68	3002	300.54
1633	271.77	1770	274.92	1907	288.57	2044	294.57	2181	293.59	2318	294.2	2455	298.79	2592	290.01	2729	303.92	2866	301.22	3003	300.08
1634	271.37	1771	274.51	1908	288.13	2045	294.12	2182	293.14	2319	293.7	2456	298.34	2593	289.57	2730	303.45	2867	300.77	3004	299.63
1635	270.96	1772	274.1	1909	287.69	2046	293.68	2183	292.7	2320	293.3	2457	297.89	2594	289.14	2731	302.99	2868	300.31	3005	299.18
1636	270.56	1773	273.68	1910	287.26	2047	293.23	2184	292.26	2321	292.8	2458	297.43	2595	288.71	2732	302.52	2869	299.86	3006	298.72
1637	270.15	1774	273.27	1911	286.82	2048	292.79	2185	291.82	2322	292.4	2459	296.98	2596	288.27	2733	302.06	2870	299.41	3007	298.27
1638	269.75	1775	272.86	1912	286.38	2049	292.35	2186	291.38	2323	292	2460	296.53	2597	287.84	2734	301.6	2871	298.95	3008	297.82
1639	269.34	1776	272.45	1913	285.95	2050	291.9	2187	290.94	2324	291.5	2461	296.08	2598	287.41	2735	301.14	2872	298.5	3009	297.37
1640	268.94	1777	272.04	1914	285.51	2051	291.46	2188	290.5	2325	291.1	2462	295.63	2599	286.98	2736	300.68	2873	298.05	3010	296.92
1641	268.54	1778	271.63	1915	285.08	2052	291.02	2189	290.06	2326	290.6	2463	295.19	2600	286.55	2737	300.22	2874	297.6	3011	296.47
1642	268.14	1779	271.22	1916	284.64	2053	290.58	2190	289.62	2327	290.2	2464	294.74	2601	286.12	2738	299.76	2875	297.15	3012	296.03
1643	267.73	1780	270.82	1917	284.21	2054	290.14	2191	289.19	2328	289.8	2465	294.29	2602	285.69	2739	299.3	2876	296.7	3013	295.58
1644	267.33	1781	270.41	1918	283.78	2055	289.7	2192	288.75	2329	289.3	2466	293.85	2603	285.26	2740	298.85	2877	296.25	3014	295.13

Chemical corporation

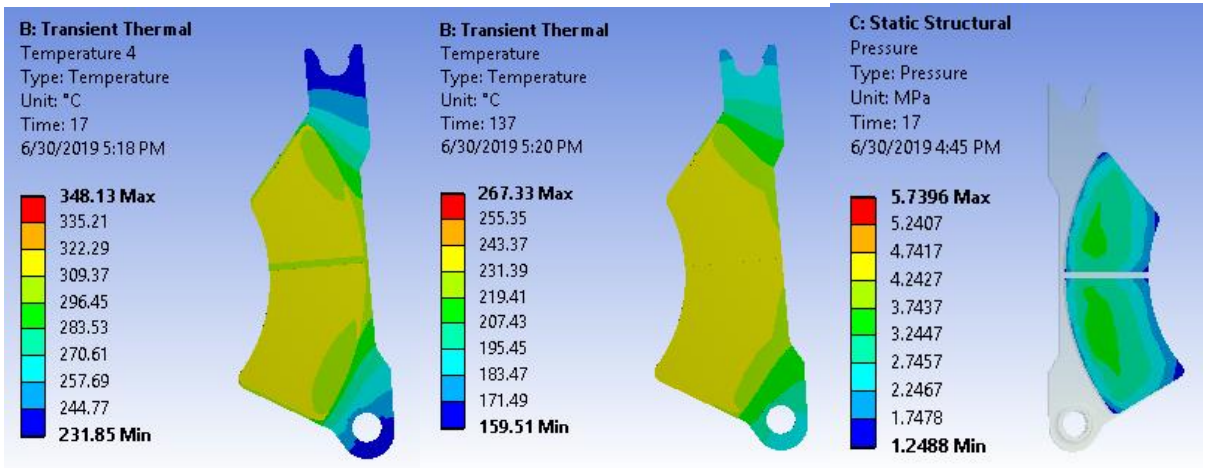

Urael church

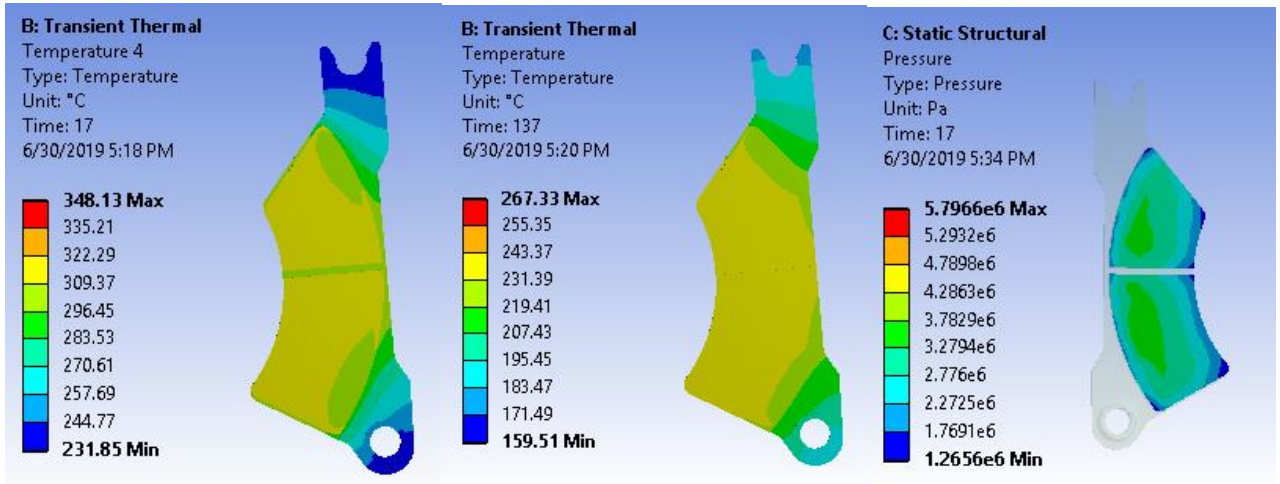

Yordanose Hotel

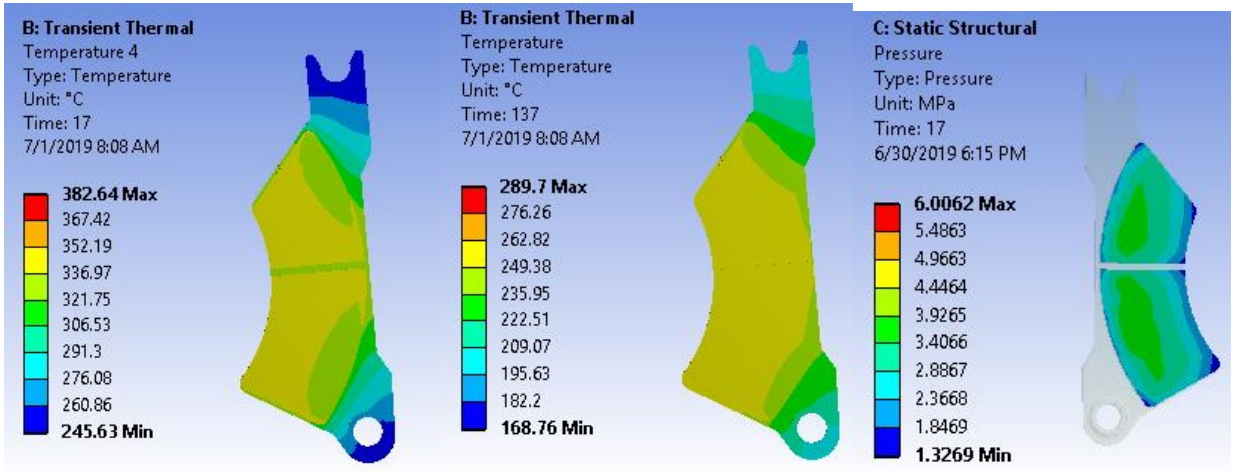

Estifanose/Meskel Square2

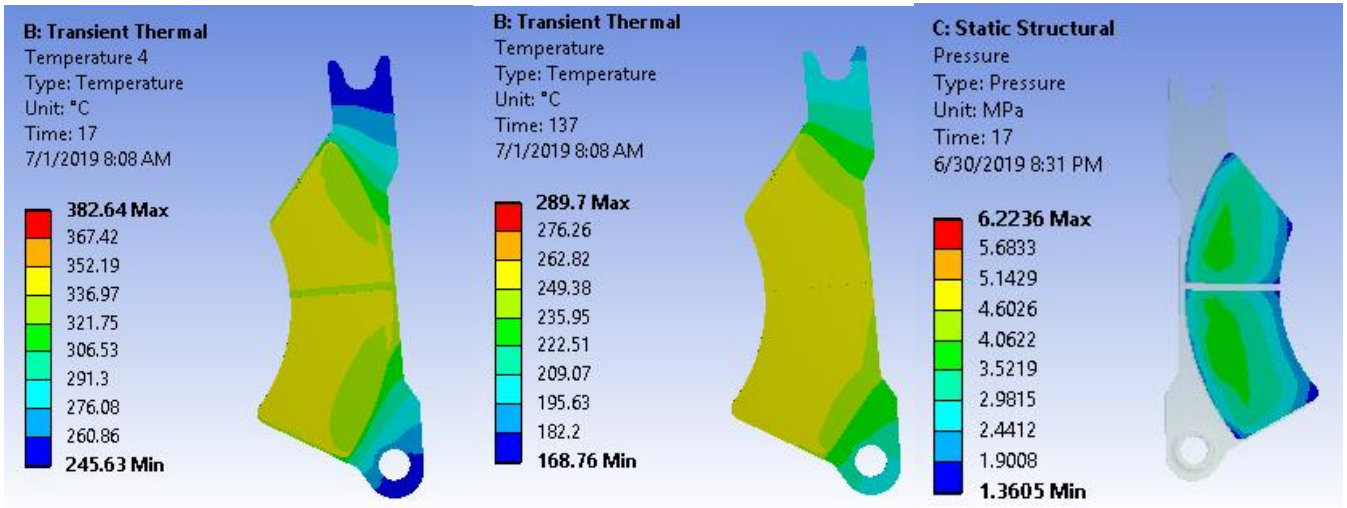

Stadium/Meskel Square 1

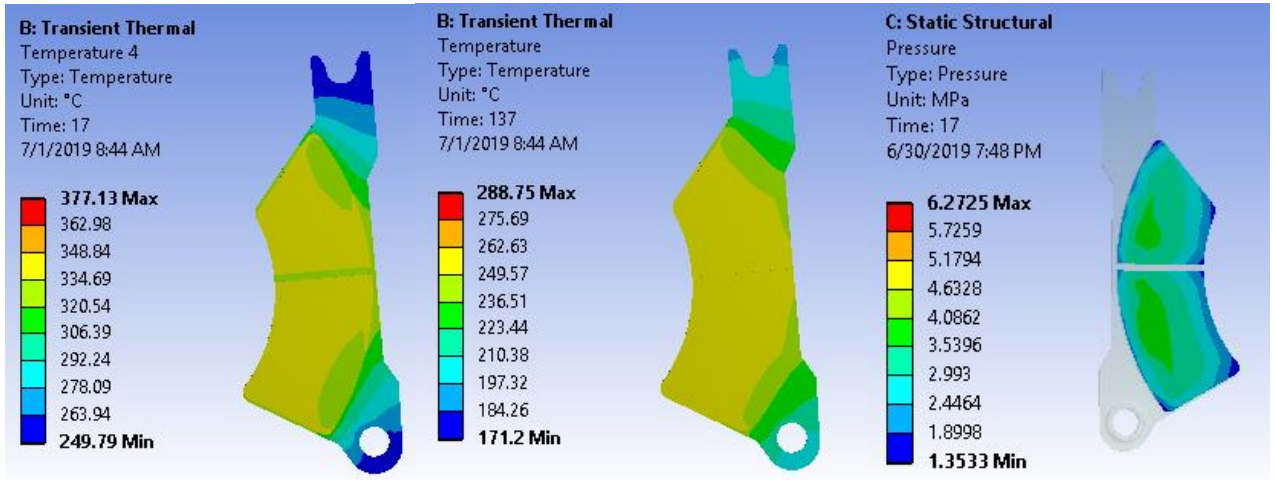

La Gare

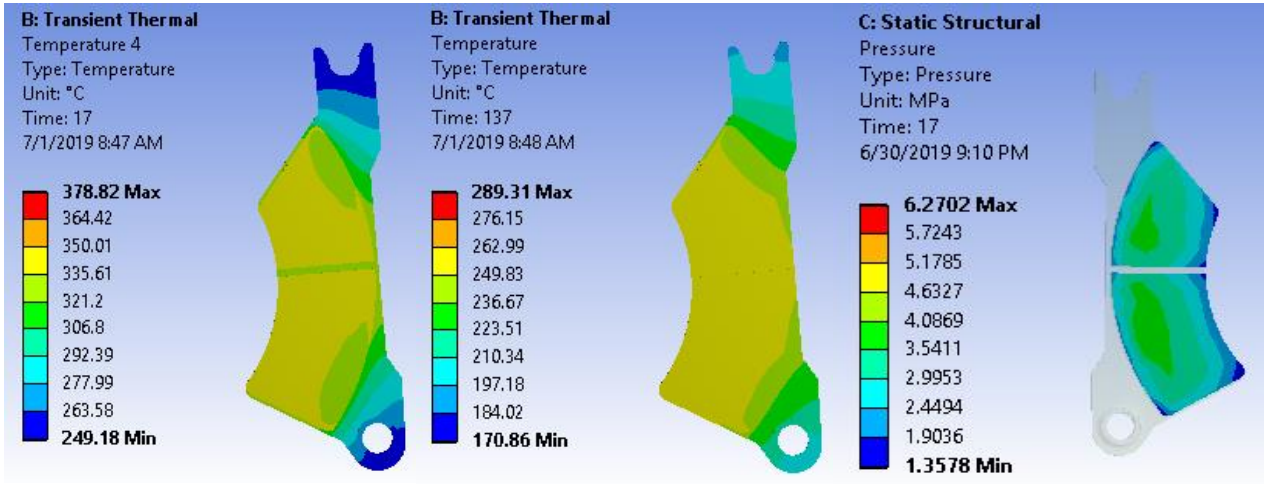

Road Authority

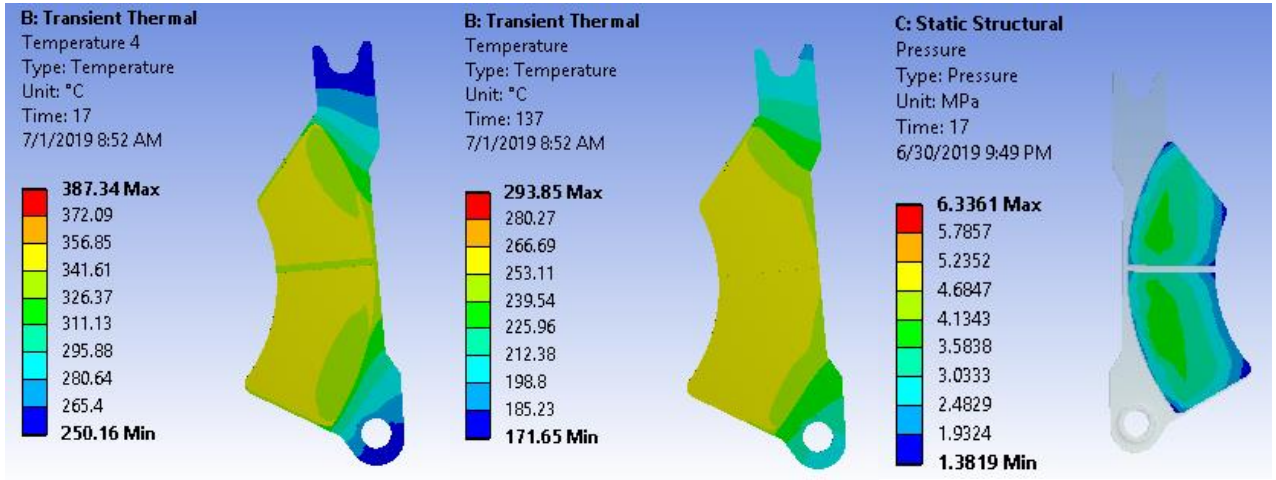

Mexico Square

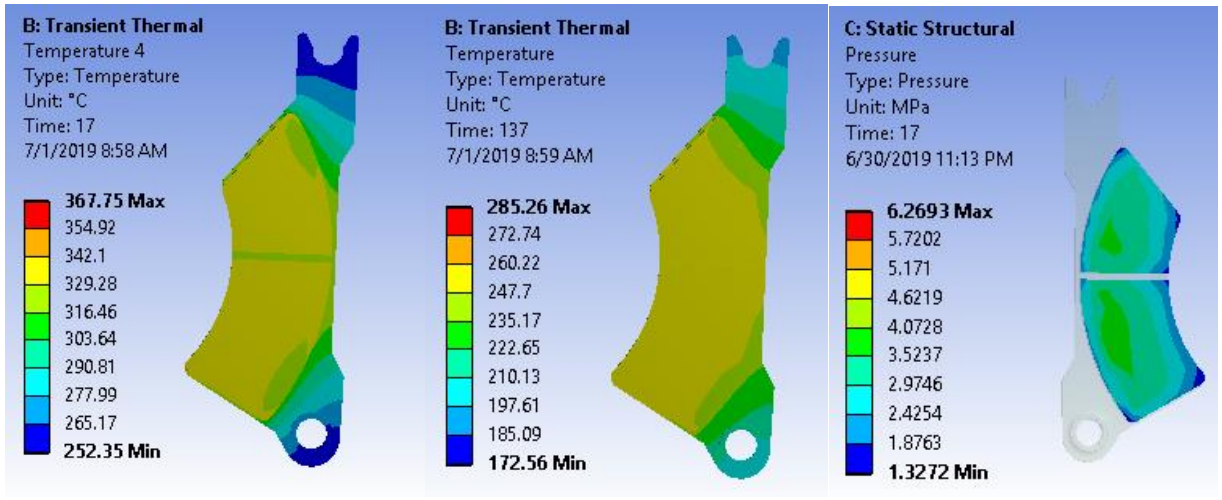

Lideta

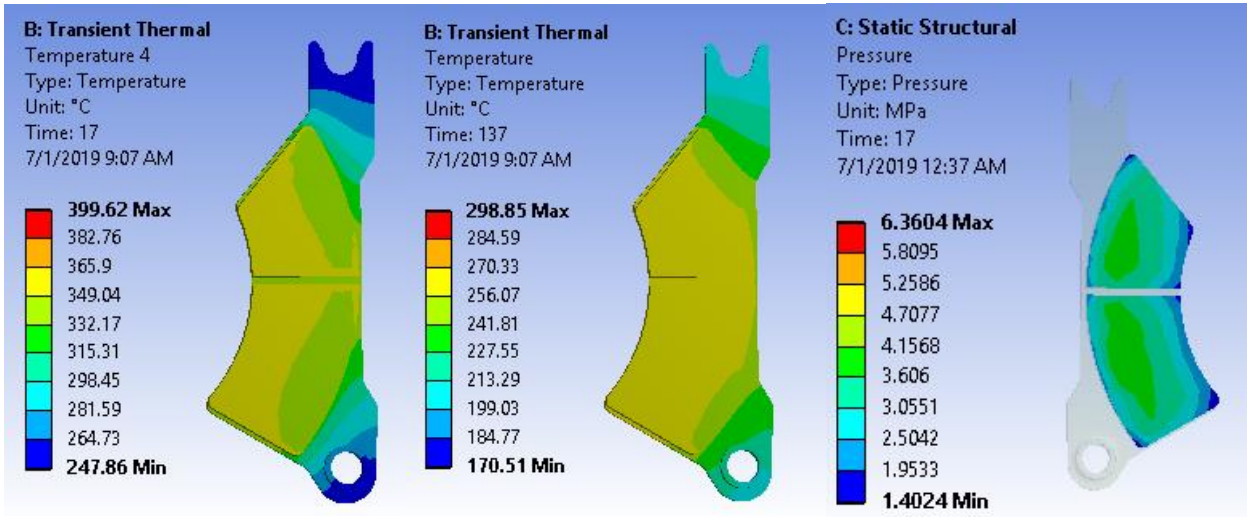

Coca Cola

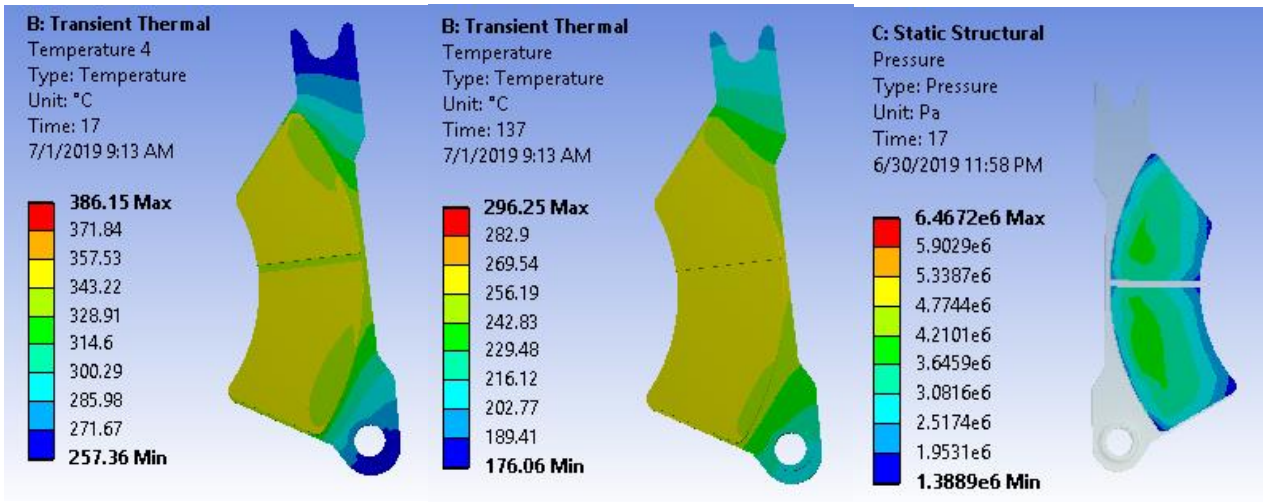

Tor Hailoch

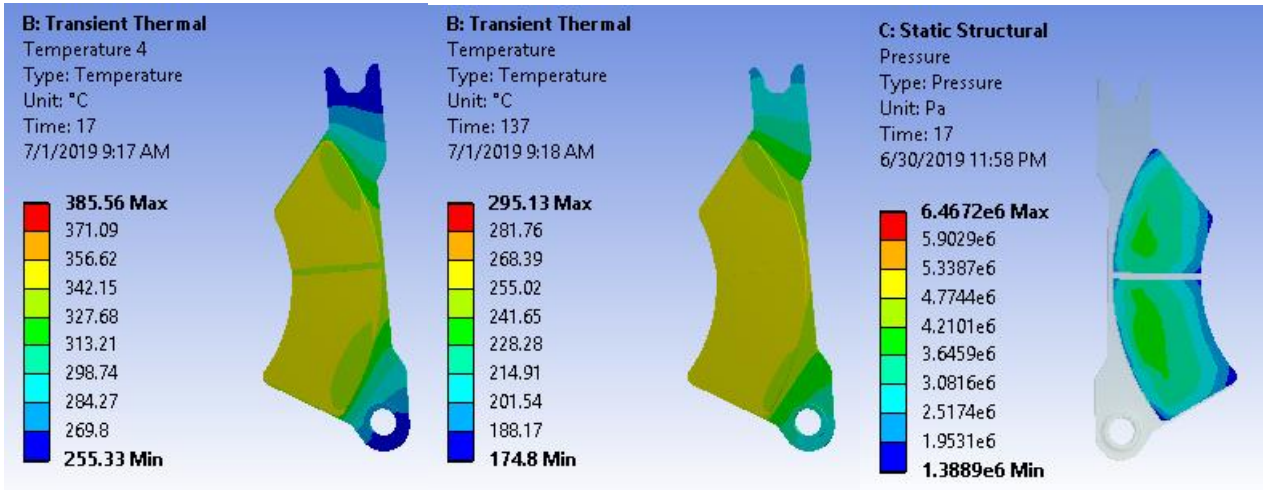
B: Transient Thermal
Temperature 4
Type: Temperature
Unit: °C
Time: 17
7/1/2019 9:17 AM
385.56 Max
371.09
356.62
342.15
327.68
313.21
298.74
284.27
269.8
255.33 Min
B: Transient Thermal
Temperature
Type: Temperature
Unit: °C
Time: 137
7/1/2019 9:18 AM
295.13 Max
281.76
268.39
255.02
241.65
228.28
214.91
201.54
188.17
174.8 Min
C: Static Structural
Pressure
Type: Pressure
Unit: Pa
Time: 17
6/30/2019 11:58 PM
6.4672e6 Max
5.9029e6
5.3387e6
4.7744e6
4.2101e6
3.6459e6
3.0816e6
2.5174e6
1.9531e6
1.3889e6 Min